Available online at www.sciencedirect.com
SCIENCE DIRECT®
Microporous and Mesoporous Materials 77 (2005) 1–45
MICROPOROUS AND MESOPOROUS MATERIALS
www.elsevier.com/locate/micromeso

Review

Ordered mesoporous materials in catalysis

Akira Taguchi, Ferdi Schüth *

Max-Planck-Institut für Kohlenforschung, Kaiser-Wilhelm-Platz 1, Mülheim an der Ruhr 45470, Germany

Received 16 April 2004; accepted 4 June 2004
Available online 30 October 2004

Abstract

Ordered mesoporous catalysts could open the door for new catalytic processes, based partly on novel principles, owing to their hitherto unprecedented intrinsic features. For the preparation of ordered mesoporous catalysts, many strategies have been described. These strategies and the essential properties of the resulting materials are described in the first part of this review. Catalytic processes over such mesoporous materials, especially such reactions where the specific features of ordered mesoporous catalysts are exploited, are described in the second part.

Keywords: Mesoporous; Catalysis; MCM-41; Ordered; Support

Contents

* Corresponding author. Tel.: +492083062367; fax: +492083062995.
E-mail address: schueth@mpi-muelheim.mpg.de (F. Schüth).

1387-1811/$ - see front matter © 2004 Elsevier Inc. All rights reserved.
doi:10.1016/j.micromeso.2004.06.030

1. Introduction

Porous materials have been intensively studied with regard to technical applications as catalysts and catalyst supports. According to the IUPAC definition, porous materials are divided into three classes; microporous (pore size < 2 nm), mesoporous (2–50 nm), and macroporous (>50 nm) materials [1]. In addition, also the term "nanoporous" is increasingly being used. However, it is not clearly defined and loosely refers to pores in the nanometer size range. Many kinds of porous materials such as (pillared) clays, anodic alumina, carbon nanotubes and related porous carbons and so on, have been extensively described in the literature [2]. Among the family of microporous materials, the best known members are zeolites which have a narrow and uniform micropore size distribution due to their crystallographically defined pore system.

In recent years, environmental and economic considerations have raised strong interest to redesign commercially important processes so that the use of harmful substances and the generation of toxic waste could be avoided. In this respect, there is no doubt that heterogeneous catalysis can play a key role in the development of environmentally benign processes in petroleum chemistry and in the production of chemicals, for instance by substitution of liquid acid catalysts by solid materials. Especially zeolites have attracted strong attention as such acids, but also as base and redox catalysts. However, zeolites present severe limitations when large reactant molecules are involved, especially in liquid-phase systems as is frequently the case in the synthesis of fine chemicals, due to the fact that mass transfer limitations are very severe for microporous solids. Attempts to improve the diffusion of reactants to the catalytic sites have so far focused on increasing the zeolite pore sizes [3], on decreasing zeolite crystal size [4], or on providing an additional mesopore system within the microporous crystals [5,6]. An important line of research has focused on the enlargement of the pore sizes into the mesopore range, allowing larger molecules to enter the pore system, to be processed there and to leave the pore system again.

The first synthesis of an ordered mesoporous material was described in the patent literature in 1969. However, due to a lack of analysis, the remarkable features of this product were not recognized [7,8]. In 1992, a similar material was obtained by scientist in Mobil Oil Corporation who discovered the remarkable features of this novel type of silica and opened up a whole field of research [9]. MCM-41, which stands for Mobil Composition of Matter No. 41, shows a highly ordered hexagonal array of unidimensional pores with a very narrow pore size distribution [10,11]. The walls, however, very much resemble amorphous silica. Other related phases such as MCM-48 and MCM-50, which have a cubic and lamellar mesostructure, respectively, were reported in these early publications as well. At approximately the same time, an alternative, but less versatile approach to mesoporous materials was described by Yanagisawa et al. [12]. Kanemite, a layered silicate, serves as a silica source, the pathway leading to the ordered mesoporous material is thought to proceed via surfactant intercalation into the silicate sheets, warping of the sheets and transformation to the hexagonally packed material. Modifying and optimizing the reaction conditions yielded highly ordered mesoporous silicates and aluminosilicates as well [13,14]. The obtained materials are designated as FSM-*n*, Folded Sheet mesoporous Materials-*n*, here *n* is the number of carbon atoms in the surfactant alkylchain used to synthesize the material. Since these early discoveries a large research effort has been invested in the synthesis and characterization of a variety of different, although related materials.

Many reviews have been published covering various aspects of ordered mesoporous materials, such as their synthesis, surface modification, application as host materials, and in catalysis [15–31]. In this review, we will first describe the general methods for the preparation of ordered mesoporous solids, then the pathways used to introduce catalytic functions, and finally highlight their applications in catalysis, with a focus on such applications which exploit the special features of ordered mesoporous materials. The treatment will cover primarily the more recent literature, because surveys of older publications can be found in previous reviews on the catalytic behavior [15,28,29]. It will not be attempted to cover the patent literature, because it is almost impossible to follow this extensive body of work and—more importantly—although many valuable findings are reported in the patents, it is generally not easy to assess the validity of the claims. It should, however, be mentioned, that the patents are covered on a rather broad basis in the early review by Corma [15].

2. Synthesis of ordered mesoporous materials

The discovery of ordered mesoporous solids of the MCM-41 type and related materials in the early 1990s has been a breakthrough in materials engineering, and since then there has been impressive progress in the development of many new mesoporous solids based on templating mechanisms related to the one used for the original MCM-41 synthesis. Depending on the synthesis conditions, the silica source or the type of surfactant used, many other mesoporous materials can be synthesized following the co-operative assembly pathway [32–34]. In addition to the co-operative pathways, also the true liquid crystal templating pathway [35] and nanocasting using already formed ordered mesoporous materials as hard templates [36,37] have been developed over the last ten years. From the viewpoint of the template used for synthesis and the interaction of inorganic species and organic template molecule, the mesoporous materials might be classified as listed in Table 1.

The first-ordered mesoporous materials were prepared from ionic surfactants, such as quaternary ammonium ions. The formation of the inorganic–organic composites is based on electrostatic interactions between the positively charged surfactants and the negatively charged silicate species in solution. The packing parameter g may be used to rationalize and also in some cases predict the product structure and the conditions for possible phase transitions. Such prediction of the structure of surfactant aggregates and the corresponding mesophases in surfactant–water systems was made possible by Israelachivili et al. [38,39], who developed a microscopic model according to which the dimensionless packing parameter g plays a key role. This number, g, is defined as $g = V/a_0 l_c$, where V is the effective volume of the hydrophobic chain of the surfactant, a_0 is the effective aggregate surface area of the hydrophilic head group, and l_c is the effective hydrophobic chain length. Although the concept was originally only developed for dilute solutions, it is surprisingly powerful also in the understanding of the phases formed in relatively concentrated systems from which ordered mesostructured materials are formed. One should note that the variables in the definition of the packing parameters are not constants for a given surfactant, but are influenced by the solution conditions, such as for instance ionic strength, pH, co-surfactant concentration or temperature [39]. A synthesis-space diagram (not a phase diagram, because different to pure surfactant–water systems, it is not only the thermodynamics which influences the formation of a certain phase) for a ternary system composed of NaOH, cetyltrimethylammonium bromide (CTAB), and tetraethylorthosilicate (TEOS) has been described in literature [40,41]. It was observed that the surfactant to silica ratio has a substantial impact on the composite structure obtained [42]. The co-operative formation mechanism was extended by Stucky and coworkers [41,43,44] to a whole series of other electrostatic assembly mechanisms, such as a reversed S^-I^+ (S = surfactant, I = inorganic species) mechanism and counterion mediated $S^+X^-I^+$ and $S^-M^+I^-$ pathways. The use of anionic surfactant via S^-I^+ or $S^-M^+S^-$ interaction has resulted mainly in lamellar and disordered mesostructures. Recently, a novel synthetic route for mesoporous silica by the use of anionic surfactants has been reported by Che et al. (named AMS-*n*, Anionic surfactant templated Mesoporous Silica) [45,46]. Here, the negatively charged head group of the anionic surfactant, such as palmitic acid or *N*-lauroyl-L-glutamic acid, interacts with the positively charged amine or ammonium groups of 3-aminopropyltrimethoxysilane or *N*-trimethyoxysilylpropyl-*N*,*N*,*N*-trimethylammonium, which are used additives for co-condensation of TEOS (tetra ethyl ortho silicate).

The mesopore size of these kinds of materials is primarily controlled by the length of the alkyl chain of the surfactant used. However, addition of auxiliary organic molecules such as aromatics [11,47], *n*-alkanes [48], or fatty acid [49] can lead to an expansion of the mesopore size. Mixing of two alkyl ammonium surfactants with different alkyl chain length can be used to fine-tune the pore size between those of the long and the short chain surfactant [50].

Many silica-based mesoporous materials, but also such with non-silica frameworks have been reported to be formed via these electrostatic assembly pathways [30]. From the catalytic point of view, materials are of minor interest as long as the pores are blocked by

Table 1
Possible pathways for the synthesis of mesoporous materials

Template	Interaction		Synthesis conditions	Examples
Ionic surfactant	Direct interaction	I^-S^+	Basic	MCM-41, MCM-48, MCM-50 [9–11], FSM-16 [13,14]
	(Ionic)	I^+S^-	Neutral-basic	(Aluminum, iron, lead oxides, etc. [33,34]) AMS [45,46]
	Intermediated interaction	$I^+X^-S^+$	Acidic	SBA-1, SBA-2, SBA-3 [43], HMS [54], TLCT [35]
	(Ionic)	$I^-X^+S^-$	Basic	(Aluminum, zinc oxides etc. [33,34])
Non-ionic surfactant	(Non-ionic)	I^0S^0		HMS [54,55]
Co-polymer		I^0N^0	Acidic	MSU [56,58], SBA-15 [62,63], TLCT [35]
(Ligand assisted)	(Co-valent bonding)	I–S		Nb-TMS [72,74], Ta-TMS [73]
Nanocasting	–	–	–	CMK-*n* [36,290]

template and the internal surface is not accessible. The thermal instability of the early materials was attributed to the existence of several relatively unstable oxidation states of the metal centers, and thus oxidation or reduction reactions during calcination would lead to structural collapse [51]. However, as will be discussed below, later on it has been possible to synthesize stable non-silica materials [52,53], and some examples of catalyses over such materials have been appeared in the literature.

Pinnavaia et al. have developed two additional approaches for the synthesis of mesoporous materials, based on non-ionic organic–inorganic interactions. They used neutral surfactants such as primary amines and poly(ethylene oxides) to prepare HMS (hexagonal mesoporous silica) [54,55] and MSU (Michigan State University material) [56], respectively. The pore systems of the latter silicas have been shown to have rather worm-like structures than long-range ordered hexagonal arrays which are characteristic for MCM-41 [57,58]. If these nonionic surfactants are used instead of ionic ones, hydrogen bonding is the driving force for the formation of mesophases. Therefore, the surfactant can be recovered by extraction, which is advantageous both from an economical and an ecological point of view. More than 90% of the template molecules can be recovered by a simple extraction with ethanol [54] or acidified water [59].

Compared to MCM-41, HMS and MSU have very similar surface areas and pore volumes, but the pore size distributions are somewhat broader. Many modifications used in the synthesis of MCM-41 can also be applied to HMS. Control of pore size by changing the alkyl chain length of the surfactant or by addition of mesitylene to the reaction mixture have accordingly been reported [60,61].

Poly(ethylene oxide) cannot only be used as such, but is also a component in very versatile surfactants used for the synthesis of ordered mesoporous materials. Poly(ethylene oxide) monoethers were used to form materials showing worm-like disordered or hexagonally ordered mesopores with pore sizes of ca. 5 nm [62]. One of the most useful groups of surfactants are the triblock co-polymers consisting of poly(ethylene oxide)$_x$–poly(propylene oxide)$_y$–poly(ethylene oxide)$_x$, (PEO)$_x$(PPO)$_y$-(PEO)$_x$, (trade name: Pluronics) which show the ability to form liquid–crystal structures. They can be used to synthesize a variety of different ordered mesoporous materials with rather large pores in various framework compositions under strongly acidic conditions [62–65]. Here the EO (ethylene oxide) units and the cationic silicate species favorably interact to form the mesostructured assembly, although the details of the mechanism are much less clear than for the synthesis of the MCM-41 type materials under basic conditions. A 2D hexagonal mesoporous material formed via this pathway (denoted as SBA-15, Santa BArbara No. 15) exhibits a thick wall of 3–7 nm thickness and large pore sizes adjustable between 6 and about 15 nm. The thick wall of this material significantly improves the thermal and hydrothermal stability compared to mesoporous MCM-41 and related silicas.

The mesopore diameter of SBA-15 depends on the synthetic conditions: increasing the gel aging temperature leads to a larger pore diameter [63,66]. One interesting feature of SBA-15 is the microporosity which is present in its mesopore wall, by which the micropores connect neighboring mesopores. By careful investigation of XRD and the modeling of the diffraction patterns, Impéror-Clerc et al. found that the walls had a ''microporous corona'' region resulting from partial embedding of the PEO part of the surfactant in the mesopore wall [67]. The authors suggested that this corona is converted to micropores upon calcination. Imaging of the platinum replica of the pore structure of SBA-15 allowed to visualize the presence of these micropores using TEM [66,68,69].

The same approach can lead to mesoporous alumina [70]. Thermally stable, ordered, mesoporous $SiAlO_{3.5}$, $SiTiO_4$, Al_2O_3, Al_2TiO_5, TiO_2, ZrO_2, $ZrTiO_4$, ZrW_2O_8, HfO_2, Nb_2O_5, Ta_2O_5, WO_3 and SnO_2 with pore sizes up to 14 nm were synthesized with amphiphilic poly(alkylene oxide) block co-polymers and inorganic salt precursors in non-aqueous solutions [64,65]. The materials contain nanocrystalline domains within relatively thick amorphous walls [71].

In the ligand assisted assembly approach, co-valent bonds are formed between the inorganic precursors and the organic surfactant molecule prior to assembly. Originally, this synthetic approach has been developed by Antonelli and Ying for the preparation of mesoporous niobium oxide [72] and tantalum oxide [73]. The synthesis of Nb-TMS (Transition-Metal oxide mesoporous molecular Sieve) and Ta-TMS involves the hydrolysis of long-chain amine complexes of niobium or tantalum alkoxides. The respective phase is formed by self-assembly of the metal–alkoxide–amine complexes. The template can be removed by extraction, leading to open porous structures with surface areas of up to 500 m^2/g. Further, in case of niobia, mesostructured materials with 3D hexagonal symmetry, a cubic phase, and a layered phase could be obtained [74]. Also hexagonal and lamellar mesostructured silica could be successfully prepared via this approach [44,75–77]. Shimojima and Kuroda used newly designed siloxane-based oligomers, consisting of an alkylsilane core and three branched trimethoxysilyl groups ($C_nH_{2n+1}Si(O-Si(OCH_3)_3)_3$, $n = 10$ or 16), in this ligand assisted strategy [77]. The structure of the obtained materials depended on the alkylchain length of the alkylsilane used; the hexagonal structure was obtained with the short chain silane ($n = 10$) while the lamellar structure

was formed by using the $n = 16$ silane. This structure change is consistent with the change of the surfactant packing parameter g upon increasing the surfactant chain length.

The methods discussed so far all rely on a co-operative interaction between the surfactant and the inorganic species by which an organic/inorganic mesostructured composite is formed. However, one can also use a preformed surfactant liquid crystalline phase which is subsequently loaded with the precursor for the inorganic material. This pathway, later labeled "true liquid crystal templating" (TLCT) [35], had already been suggested as one possible mechanism for the formation of MCM-41 in the original publication by the Mobil-group [10]. The first realization was reported by Attard et al. [35] who hydrolyzed tetramethylorthosilicate (TMOS) within a liquid crystalline phase. This phase was destroyed upon formation of the methanol but reformed after evaporation of the alcohol. This method was later found to be useful also for the synthesis of mesoporous metals [78–81] or mesostructured assemblies of chalkogenide nanoparticles [82]. The boundary between the co-operative pathway and the TLCT mechanism, however, is not sharply defined because the pure surfactant mesophase used in the TLCT method may be intermittently destroyed and then reformed during the synthesis.

A clearly distinct method is the nanocasting first reported by Ryoo and co-workers in 1999 [36]. Here no surfactant template is used, but instead the pore system of an ordered mesoporous silica is used as a hard template. The pores are infiltrated with a carbon precursor such as sucrose or furfuryl alcohol which is subsequently converted to carbon by high temperature treatment in inert gas (Fig. 1). After leaching of the silica with HF or NaOH, a negative of the original mold is obtained (denoted as CMK-*n*). Also small ordered mesoporous metal domains could be prepared by this pathway although it is not fully clear how well the perfection and long range order of the materials is [83]. While this method is already well established to produce carbon-based materials and ordered mesoporous polymers [84,85], silica as a hard template for the formation of an oxide was only recently reported for some examples, such as CeO_2 [86], Cr_2O_3 [87], NiO [88], OsO_4 [89], In_2O_3 [90,91] and Co_3O_4 [91,92]. This is probably due to the fact that many oxide materials are not compatible with the conditions of silica leaching.

Alternatively, non-carbon materials can be synthesized via the nanocasting route by repeated nanocasting, where first an ordered mesoporous carbon is synthesized which is then in turn used as a hard template for the synthesis of an oxide. This has been demonstrated to be possible for the example of silica so far (Fig. 1) [37,93]. Although on first sight the complex procedure brings only back the starting situation, additional control of the textural parameters, such as the fraction of micropores in the materials, is possible [94]. Considering the range of methods reported and their versatility to produce ordered mesoporous material, it is not hard to predict that compositional variability will continue to increase over the years to come.

3. Control of local environment and morphology

One of the interesting features of ordered mesoporous solids for catalysis is the multitude of possibilities to modify them. The modifications can be used to adjust

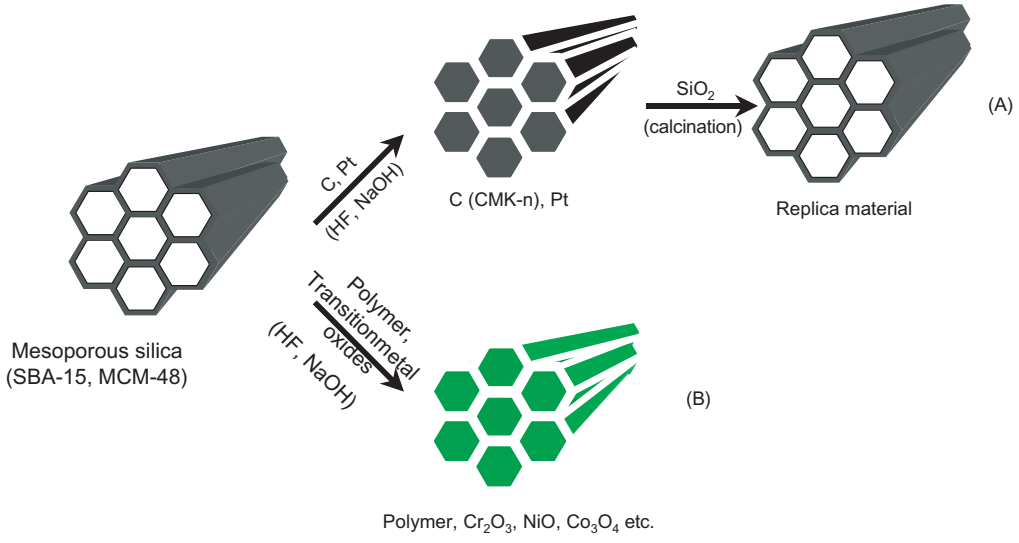

Fig. 1. Schematic description of the nanocasting pathway. (A) Loading with carbon or platinum and following dissolution of mesoporous silica gives the corresponding porous materials with negative replica structure. Subsequent back casting with silica source and removal of carbon by calcination allows to obtain positive replica porous silica material. (B) Incorporation of polymer or metal oxides instead of carbon or platinum also allows to obtain new mesoporous materials.

surface functionality, to incorporate catalytic functions or to change textural properties. These methods, with a focus on such modifications which are useful for the application of the materials as catalysts, will be discussed in the following.

Recently, the thermal, hydrothermal, and mechanical stabilities of various mesoporous silicas, e.g. MCM-41, MCM-48, HMS, FSM-16, KIT-1, PCH (porous clay heterostructure) [95] and SBA-15, have been studied by Galarneau et al. [96], Cassiers et al. [97] and Igarashi et al. [98]. It was discovered that the thermal stability strongly depends on the wall thickness of the mesoporous materials and the silica precursor used in the synthesis. Hydrothermal stability is influenced by the wall thickness as well, but the degree of silica polymerization has also a very strong influence on hydrothermal stability (Table 2). Mechanical stability, on the other hand, is only little influenced by the nature of the mesoporous materials and is usually sufficient for application of ordered mesoporous solids in most catalytic applications. Since hydrothermal stability is essential for most possible applications of mesoporous materials in catalysis, several approaches were developed to improve this property. The strategies that have been investigated include the addition of salts during the hydrothermal synthesis [99], modification of the surface by silylation [100] or post-synthesis grafting of inorganic compounds to increase the wall thickness or to chemically stabilize the wall surface [101].

In order to decrease the population of surface silanols, the number of which influences the structural stability [97,98], silylation of surface hydroxyls is widely used. This treatment drastically increases the surface hydrophobicity, and therefore, the resulting materials have improved hydrothermal stabilities. Direct incorporation of organic groups, either pending on the wall [102,103] or incorporated as bridges between silicon atoms in the wall [104] is possible, for instance, by the use of alkylalkoxysilanes as silica source. Since the alkyl-C-bond is not affected during synthesis, the organic groups are retained in the final material. Such modified silicas and their properties are discussed in several recent reviews [105–109]. Grafting of inorganic components, such as Al, Ti, V, etc., is also effective in achieving surface silanol modification. In addition to decrease of the number of structural defect sites in the silica framework, this treatment also leads to increased pore wall thickness. Furthermore, such treatment might simultaneously be used to introduce catalytic functions into the materials [110,111].

The activity of solid catalysts is sometimes influenced by an additional interaction between substrate and support surface. For example, enhancement of catalytic activity in the epoxidation of cyclohexene with alkyl hydroperoxides was observed when the surface of MCM-41 had been modified with Ge(IV) prior to the grafting of titanocene dichloride ($TiCp_2Cl_2$) [112]. The turnover frequency increased up to 140% compared to the catalyst supported on siliceous MCM-41. The EDX-TEM and XAS measurements revealed that the germanium is evenly spread over the MCM-41, indicating a strong interaction of Ge and silica support. Titanium centers attached via oxygen to two silicon and one germanium atom are responsible for the increased activity of this catalyst. The activity for cyclooctene epoxidation with *tert*-butylhydroperoxide (TBHP) of an oxodiperoxo molybdenum complex grafted on mesoporous material was improved by the use of Al-MCM-41 instead of siliceous MCM-41 [113]. Two possible explanations are (i) the Al sites near the active Mo complex could activate the TBHP molecule for proton transfer to an $Mo(O_2)$ unit in the activation of the

Table 2
Effect of thermal and hydrothermal treatments on the surface area and primary pore volume of mesoporous materials [97]

	Wall thickness (nm)	Surface area (m^2/g)				Pore volume (cm^3/g)			
		550 °C	850 °C	400 °C, 30 vol% steam, 120 h	100 °C, 100 vol% relative humidity, 16 h	550 °C	850 °C	400 °C, 30 vol% steam, 120 h	100 °C, 100 vol% relative humidity, 16 h
MCM-41(T)[a]	0.97	1128	403[b]	1019	145	0.95	0.26[b]	0.47	–[d]
MCM-41(FS)[a]	1.10	1027	795	864	106	0.92	0.53	0.58	–[d]
MCM-48(T)[a]	0.93	1433	108[b]	1318	197	1.14	–[a]	0.93	–[a]
MCM-48(FS)[a]	0.94	1319	1094	1130	168	1.22	0.74	0.94	–[a]
HMS	1.07	1021	213[b]	830	228	0.81	–[a]	0.48	–[a]
FSM-16	0.99	1172	476	789	67	0.78	0.20	0.36	–[a]
KIT-1	1.07	1059	967	–[c]	974	0.88	0.68	–[c]	0.78
PCH		899	441	728	335	0.50	0.25	0.43	–[c]
SBA-15	2.97	632	446[b]	500	281	0.63	0.48[b]	0.55	0.47

[a] Prepared from TEOS (T) or fumed silica (FS) as a silica source.
[b] Data from 750 °C.
[c] Not measured.
[d] No capillary condensation step was observed in the N_2 isotherm.

organoperoxide, and/or (ii) a Lewis acid site close to the molybdenum species could co-ordinate to the ligand of the Mo complex and reduce the donor strength of the ligand-Mo bond which leads to an increase in the catalytic activity.

The hydrophobic/hydrophilic properties of the catalyst surface sometimes also have a strong influence on the catalytic activity. In the acetalization of D-glucose with *n*-butanol on Al-MCM-41, the catalytic activity is influenced by the hydrophobic properties as well as the concentration of active acid sites [114]. In this reaction, the initial rate for the disappearance of D-glucose is increased with increase of the Si/Al ratio. If the Si/Al ratio of MCM-41 is increased, the hydrophobicity of the catalyst will increase as well. Due to the difference of polarity of D-glucose (hydrophilic) and *n*-butanol (hydrophobic) the more polar glucose could preferentially and strongly be adsorbed. These examples show that in many cases fine-tuning of surface polarity and the active site is required in the design of solid catalysts. This holds especially for catalysts based on ordered mesoporous materials, since due to their pore system with relatively narrow pores the reacting molecules are exposed to a local environment determined by the surface properties of these pores for a relatively long time.

The most well-known example for the effect of surface hydrophobicity is the olefin epoxidation over titanium-modified materials. Silylated mesoporous titanosilicates which are more hydrophobic compared to the unmodified silicas, have enhanced activity in olefin epoxidation [115–117]. When alkylhydroperoxides are used as oxidants, the substrates have to compete with water. An increase in activity is then expected for a more hydrophobic support, because the substrates are favored in the pore system and therefore gain easier access to the catalytically active titanium centers. Moreover, in Ti-MCM-41 with larger pores compared to zeolites, the alkylhydroperoxide can easily penetrate the mesopore system, reducing diffusion limitations or complete exclusion of the hydroperoxide. In addition, the removal of the silanols may reduce the undesired solvolysis reaction of the formed epoxides by water.

As stated above, in comparison to microporous zeolites, ordered mesoporous materials overcome the pore size constraint of zeolites and allow more facile diffusion of bulky substrates. Unrestricted diffusion of reactants and products for mesoporous materials was observed even after the incorporation of large catalytically active sites in the mesopore system [118,119]. Since diffusion limitations depend on the size and morphology of the primary catalyst particles, variation of these factors should help to elucidate mass transfer effects. Wong et al. [120] studied the effect of the morphology of MCM-41 on catalytic performance. They reported various different synthesis procedures and characterized transition metal oxide catalysts supported on tubular and particulate MCM-41 [121,122]. They tested the catalytic performance of several molybdenum oxide catalysts for ethylbenzene dehydrogenation and showed that Mo supported on tubular MCM-41 has a higher activity (3.07×10^{-3} mol/h g) than that on MCM-41 with a usual particulate morphology (2.60×10^{-3} mol/h g). In addition, the catalyst based on tubular MCM-41 had a lower deactivation rate. A similar trend has recently been published in catalytic cracking of 1,3,5-triisopropylbenzene over Al-MCM-41 with tubular and particulate morphology [123]. The high porosity of the tubular MCM-41 and the presence of defects are proposed to be responsible for the better performance, by improving the inter-channel diffusion of reactants and products. This is on first sight in agreement with a recent NMR study of cyclohexane diffusion in tubular and particulate materials where intraparticle diffusion coefficients in tubular materials were observed to be higher [123]. However, the study was performed close to room temperature, and activation energies were reported to be 15 kJ/mol for the tubular sample and 27 kJ/mol for the particulate one. Under reaction temperature, diffusion can thus be expected to be higher in the particulate sample. Thus, more work seems to be necessary to elucidate mass transfer effects in catalysis over ordered mesoporous materials, especially, since the differences between different morphologies do not seem to be very pronounced.

In order to obtain efficient solid-phase catalysts, morphology control of mesoporous silica may help to optimize the material for specific applications. The synthesis of thin films [124–126], fibers [127–130], tubes [121,131], spheres [125,132–134] or monoliths [135] has been reported, following various pathways, which include either self-organization, or shaping procedures, such as spray-drying [132], aerosol processing [133], spin- and dip-coating [126,136], etc. Syntheses in the presence of special additives, such as polystyrene latices or water-soluble polymers yielded porous silicas with mesoporous–macroporous hierarchical porosity [137,138].

4. Preparation of catalysts—strategies and properties

Ordered mesoporous silicas are not often used as catalysts as such. Much more frequently, additional catalytic functions are introduced, by incorporation of active sites in the silica walls or by deposition of active species on the inner surface of the material. The advantage of using ordered mesoporous solids in catalysis are the relatively large pores which facilitate mass transfer and the very high surface area which allows a high concentration of active sites per mass of material. There are many possible pathways to modify mesoporous materials when one wants to give them a new catalytic function as schematically shown in Fig. 2. Metal ions substituting

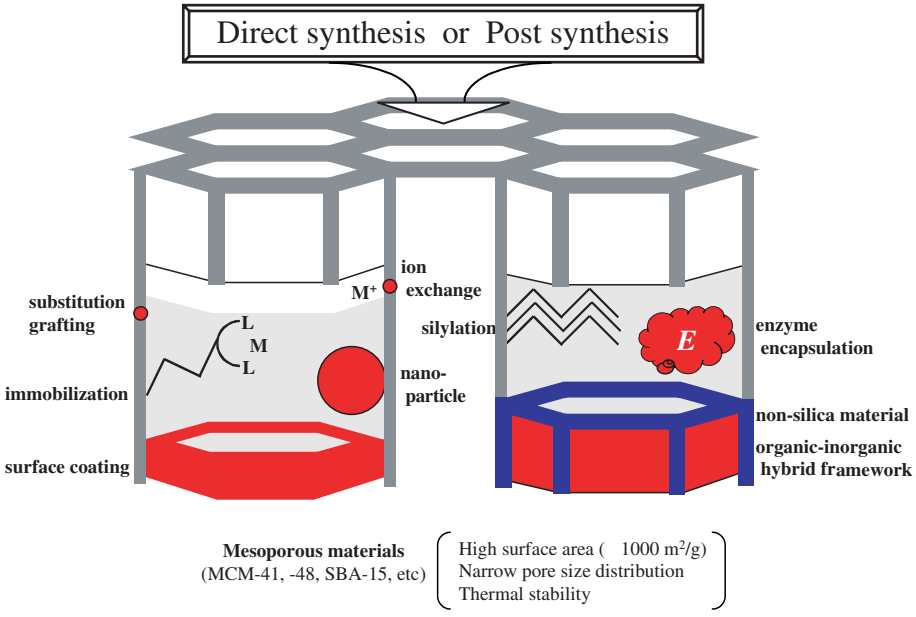

Fig. 2. Schematic sketch of the various methods for the functionalization of mesoporous material. There are many possible strategies and pathways to introduce novel functions in mesoporous materials.

silicon atoms in the framework, similar as in zeolites, can act as acid or redox active sites and may be used for different classes of catalytic reactions. One should bear in mind, though, that the wall structure of ordered mesoporous silica rather resembles amorphous silica. Incorporation of other metal centers therefore does not lead to the formation of defined sites as in zeolites, but to a rather wide variety of different sites with different local environments. Therefore, the catalytic properties of such materials are closer to those of metal substituted amorphous silica than to those of framework substituted zeolites. Possibly more interesting is to exploit the exceedingly high surface area of these materials in support applications for metal or metal oxide particles or to deposit isolated species onto the wall surface. Interestingly, these active sites can be constructed both directly or via post-synthesis procedures by a multitude of pathways, which means that the properties of these active sites are variable and controllable, depending on the synthetic procedure.

The number of combinations of different modifications of ordered mesoporous materials is high, since many properties can be changed independently of each other. One may think about surface coating of mesoporous materials with organic or inorganic species, which drastically changes the microenvironment inside the mesopores. On the other hand, the pore system with large pore opening enables the fixation of various regio- and enantioselective complexes; this can be advantageous compared to conventional microporous or macroporous supports since the size of the pores can be exactly adapted to the requirements of the anchored species. The open mesoporous structure provides highly dispersed and spatially uniform active sites. Furthermore, the composition of the mesoporous support material itself could be changed by wall incorporation of different components, which is another adjustable parameter of the materials. Since most of these factors could be varied independently, different materials could be created in an almost combinatorial fashion.

Many of the modification steps make use of the silanol groups present on the silica surface of the ordered mesoporous silica, because they are the anchor sites for metal species or silane coupling agents. There are many indications that the density of silanols in ordered mesoporous materials, especially in MCM-41, is lower than in conventional hydroxylated silica. For conventional hydroxylated silica, the density of silanol groups is remarkably constant, irrespective of the origin of the silica, at about 4–6 Si–OH/nm^2 [139]. This, however, can be different for ordered mesoporous materials. Concentrations of between 1.4 and 1.9 groups/nm^2 have been determined for the cubic MCM-48 [140]. This is close to the data reported by other groups. From the published data, a concentration between 2 and 3 groups/nm^2 can be estimated for MCM-41 as well as MCM-48 [141,142]. However, direct comparison with fully hydroxylated silica is difficult, since from the published data it is often not clear, to what extent the surface of these materials is dehydroxylated by the thermal pretreatment, or whether a rehydroxylation step was performed under controlled conditions. For SBA-15 with its larger pores pretreated at 200 °C under vacuum, a concentration of around 1.0 OH/nm^2 was reported, which roughly corresponds to the value expected after such a pre-treatment also for conventional silica

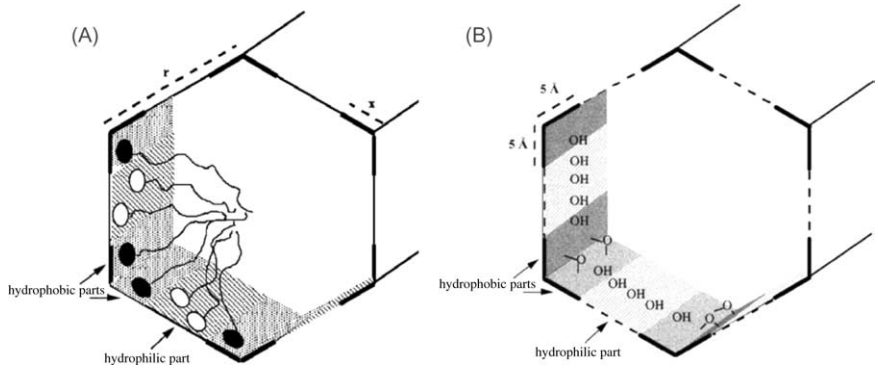

Fig. 3. Schematic view of the inhomogeneous silanol group distribution in the hexagonal pore of MCM-41 mesoporous silica. (A) EPR spectra suggest a direct interaction of the charged head of 4-alkyldimethylammonium-2,2,6,6-tetramethylpiperidine-1-oxyle (white head group) with the polar surfaces sites in the hydrophilic part, the number of which increases with the pore diameter of MCM-41. (B) The hydrophilic surfaces correspond to the section on the flat sides of the hexagon. Around the pore corners, a condensed silica surface is generated with a low concentration of silanol [96,145].

[143,144]. One should also keep in mind that there is evidence for a non-homogeneous distribution of the silanols over the surface of MCM-41: more hydrophobic and more hydrophilic patches co-exist in these materials and their relative concentration changes with surface area and pore size (Fig. 3) [96,145]. This may lead to inhomogeneous distribution of groups anchored to the surface. Even if the silanol groups are homogeneously distributed, the possibly lower silanol density compared to conventional hydroxylated silica may correspond to a lower podality (on average) of the anchored species which could result in a higher susceptibility to hydrolytic bond cleavage.

In the following, we will briefly discuss the different types of active species found in catalysts based on mesoporous silica and the pathways used to generate them. The basic properties of the resulting materials will also be described.

4.1. Highly dispersed heteroatoms and oxidic species

Much effort has been focused on the introduction of heteroatoms, such as B, Fe, Ga, Ti, V, Sn, and particularly aluminum, in the siliceous framework to modify the composition of the inorganic walls. This is especially important with respect to the catalytic applications, since substitution of silicon allows fine-tuning of the acidity or creation of redox properties, similar as observed in amorphous aluminosilicates or zeolites. Modification of the framework composition is possible by the direct synthesis, i.e. from mixtures containing both silicon and the heteroelement to be incorporated, or by post-treatment of an initially prepared silica mesoporous material. The results of these two different methods are not necessarily identical. While the direct method typically will result in a relatively homogeneous incorporation of the heteroelement, post-synthesis treatment will primarily modify the wall surface and thus lead to increased concentration of the heteroelement on the surface. This effect has, for instance, been used by Mokaya [110] to synthesize aluminum modified materials with enhanced hydrothermal stability. The increased stability was explained by the coating of the silica surface with alumina species which are less susceptible to hydrothermal degradation. The nature of the reagents used for grafting can strongly influence the properties of the resulting materials. This was nicely demonstrated for Sn(IV) modified materials obtained by grafting with R_nSnCl_{4-n} precursors. Tin reagents with two or three chloro substituents and correspondingly two or one alkyl substituents avoid the generation of inactive polymeric species [146].

Incorporation of aluminum is of special interest if, as in zeolites, this results in the formation of Brønsted acidity and ion exchange sites. The ^{29}Si MAS NMR results indicate the amorphous nature of the pore walls. Since the O–Al–O angle is less flexible than the O–Si–O angle, Al-MCM-41 materials are commonly less well ordered on the mesoscale and show a broader pore size distribution than their pure silica analogues [10,147].

Adsorption of bases such as ammonia and pyridine on Al-MCM-41 allows to determine the strength of acid sites via temperature programmed desorption and FT-IR [147–153]. One can distinguish with these methods between Brønsted and Lewis acidity and recognize weak and strong acid sites, which are formed depending on the Si/Al ratio and the nature of the trivalent element (Al, Fe, Ge). Since the local environment around the acid sites corresponds to amorphous silica–alumina, however, framework substituted materials exhibit a substantially weaker acidity than zeolites, and rather correspond to amorphous silica–alumina in number of acid sites and acid strength distribution (Fig. 4) [154].

Typically, directly synthesized aluminum containing mesoporous silicas, i.e. synthesized from precursor solutions already containing aluminum, have both

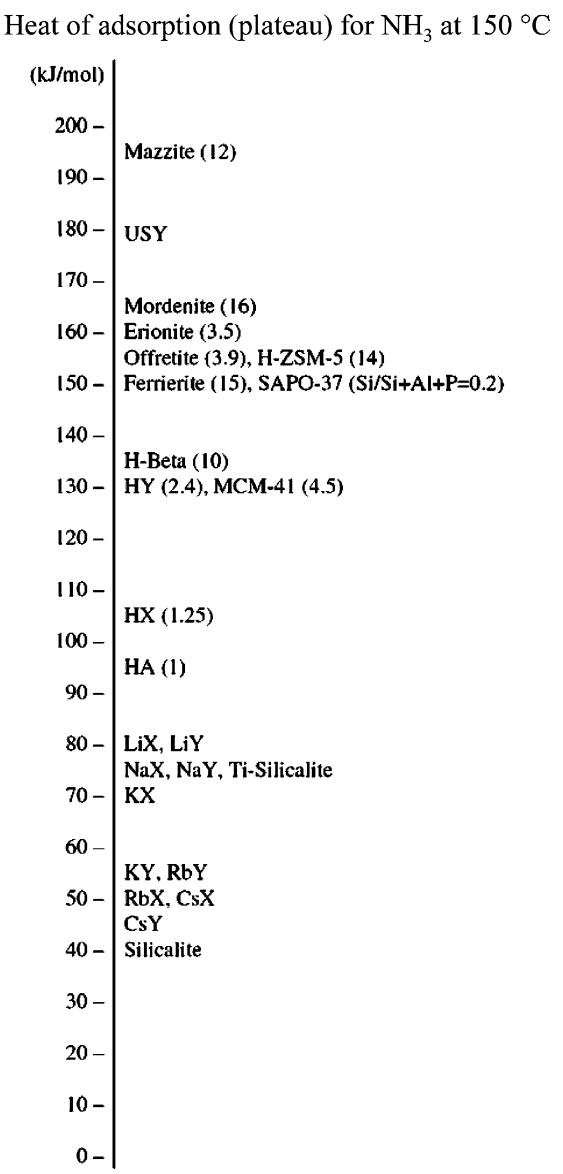

Fig. 4. Acidity of various aluminosilicates studied with NH_3 adsorption calorimetric analysis. Numbers in parentheses show the Si/Al ratio [154].

tetrahedrally and octahedrally co-ordinated aluminum [151,155–158]. Change of the aluminum source can lead to the formation of exclusively tetrahedrally co-ordinated aluminum. If $Al(OH)_3$, aluminum *iso*-propoxide ($Al(OPr^i)_3$) or $NaAlO_2$ are used as aluminum source, Al-MCM-41 prepared from $NaAlO_2$ gave the strongest Brønsted acidity [158]. Microcalorimetry studies of ammonia adsorption revealed that a sample prepared from $Al(OH)_3$ contains a wide distribution of acid site strength while samples prepared with $Al(OPr^i)_3$ or $NaAlO_2$ contain sites with a distinct strength around 130–150 kJ/mol (Fig. 4). By using aluminum sulfate, Al-MCM-41 can be prepared which has all aluminum atoms in tetrahedral co-ordination down to a framework Si/Al ratio as low as 10, although ion exchange of Na^+ against NH_4^+ and following calcination lead to the removal of a small fraction of the aluminum from the framework [151,156]. It is also possible to prepare aluminum incorporated SBA-15 via a direct synthetic route [159]. Washing the material in NH_4Cl solution can eliminate the octahedrally and pentagonally co-ordinated Al species, the absence of which was confirmed by ^{27}Al MAS NMR. The Al-SBA-15 shows higher hydrothermal stability and has higher activity in cumene cracking than Al-MCM-41.

As in zeolites, different heteroelements provide different strength of the resulting acid sites. The Brønsted acid strength of Al-, Ga-, and Fe-substituted MCM-48 investigated by NH_3-TPD were in the order of Al > Ga > Fe, whereas the Lewis acid sites showed an order Ga ≈ Al ≫ Fe [152]. Adding heteroelements to the synthesis mixture does not only lead to their incorporation. Other properties of the synthesis product may be changed as well. The content of Ga, i.e. the concentration of $Ga(NO_3)_3$ in the synthetic gel, influences the particle size of Ga-MCM-41 [160]. The average particle size observed by dynamic light scattering increased with increasing Ga content from 3500 nm (Si/Ga = ∞) to 10,000 nm (Si/Ga = 25).

For post-treatment to induce acidity, various kinds of reagents can be used, and the resulting materials often provide the desired catalytic properties. A comparative study of the acidity of directly synthesized and post-treated Al-MCM-41 has been published by Chen et al. [153]. From the FT-IR-based acidity analysis with pyridine as a probe molecule, one can conclude that Al-MCM-41 directly prepared from $Al(OPr^i)_3$ and TEOS in a mixed gel has the highest concentration of acid sites. The $Al(OPr^i)_3$ grafted materials show lower acid site concentration than $AlCl_3$ grafted samples even for similar Si/Al ratios (11.8–1.3). The total concentration of acid sites normally increases linearly with increasing loading of aluminum [153]. However, at higher loading levels, agglomeration of aluminum species takes place and the concentration of acid sites becomes almost independent of the aluminum content of the materials [161].

Not only aluminum but also other elements such as Sn [146,162] Zn [162] or Zr [163] can be incorporated by post-treatment, and resultant materials provide interesting catalytic activity. For example, Zhu et al. [163] reported that zirconium 1-propoxide grafted SBA-15 has higher activities in the Meerwein–Ponndorf–Verley (MPV) reduction of 4-*tert*-butylcyclohexanone than SBA-15 grafted with aluminum 2-propoxide.

From the viewpoint of the surface acidity, thermal stability or hydrothermal stability, one of the most interesting developments involves zeolitization of the wall of mesoporous silica. Generally, two methods seem feasible for this process: (i) the silica in the walls of a formed ordered mesoporous material could be converted to zeolitic units, or (ii) the mesoporous silica could be

synthesized from solutions which already contain zeolitic structural elements. Kloetstra et al. [164] followed the first pathway and tried to re-crystallize the amorphous aluminosilicate wall to the zeolitic ZSM-5 structure. Using glycerol as a solvent, Na^+ and TPA^+ ion exchanged Al-MCM-41 was treated in an autoclave at 120 °C. However, the presence of zeolitic species in the wall could not clearly be proven. The alternative pathway seems to be more successful. In a first step, zeolite synthesis gels are prepared and aged under conditions where no bulk zeolite particles form. Small structural fragments are thought to be present in such solutions and some indications that this is true do exist. In a second step, the surfactant template is added, and a mesoporous material is formed. Although difficult to analyze, the catalytic, spectroscopic and textural properties suggest that the walls indeed contain structural fragments of zeolites. Several publications report the formation of mesoporous materials with zeolitic fragments in the walls which were synthesized following this method [165–169]. Alternatively, the walls of mesoporous silica can also be coated with zeolitic fragments, as reported by Trong On and Kaliaguine [170–172]. The FT-IR spectrum after pyridine adsorption, using ZSM-5 coated SBA-15 as an example, shows the two intense absorption bands characteristic for Brønsted and Lewis acid sites, which are not observable for the parent mesoporous SBA-15 [170]. In addition, the material was very stable when exposed to boiling water at 100 °C or steam at 800 °C. Such materials may have good perspectives for industrial applications, because they combine the acidity of zeolites with the improved mass transfer of mesoporous materials.

The substitution of trivalent elements in a silica framework requires the presence of extra framework charge compensation cations. Such counter ions are usually exchangeable and can be used to introduce novel functionality into the mesoporous silicate. For example, the cations in aluminosilicates were successfully exchanged with Cs^+, Zn^{2+} or Fe^{3+}, and the resulting materials show catalytic activity in the Diels–Alder reaction of cyclopentadiene and methyl acrylate [173] or in the selective catalytic reduction of NO [174]. Not only inorganic cations but also cationic organometallic compounds, such as $[Fe(phenanthroline)_3]Cl_2$ [175], $[Fe(8\text{-quinolinol})_3]Cl_2$ [176], $[Mn(2,2'\text{-bipyridine})_2]NO_3$ [177], [Mn(porphyrin)]Cl [178], or [Mn(salen)]Cl [179,180], are also exchangeable. However, one should keep in mind that the ion-exchange procedure sometimes leads to a partial elimination of the substituted trivalent element [156,181,182]. In addition, the counter ions may play a role in the stabilization of the mesostructure; hydration of the H^+ form of B-MCM-41 resulted in an easy extraction of framework boron, while the tetrahedral framework boron is stable when Na^+ and NH_4^+ are present as counter ions [181].

In order to modify the catalytic activity of the mesoporous materials, especially to create redox active sites, several other metal ions were incorporated into the silica framework or grafted on the surface. Similar to zeolites, the incorporation of transition metal ions, such as Ti, V, or Mn, could isolate these active centers and thus make them highly efficient. The catalytic behavior is strongly influenced by the nature, the local environment and the stability of the metal introduced, and by the hydrophobic properties of the surface. As discussed above, however, the materials may more resemble substituted amorphous silica than framework substituted zeolites with respect to their properties and catalytic performance.

Incorporation of Ti in mesoporous materials is generally achieved via a direct synthesis procedure which involves addition of a titanium source, such as titanium ethoxide ($Ti(OEt)_4$) in H_2O_2 or titanium isopropoxide ($Ti(OPr^i)_4$) in ethanol, to the gel for hydrothermal synthesis [183,184]. One of the problems in the preparation of substituted mesoporous silica with a homogeneous titanium distribution is due to the great reactivity differences between the usual Ti and Si precursor species, such as the alkoxides. Use of chelate reagents is one of the promising methods to circumvent this problem [185,186].

In order to create highly dispersed and isolated Ti-species, grafting is a viable alternative to direct synthesis. These systems were prepared for use in either oxidation catalysis or photocatalysis. Grafting of a titanium precursor such as titanocene dichloride [112,187] $TiCl_4$ [188,189], $Ti(OEt)_4$ [190], $Ti(OPr^i)_4$ [191,192], or tetrakis(dimethyl amido)titanium [191], and following post-treatment, such as calcination, provide highly dispersed Ti-species.

Titanium isopropoxide was grafted on SBA-15 with Si/Ti ratios between 80 and 5 with high dispersion [192]. The fraction of tetrahedral Ti measured by XPS decreased from 83% to 25% with increase of the Ti content. At Si/Ti of 5, the average number of Ti atoms per unit surface area is 2.4 Ti/nm^2. Compared to the value of 5.5 Ti/nm^2 for the (0 1 0) plane of anatase, the number suggests that the titanium does not form a complete "TiO_2" monolayer.

Deposition–precipitation is also effective to obtain highly dispersed titanium species [117]. The impregnation of a mixture of quaternary ammonium hydroxide and partially hydrolyzed tetrabutyl orthotitanate (TBOT) with SBA-15 or MCM-41, and following filtration, washing and calcination gave anatase-free mesoporous titanosilicates with Si/Ti ratios between 116 and 16. The role of the quaternary ammonium hydroxide is probably to promote the dispersion of the titanium species. However, the exact nature of the short alkyl groups did not strongly influence the result of the synthesis.

The template ion-exchange method is a new preparation technique for atomically isolated metal centers [193,194]. Ion exchange of alkylammonium cations present in as-synthesized MCM-41 against transition metal cations, and following calcination can provide evenly dispersed metal centers on the mesopore surface. Mn-MCM-41 synthesized this way has a higher activity for the catalytic epoxidation of aromatic olefins than Mn–SiO_2 and Mn-Al_2O_3 prepared by conventional impregnation methods, or than Mn-ion exchanged ZSM-5. It has been described that this method can be applied for the preparation of Ti- and V-modified mesoporous silica [195,196], but is not suitable for iron exchange [197].

Gas phase deposition of active elements is a promising technique, provided the precursors are volatile reagents [198–200]. The loading amount depends on the silanol number and not on the geometrical surface area [198]. The ^{51}V NMR and UV–vis spectroscopic studies revealed that VO_x centers were, in the absence of water, grafted in pseudotetrahedral co-ordination with $O_{3/2}V{=}O$ configuration by three Si–O–V bonds [199]. Most of the VO_x species are present as tetrahedrally co-ordinated oligomers with an average ensemble size of 5.6 after calcination. Grafting of VO_x structures on the mesoporous silica surface was also achieved using dimethyldichlorosilane (DMDCS) as a coupling agent [201–203]. Pure silica MCM-48 was first silylated using appropriate amounts of DMDCS, then hydrolyzed in water to create Si–O–$Si(CH_3)_2OH$ species on the surface. The silylated material was used to anchor $VO(acac)_2$, followed by calcination in air at 450 °C resulting in a hydrophobic material with an improved stability towards leaching and with the V^{5+} centers still accessible to water adsorption.

4.2. Highly dispersed metal-, metal oxide- or metal sulfide-nanoparticles

The deposition of catalytically active nanoparticles on support materials with high dispersion is an important and effective strategy for the design of catalysts. Ordered mesoporous materials with their intrinsically high surface areas are excellently suited for this purpose. Pore blockage is not a severe problem up to relatively high loading, since for many mesoporous materials the primary particle size is rather small and the pores thus short. Compared to other support materials, the ordered mesoporous solids have the advantage of stabilizing metal or metal oxide particles, since they cannot grow to sizes larger than the pore size unless they move to the external surface of the particles. Compared to the microporous solids with their narrow and well defined pores, they allow the access of bulky reagents.

Metal nanoparticles have been used in catalysis for many decades, since supported noble metal catalysts typically have noble metal particles sizes in the nanometer ranger. These materials have great potential as catalysts because of the large surface area and high fraction of atoms present at the surface of the particles which is the reaction site in heterogeneous catalysis [204]. Unfortunately, small particles are unstable with respect to agglomeration to the bulk material due to their high surface energies. In most cases, this agglomeration leads to the loss of the properties associated with the colloidal state of these metallic particles. Therefore, stabilization of nanoparticles is required which is typically brought about by a suitable support material.

Several pathways for depositing the active compound on mesoporous supports are available (Table 3). Direct inclusion of metal particle in the synthetic gel of mesoporous materials has been studied in the cases of Pt and Rh [205,206]. Junges et al. [205] reported a preparation of Pt/MCM-41 by adding different platinum precursors to the synthetic gel. The neutral Pt precursor $[Pt(NH_3)_2Cl_2]$ was found to be more suitable for the preparation of small particles compared to the cationic $[Pt(NH_3)_4](NO_3)_2$ or anionic $K_2[PtCl_6]$ species. Under neutral synthesis conditions, in the direct synthesis of Pt/MSU-1, anionic $(NH_4)_2PtCl_4$ was found to be preferable over cationic or neutral precursors [206].

The conventional methods, such as impregnation techniques, often yield nanoparticles of various sizes in the mesopores and on the external surface of the support materials. Yao et al. introduced a new technique designated as vacuum evaporation impregnation. The MCM-41 was suspended in an aqueous solution of $[Pt(NH_3)_4](NO_3)_2$ at pH 5, heated at 70 °C and the water was evaporated in vacuum. The obtained material shows a very high Pt dispersion (1.03) at a loading level of 1.3 wt%, measured by CO chemisorption [207]. The use of supercritical fluids, which have excellent properties such as low viscosity, high diffusivity and controllable solubility of dissolved species, are a novel method to overcome the limitations of conventional solvents [208]. Recently, the synthesis of Pt and Rh–Pt alloy particles supported on FSM-16 via supercritical CO_2 has been reported [209,210]. Incorporation of anionic precursor species into silica from aqueous solution is often difficult, since the silica surface itself is negatively charged at pH values above approximately 2. Yang et al. [211] have developed a method to invert the surface charge of silica by attaching a tetraalkylammonium ion to the silanol groups via a functionalized alkoxysilane. This group can be used as an anchor to create well distributed gold particles within the pores [212]. The catalysts show remarkable low temperature activity in low temperature CO oxidation, thus demonstrating, that no strong interaction of the gold particles with the support is necessary for this property [213].

Immobilization of polynuclear molecular transition metal complexes in porous materials is also a promising method for the preparation of supported metal cata-

Table 3
Preparation of mesoporous silica supported metal and metal carbonyl nanoparticles and their application for catalysis

	Preparation method	Catalysis	References
Pt	Inclusion in synthetic gel	CO oxidation	[205,206]
	Vacuum evaporation		[207]
	Super critical CO_2		[209]
	Ion exchange to positively charged trimethylalkyl ammonium functionalized surface, and reduction		[211]
	Ship-in-the-Bottle	Water–gas shift reaction, alkene hydrogenation	[216,217]
Ph (Rh–Pt)	Super critical CO_2	Butane hydrogenolysis to ethane	[210]
Au	Ion exchange to trimethylalkyl ammonium functional group, and reduction	CO oxidation	[213]
	Chemical vapor deposition	CO oxidation	[378]
Ru, Ru–Sn, Ru–Pt, Cu–Ru	Impregnation of carbonyl cluster together with organic counter cations	Hydrogenation	[218,219,221]
Pd	Vapor phase diffusion–deposition of $Pd(\eta\text{-}C_5H_5)(\eta^3\text{-}C_3H_5)$	Heck reaction	[369,370]
	Deposition–precipitation	Phenol hydrogenation	[435]
Pd, Au	Inclusion in synthetic gel/incipient wetness	CO oxidation	[379]
Co	Vapor phase diffusion–deposition of $Co_2(CO)_8$		[214]
Co, Co–Ru	Incipient wetness	CO hydrogenation, Fischer–Tropsch	[373–376]
Ni	Incipient wetness	Benzene hydrogenation	[377]

lysts, because fine tuning of the metal complexes in terms of electronic states and steric environment is substantially easier than with the metal salts used in the conventional catalyst preparation. Metal carbonyl complexes react with the surface silanol groups at elevated temperature. Continuous adsorption of $Co_2(CO)_8$ on MCM-41 in a flow reactor resulted in a maximum Co deposition of 20 wt%. The metal loading increased up to 41 wt% using the pulse deposition method [214,215].

Platinum carbonyl clusters like $[Pt_{15}(CO)_{30}](NR_4)_2$ or $[Pt_3(CO)_6]_5(NR_4)_2$ (R = methyl, ethyl, butyl, hexyl or methylviologen) can be successfully prepared in FSM-16 by the "Ship-in-the-Bottle" technique [216,217]. Careful evacuation leads to a desorption of the carbonyl groups, and the catalysts show remarkable catalytic activities for hydrogenation of ethene and 1,3-butadiene. A super-structure of ruthenium carbonyl clusters with anionic $[H_2Ru_{10}(CO)_{25}]^{2-}$ and the cationic PPN^+ (PPN^+ = bis(triphenylphosphane)iminium) ion, $[(C_6H_5)_3P{=}N{=}P(C_6H_5)_3]^+$, uniformly stacked throughout the MCM-41 mesopore, have been observed by HRTEM [218]. The distance of "rosary"-like black dots along the mesopores, the distance between which being ~2.95 nm, is consistent with the distance expected for clusters with two PPN^+ ions in a tilted arrangement in between. After careful removal of the carbonyl group and the organic counter cations, the obtained nanoparticles become less ordered, but still show hexene and cyclooctene hydrogenation activity.

Using mixed metal carbonyl clusters as starting materials has advantages for the production of efficient bimetallic nanoparticle catalysts. Good bimetallic hydrogenation catalysts based on MCM-41 supported Cu–Ru ($[Ru_{12}C_2Cu_4Cl_2(CO)_{32}][PPN]$) [219], Ru–Sn ($[PPN][Ru_6C(CO)_{16}SnCl_3]$) [220], Pt–Ru ($[Ph_4P]_2$-$[Ru_5PtC(CO)_{15}]$, $[PPN]_2[Ru_{10}Pt_2C_2(CO)_{28}]$) [221], have been reported by the group of Thomas and Johnson. The core structure of the bimetallic clusters changes dramatically after removal of carbonyl groups [222,223], however, these systems are good models to investigate the activity of bimetallic catalysts. For example, in the hydrogenation of benzoic acid with Ru_5Pt and $Ru_{10}Pt_2$ supported on MCM-41 [221], different activities are observed; $Ru_{10}Pt_2$ shows a higher activity and selectivity to cyclohexane carboxylic acid than Ru_5Pt. However, the Ru/Pt ratio of both catalysts is identical, but the structures differ. Such model systems are thus suitable to elucidate structure–activity relationships (Fig. 5).

Also many different metal oxides have been supported on ordered mesoporous materials. Other than in the examples discussed above in Section 4.1, we are dealing with extended oxide structures, even if the particles are very small. The borderline between surface grafted species and supported bulk oxides is certainly not well defined. However, in several cases even the XRD patterns of the supported oxide phase could be identified and one can definitely consider the material to be a supported oxide. SBA-15 loaded with ZrO_2 retains its mesostructure up to a calcination temperature of 1000 °C [224]. Tetragonal ZrO_2 is present in samples calcined above 900 °C, while the phase transformation from tetragonal to monoclinic normally takes place around 450 °C. This may be related to the small size of zirconia present in the mesoporous material, since it has been shown that also small size zirconia particles precipitated from solution have transition temperatures of up to 900 °C [225]. The tetragonal ZrO_2 in the SBA-15 mesopores shows about three times higher capacity for sulfate adsorption than bulk ZrO_2 [226]. Iron oxide has been deposited on MCM-41 and MCM-48 by the

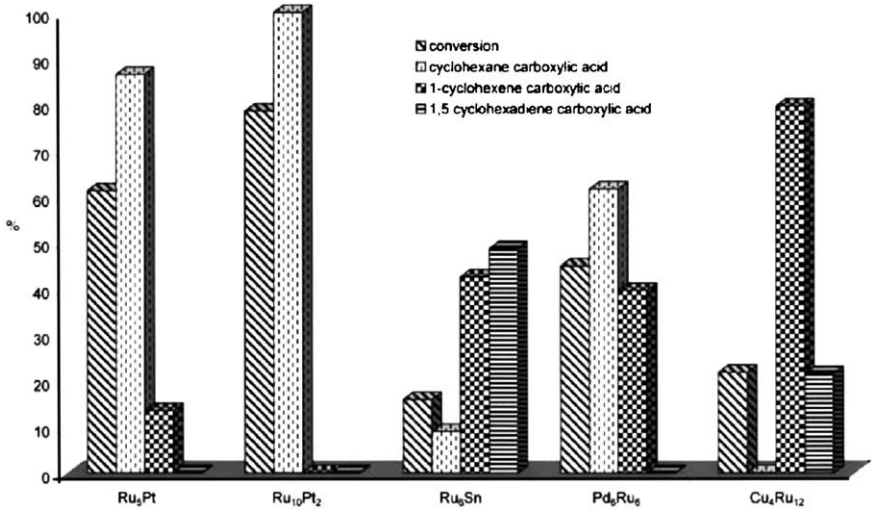

Fig. 5. Relative performances and selectivities of the Ru_5Pt and $Ru_{10}Pt_2$ catalysts in MCM-41 compared to other bimetallic nanocatalysts for the hydrogenation of benzoic acid. Benzoic acid 2.5 g (dissolved in ≈75 ml of ethanol); 50 mg catalyst; 20 bar H_2; 373 K, 24 h [221].

incipient wetness technique [227–229]. The UV–vis spectroscopy results indicate that the band gap of the resulting iron oxide particles is widened from 2.1 to 4.1 eV, depending on the pore diameter of the mesoporous silica used [227,228]. MCM-41 supported γ-Fe_2O_3 prepared by vapor-phase deposition with $Fe(CO)_5$ as precursor exhibits a superparamagnetic behavior [230]. The magnetization of Fe_2O_3 increased when the sample was calcined at high temperature, although partial phase transformation from γ- to α-Fe_2O_3 was observed.

Many other elements are directly or indirectly incorporated in the structure of mesoporous materials. Cu(II) acetate dimer was impregnated on MCM-48 from copper acetate solution [231]. The ESR spectrum of the dried sample suggests the presence of dimer species but not of the monomer. The Mn_{12} oxocluster, $[Mn_{12}O_{12}(O_2CR)_{16}(H_2O)_4]$ (R=CH_3, CH_3CH_2), can be incorporated in the channel system of MCM-41 with a pore diameter of 2.58 nm under reflux [232]. Small differences of magnetic properties were observable in the resultant composite as compared to the microcrystalline unsupported cluster. The difference was attributed to a partial substitution of carboxylate groups of the cluster with silanol groups of MCM-41. Basic and amphoteric oxides, such as MgO, Cs_2O, Ga_2O_3 and In_2O_3 supported on mesoporous materials can also be prepared by impregnation of suitable precursor such as cesium acetate or gallium nitrate, and following calcination [233–236]. On the basis of CO_2 temperature programmed desorption (TPD) measurements, it was inferred that the Cs_2O loaded Al-MCM-41 has a higher amount and stronger basic sites than Al-MCM-41 ion exchanged with Cs^+ [233]. Nitrogen sorption studies revealed that the framework of Al-MCM-41 collapsed with increasing Cs_2O loading level. The framework of Al-MCM-41 with high Si/Al ratio is more stable, because the collapse of the framework is rather a result of breaking of the Si–O–Si bonds than that of the Si–O–Al ones [237]. Ga_2O_3 or In_2O_3 supported on MCM-41 show catalytic activity in Michael addition of diethyl malonate to neopentyl glycol diacrylate [233] or Friedel–Crafts type benzene benzoylation and acylation [235] reactions. Highly dispersed rare earth oxides on SBA-15 were reported recently (Fig. 6) [238]. TEM images, nitrogen sorption measurements, XRD and IR measurements support the notion of a thin layer coating of the SBA-15 surface. Such mesoporous silicas thinly coated with another oxide might give access to a wide range of materials with different surface properties, but the high surface area of ordered mesoporous silica.

Because of the lowering of the formation temperature when the citrate method is used, $LaCoO_3$ nanoparticles can be crystallized in the mesopores of ordered mesoporous silica (pore diameter 3.4 nm) [239]. Catalysts with a high dispersion of the oxide show good methane oxidation activity, although diffusion limitations were observable in the high loading case.

Inclusion of nanocrystals of well-defined catalytic phases is another option for the design of supported oxide catalyst. Zeolite seeds [170–172], as mentioned above, and polyoxometalates [240–244], for example, have been supported on mesoporous silica. Although polyoxometalates, especially 12-tungstophosphoric acid ($H_3PW_{12}O_{40}$), provides strong acidity, the polyoxometalates normally have a low surface area in the solid state and therefore, only a limited number of acid sites on the external surface are available for the catalytic reactions [245–247]. Mesoporous silica provides an excellent support for the dispersion of heteropoly acids [242–244]. Isopolyanions such as $W_{10}O_{32}^{4-}$ [248] $Mo_7O_{24}^{6-}$ [249–251] and the Al_{13}^{7+} Keggin cation [111], which are all defined

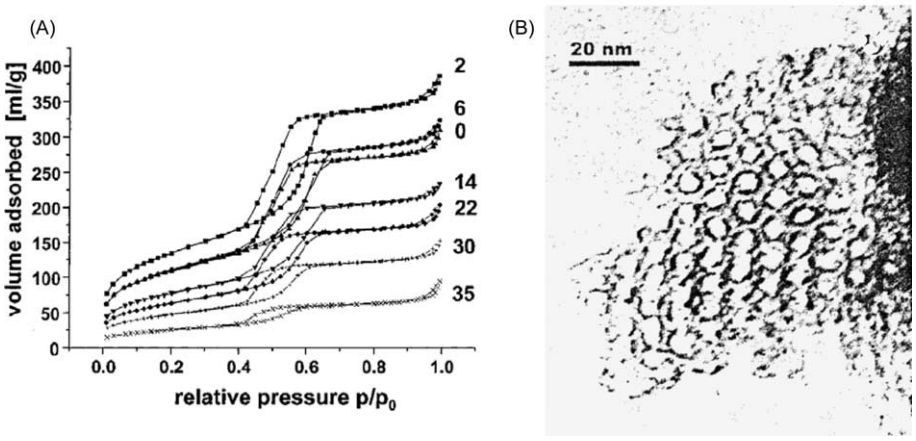

Fig. 6. (A) N_2 sorption isotherms of SBA-15 supported europium doped Y_2O_3 with different rare earth contents (given in the figure as wt%). The hysteresis loop of the capillary condensation step is shifted to lower relative pressure without being substantially widened. (B) TEM images of SBA-15 supported europium-doped Y_2O_3 viewed parallel to the channel axis. The Eu:Y_2O_3 content is 28 wt% [238].

metal oxide clusters, can be regarded as excellent precursors for supported oxides.

Tetrahedrally co-ordinated titanium is a good catalyst for alkene oxidation. Immobilization of the titanium silsesquioxane, $[\{(c\text{-}C_6H_{11})_7Si_7O_{12}\}Ti(\eta^5\text{-}C_5H_5)]$, in MCM-41 has been reported [252]. In the heterogenized state this silsesquioxane shows good cyclooctene epoxidation activity using TBHP as an oxidant. However, undesired leaching of this component was observed under reaction conditions. The leaching can be completely stopped when MCM-41 was treated with the silylating agent $SiCl_2Ph_2$ prior to the catalytic reaction.

Not only loading of ordered mesoporous solids with metals or metal oxides but also with chalcogenides is successful. MCM-41 supported MoS_2 was prepared by incipient wetness impregnation with $(NH_4)_2MoS_4$, followed by in situ activation under H_2/H_2S gas at 350 °C, which resulted in a good catalyst for hydrodesulfurization (HDS) of dibenzothiophene [253]. Ultrasonic treatment of a mixture of SBA-15, elemental sulfur and $W(CO)_6$ in diphenylmethane can introduce amorphous WS_2 into the mesopores of SBA-15 [119]. Following sulfidation of the composite with dimethyldisulfide in toluene under hydrogen flow at 320 °C gave an active HDS catalyst. Nitrogen sorption and high-resolution TEM measurements revealed that WS_2 is occluded in the mesopores in form of crystalline nanoslabs (Fig. 7).

4.3. Anchoring of molecular catalysts to the surface

Since heterogenized molecular catalysts are considerably easier to handle, retrieve, and re-cycle than their homogeneous counterparts, immobilization of homogeneous catalysts on solid supports is of high commercial interest. Ordered mesoporous silica has often been used for immobilization of molecular catalysts due to the high surface area. Often, immobilized catalysts suffer from reduced activity upon immobilization, but occasionally, the catalytic performance might improve as compared to the homogeneous case [254,255]. Immobilized $Mn(bpy)_2^{2+}$ (bpy = 2,2′-bipyridine), for example, exhibits a higher catalytic activity in terms of peroxide oxidation activity and selectivity for styrene oxidation than the corresponding homogeneous catalyst [177].

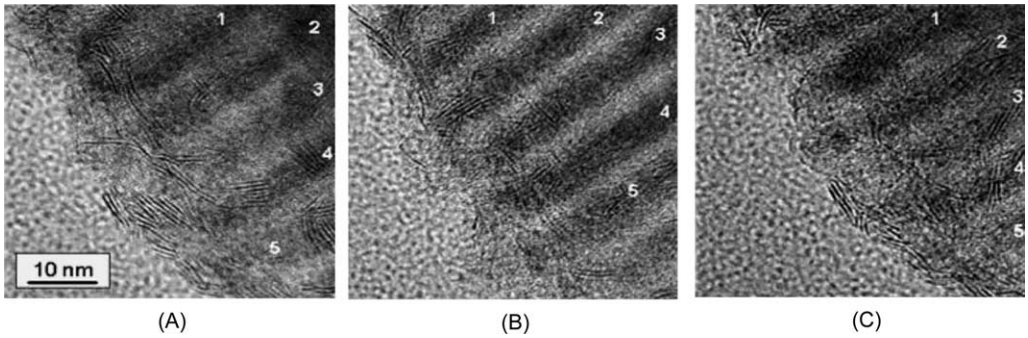

Fig. 7. TEM pictures of the 60 wt% WS_2/SBA-15 prepared via an ultrasonic treatment method. Various planes of WS_2 nanoslabs with different orientations were observed depending on the tilt of the samples in the TEM. (A) −10°; (B) 0°; (C) +10°. The same mesopore is marked by the same number (1–5) [119].

This is due to the fact that $Mn(bpy)_2^{2+}$ easily forms a dimer and in this state preferentially decomposes peroxide rather than oxidize any substrate. The effective isolation of catalytic centers in an immobilized catalyst prevents this dimerization. This effect has not only been observed for mesoporous silicas, but also isolation of $Mn(bpy)_2^{2+}$ in zeolite cages improves the activity of this system, as reported by Knops-Gerrits et al. [254].

The standard reactions used for the surface modification of silica, i.e. reaction with various functional silanes, can be used also to modify the surface of ordered mesoporous silica. However, one has to keep in mind the possible limitations arising from the lower concentration of silanol groups on the surface (see above). Excellent surveys over the methods to create different functional groups on the surface which can be used for the anchoring of other species can be found in several recent reviews [22,26,105,108].

In the simplest case, the molecular catalysts can just be adsorbed on the silica surface [252,256–258]. Bianchini et al. [259,260] reported the immobilization of a rhodium phosphine complex, e.g. (sulfos)Rh(cod) (sulfos = $^{-}O_3S(C_6H_4)CH_2C(CH_3PPh_2)_3$; cod = cycloocta-1,5-diene), on amorphous silica which occurs via hydrogen bonding between the sulfonate tail of the ligand functional group and the surface silanol groups (Scheme 1). The IR, Rh K-edge EXAFS and CP MAS ^{31}P NMR studies support the existence of an interaction between complex and silica surface. However, since the interaction is normally relatively weak in these cases, leaching easily occurs if polar or protic solvents such as methanol or ethanol are used.

The leaching problem is most frequently encountered for incorporated enzymes. The large pore sizes and the open-pore structure of mesoporous materials, as compared to conventional amorphous silica encapsulated enzyme, allow the loading of enzyme into the pores with free access of substrates [261–264]. However, it appears that the open-pore structure of mesoporous silica leads to easy leaching of the encapsulated enzyme. In order to minimize leaching, suitable polarity of solvent or a close fitting of the enzyme to the pore in order to maximize the van der Waals interaction are required [261,264,265]. Silylation to partially close the channels of mesoporous silica is one of the methods to prevent leaching [261]. Functionalization of the mesopore surface with carboxylic acid, thiol or amine groups etc. can change the surface polarity and improve the immobilization [263,266].

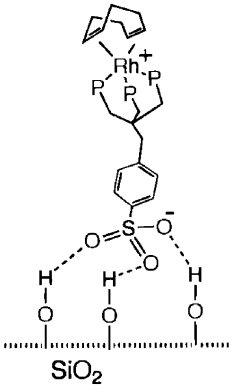

Scheme 1.

However, even if leaching can be reduced by one of the methods discussed above, it may still pose a serious problem if solvents are present in which the immobilized species is readily dissolved [256,257]. Therefore, often a co-valently attached anchor group is used to immobilize the molecular catalyst in the pore system. Fig. 8 gives a sketch of the more frequently used anchor groups which have been reported for the immobilization of molecular catalysts. Functional alkoxysilanes are favored for this purpose. These precursors are readily commercially available with different functional groups, such as alkylamine or alkylthiol, which can be further functionalized to provide optimal binding to the silica surface. One should keep in mind that for immobilized molecular catalysts, the selectivity for a certain product might change depending on the length of the tether [267,268] or specific functional group integrated in the tether [269].

Attachment of the molecular catalyst can be achieved via a wide variety of methods, following two principally different approaches. Either first ligands for the metal are immobilized with which the metal is reacted in a subsequent step, or the surface functional group is provided

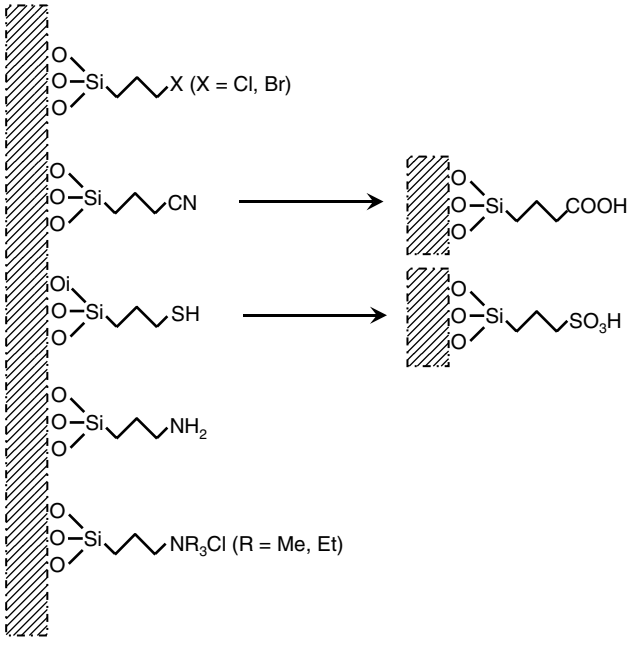

Fig. 8. Sketch of frequently used functionalized alkylsilanes for anchoring molecular catalysts. These functional groups can also be used as active sites in adsorbents or catalysts by themselves.

with a chemical function which reacts with a ligand side group to provide the bond of the complex to the surface. An example for the anchoring of an enantioselective palladium catalyst has been reported by Johnson and Raynor et al. [270] (Fig. 9). Following the first strategy (pathway (A)), a phosphine modified ferrocene was attached to the surface of the silica via an alkoxysilane, then reaction with $PdCl_2$ resulted in the formation of the catalyst, with the Pd co-ordinated to two chloride and the two phosphine ligands. Alternatively, as an example for the second strategy (pathway (B)), a silane functionalized ferrocene ligand could be synthesized including $PdCl_2$ anchored to the grafting reagent [271]. The palladium phosphine was then loaded into the mesoporous MCM-41. These methods should produce the same active site, although the reactivity may slightly differ. From the viewpoint of characterization of the catalysts prepared, the latter approach is preferable because the active site can be analyzed before linkage (assuming that it is not destroyed upon linking).

A particularly useful route for the surface modification of ordered mesoporous silica is the silylamide route introduced by Anwander [272–275]. This route allows to anchor a metal complex to the surface and simultaneously caps all remaining silanol groups by reaction with the silylamines formed in the immobilization reaction (Fig. 10). Following ligand exchange of the resultant silylamide–MCM complex with various ligands, such as fod (1,1,1,2,2,3,3-heptafluoro-7,7-dimethyl-4,6-octanedionate), provides highly dispersed metal centers possessing stable Si–O–metal linkages. Because of the steric hindrance between pore wall and bulky ligand, an immobilized catalyst, yittrium-fod for example, had an increased diastereoselectivity in the Diels–Alder-cyclization of *trans*-1-methoxy-3-trimethylsilyloxy-1,3-butadiene with benzaldehyde of 70% instead of the 41% observed for the free catalyst [273,275].

While the better separability is a good incentive for immobilization of molecular catalysts, it is even more rewarding, if the immobilized systems have an improved activity, regio- or enantioselectivity compared to the homogeneous counterparts. Such improvements have been observed, and the enhancement of selectivity might be explained by the steric constraints which the support with the uniform mesopores imposes on the catalytically active species; the reaction must take place in the restricted space between catalytic center(s), chiral ligand group and the pore walls (Fig. 11) [276]. The confinement of the substrate in the mesoporous channel could then lead to a larger influence of the chiral directing group on the orientation of the substrate relative to the reactive catalytic center when compared to the

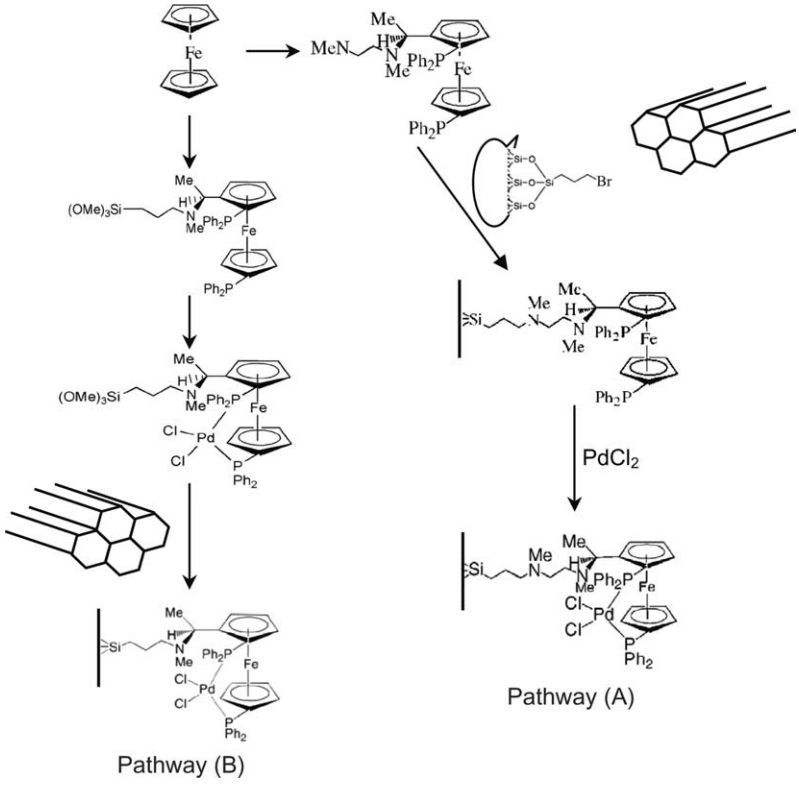

Fig. 9. Schematic sketch of the synthetic routes for immobilizing Pd-1,1′-bis(diphenylphosphino) ferrocene. (A) Phosphine modified ferrocene is attached to bromopropyl silane which was previously grafted to the mesopore surface, then the active center, $PdCl_2$ is complexed with the phosphine groups. (B) Silane modified ferrocene ligand, including the Pd center, is first prepared and then grafted to the silica surface [270,271].

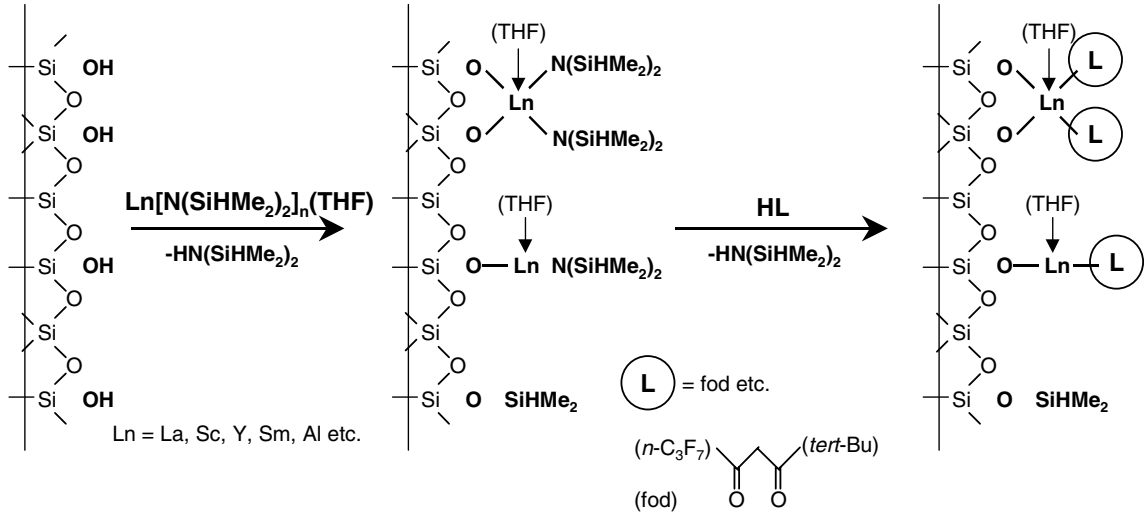

Fig. 10. Schematic sketch of the silylamide route. Lewis acidic elements, such as aluminum or lanthanoids, are immobilized with simultaneous surface silylation. Subsequent ligand exchange (e.g. fod) releases the silylamine and activates the catalytic center [272–275].

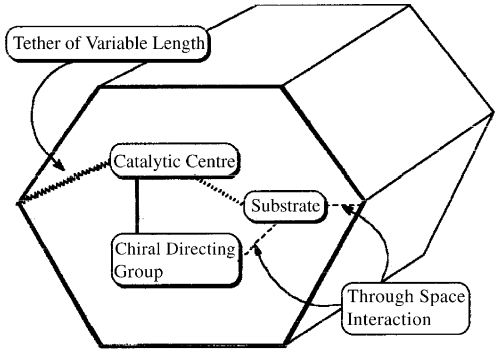

Fig. 11. Schematic representation of the confinement concept [276].

situation in the homogeneous reaction [276]. For example, in the allylic amination of cinnamyl acetate and benzylamine, the Pd(II)-1,1′-bis(diphenylphosphino) ferrocene tethered to mesoporous silica (Fig. 9, pathway (A)) produces a branched product with 51% selectivity, while the selectivity in the homogeneous case and a catalyst linked to amorphous silica are close to zero and 2%, respectively (Scheme 2) [270]. In addition, the enantioselectivity of the catalyst immobilized on ordered mesoporous silica is dramatically changed from 43% on amorphous silica to close to 100%. These results with an MCM-41 supported catalyst show that a significant improvement in regio- and enantioselectivity can occur, which is attributed to the spatial restrictions imposed by the mesopore. A similar pore confinement effect has been proposed not only for mesoporous silica but also for zeolite (USY) supported organometallic catalysts [277]. Careful control of pore diameter as well as design of active centers will be necessary to develop other effective solid catalysts which use confinement effects to improve the performance of molecular catalysts.

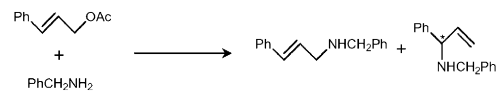

Catalyst*	Conversion (%)	Regio selectivity (%) (straight chain)	(branched)	ee (%)
homogeneous (S)	76	99+	-	-
amorphous silica (S)	98	98	2	43
MCM-41 (S)	99+	49	51	99+
MCM-41 (R)	99+	50	50	93

*Symbols in parentheses denote chirality of the directing group.

Scheme 2.

4.4. Fully non-siliceous materials

The discovery that surfactant micelles can be used for the templating of ordered mesoporous materials also opened up routes for new synthetic strategies in the preparation of various other oxides with high surface area and ordered pore systems [16,23,24,30,278]. Mesoporous materials composed of transition metal oxides are attractive solid catalysts, catalyst supports and host materials for nanocomposites. Unfortunately, thermal stabilities of these obtained mesoporous materials are in many cases less satisfactory than for silica. The incomplete condensation of the inorganic framework, change of the valence and/or co-ordination state of the wall component during calcination, as well as thin wall thickness and re-crystallization of the oxide forming the walls, are the reasons for this low thermal stability. Nevertheless, many different non-silica materials have been synthesized over the last ten years, treated in more detail in several reviews [16,24,30,278]. If the as-synthesized material is not stable towards calcination as it is, post-synthesis stabilization, for instance with phosphoric acid, which is successful in the case of aluminum [279], titanium [53] and zirconium [280], provides the

additional condensation necessary to produce a material which can be calcined.

If a block co-polymer is used as template, products with relatively thick walls are formed which helps to solve some of the problems mentioned above [64,65,281]. Re-crystallization, for instance, is less of a problem, since the walls are sufficiently thick to accommodate crystalline oxide nanoparticles. A whole series of different oxides, some with amorphous walls, some with crystalline walls, could be synthesized following the synthesis procedure developed first for SBA-15. For the synthesis of non-silica compositions, typically metal chlorides are reacted in alcoholic solutions in the presence of triblock co-polymer templates [64,65].

Several reports of the synthesis of non-silica mesoporous materials have been published, together with catalysis results. For example, vanadium incorporated mesoporous titania was used for propene oxidation [282]. It was found that the rate of CO and CO_2 formation was 1.7 and 5.0 times higher than that measured over vanadium impregnated commercial TiO_2. Methanol decomposition over Pd supported on mesoporous titanium oxide has also been investigated [283]. The activity of this catalyst was also higher than over Pd supported on commercial titanium oxide.

The "one-pot" co-condensation reaction of differently functionalized alkoxysilanes in the presence of a templating reagent is an alternative route in the preparation of organic–inorganic hybrid materials. Although one does not obtain materials with a framework consisting completely of non-silica elements, the materials can have remarkable properties, which justify to specifically mention these materials. Many organosilane reagents such as alkyltrialkoxysilanes ($RSi(OEt)_3$), or especially silsesquioxanes with bridging organic groups, such as $(EtO)_3Si–R–Si(OEt)_3$ with R = methylene, ethylene, phenylene, vinylene, or benzene are used [102–104,284–286]. Using 3-aminopropyltrialkoxysilane as a co-precursor, Macquarrie prepared HMS type mesoporous silica with pendant 3-aminopropyl chains in the mesopores [103]. After solvent extraction of the templating agent, this aminopropylated mesoporous silica was used as a base catalyst in the Knoevenagel condensation of aldehydes and ketones with ethyl cyanoacetate. In terms of the turnover number, estimated from the number of mole of products and that of the NH_2 group attached, compared to aminopropyl functionalized amorphous SiO_2, significant improvements were observed in hybrid mesoporous silica [284]. The organic group implanted in the pore walls can be functionalized by post-treatment. For example, Inagaki et al. [286] reported the sulfonation of benzene–silica hybrid mesoporous material. In these materials the benzene moieties are fully incorporated in the walls as integral parts of the wall structure ($O_3{\equiv}Si–C_6H_4–Si{\equiv}O_3$). Treatment with 25% SO_3/H_2SO_4 solution gave a sulfonic acid-functionalized mesoporous material. The resultant sulfonated materials were stable up to 500 °C in air or nitrogen. It was also possible to substitute framework Si with Ti in these inorganic–organic nanocomposites [115,287,288]. Bhaumik and Tatsumi [115,287] synthesized methyl-, vinyl-, allyl-, 3-chloropropyl-, pentyl-, and phenyl-modified mesoporous titanosilicates from mixtures of TEOS, organotriethoxysilane, TBOT, CTAB, tetramethylammonium hydroxide (TMAOH), and H_2O. The efficiency of Ti incorporation is higher when organosilane is used as Si source in conjunction with TEOS instead of TEOS alone. The highest Ti incorporation was achieved with a Si/Ti ratio of 38.9 in 3-chloropropyl modified material, with large pores and high surface area (1218 m^2/g).

Interesting non-silica materials can be synthesized, if the siliceous ordered mesoporous materials are used as hard templates in a nanocasting process (Fig. 1). This method was especially useful for the synthesis of a new class of mesoporous platinum and carbon [36,289–292]. After loading platinum or carbon in mesoporous silica and following dissolution of the silica mold with HF or NaOH solution, mesoporous Pt or carbon materials with the negative replica structure of MCM-41 [293], MCM-48 [294,295], or SBA-15 [66,68,69] could be obtained. A second nanocasting step, in which these ordered carbon materials are filled with an inorganic precursor, and following removal of the carbon template results in the formation of a direct replica porous material of the original mold [37,93,296]. Although this double replication for silica is inefficient because the properties of the final product are not drastically different from the starting material, some differences to the texture and structure of the original silica may exist, such as a different fraction of micropores in the materials [94]. It may be valuable, though, for other compositions that are more difficult to synthesize directly via surfactant-based pathways. Very recently, on the other hand, ordered mesoporous transition metal oxides such as CeO_2, Cr_2O_3, NiO, OsO_4, Co_3O_4 or In_2O_3 were reported, using SBA-15 as a template [86–92]. The negative replica structure of these transition metal oxides obtained from the SBA-15 original is restricted with respect to pore size engineering. Nevertheless, functional materials may be accessible via this route, and also backcasting from such materials can be envisioned.

Mesoporous materials with zeolitic microporous walls have already been described. In addition to the pathways described in this connection, using carbon as a meso/macropore template is another possibility to create bimodal zeolite monoliths. Jacobsen et al. [297] impregnated fine carbon black particles having average particle diameters of 12 nm with a zeolite synthesis gel. After hydrothermal treatment to crystallize ZSM-5, the carbon particles were removed by calcination. The pores created by combustion of carbon particles resulted

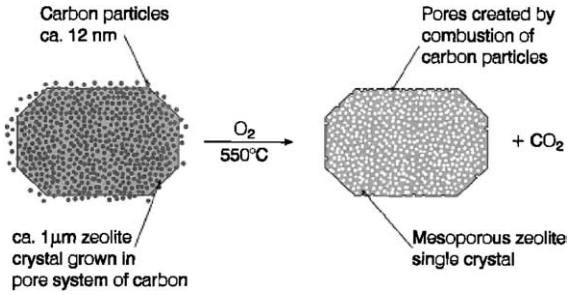

Scheme 3.

in the formation of mesopores in the zeolite crystals (Scheme 3). Also crystallization of MFI type zeolites in the presence of carbon nanofibers induced the formation of a mesopore system in zeolite single crystals [6]. Tao et al. used mesoporous carbon aerogel as a mold for ZSM-5 particle growth [298].

It should be mentioned at the end of this section, that 3D meso- or macroporous materials can be prepared by Latex spheres as template [299,300]. Not only silica but also many kinds of non-silica porous materials, such as TiO_2, ZrO_2, Al_2O_3, Fe_2O_3, WO_3 and MgO, which are useful for catalysis or as catalyst supports, has been reported [301,302]. Macroporous vanadyl pyrophosphate having $(VO)_2P_2O_7$ crystals in its wall has been reported, although the catalytic activity of these VPO type materials is not clear [303,304]. 3D macroporous materials having the MFI zeolite structure in the walls are also accessible by using Latex spheres [137]. The small wall thickness of these zeolite monoliths is expected to improve the reaction efficiency because of the short diffusion path. Such an effect has been reported by Christensen et al. [305], an improved selectivity to ethylbenzene in benzene alkylation over a mesoporous zeolite as compared with conventional zeolite particles.

5. Catalysis

5.1. Highly dispersed active sites — as an extension of microporous zeolite catalysts

Possibly the greatest hope in the initial phase of research on ordered mesoporous materials was their expected use in FCC catalysis. In this respect, substantial efforts have focused on the potential activity of Al-MCM-41 in processing bulky hydrocarbon molecules. However, their relatively low hydrothermal stability and the relatively low acid strength limit their suitability in this field. In other reactions that require milder acidity and also involve bulky reactants and products, such as mild hydrocracking reactions, however, mesoporous materials exhibit great potential [15]. Furthermore, one of the most important features of ordered mesoporous oxides is their exceptionally high surface area. This can be exploited to create highly dispersed active species on interacting and non-interacting support materials. Ordered mesoporous oxides have been used as supports for metals, metal oxides and as a host material for anchoring stereo- and enantioselective species, such a certain molecular catalysts.

In the following, we will focus on catalytic examples which exploit the possible high dispersion of the active site, such as in framework substituted materials, by supported metals or metal oxides, or grafted molecular species. Mesoporous materials with narrow pore size distribution may in future replace zeolite catalysts in some commercial applications, and in many research applications they already now have a comparable and superior performance compared to conventional microporous zeolites or amorphous silica–alumina catalysts, although it is not always clear that the right zeolite catalyst had been chosen as a benchmark. The early part of the following section presents some interesting developments in acid–base and redox catalysis over ordered mesoporous materials. In the later part we will mainly focus on metal or metal oxide supported catalysts and grafted molecular species.

5.1.1. Acid catalysis

5.1.1.1. Cracking and other petrochemical conversions. Mesoporous materials have been extensively investigated with regard to their use in cracking and hydrocracking reactions. The patent literature contains many examples, but cannot be reviewed in detail here. Many references to the early patent literature, however, can be found in the review given by Corma [15]. Unfortunately, the disadvantages of low acid strength and low hydrothermal stability of MCM-41 catalysts are a counterbalance to the advantage of the accessibility of the pores even for larger molecules. Nevertheless, MCM-41 catalysts show substantial cracking activity for bulky substances such as palm oil and asphaltene [306,307]. FSM-16 analogous mesoporous silicas are active in the thermal degradation of polyethylene to fuel oil [308]. The initial rate of degradation was as fast as over amorphous silica–alumina and the yield of liquid products was higher.

For small molecules, such as 1-butene, *n*-hexane, *n*-heptane or small cyclic hydrocarbons such as tetralin and decaline, the cracking activity of MCM-41 is much lower than that of USY or Beta zeolites, and similar to that of amorphous silica–alumina [154,309–313]. In addition, steam treatment, which was used as a way to simulate fluidized catalytic cracking, results in a collapse of the mesopore structure and a decrease in activity far below that of steam-treated aluminosilicate [312]. The perspectives of the materials in FCC applications thus seem to be limited.

There is also the possibility to induce activity in acid catalyzed reactions by suitable modification of silica or

aluminosilicate MCM-41. Sulfated ZrO_2 supported on MCM-41 shows comparable activity with bulk sulfated ZrO_2 catalyst in both cumene and 1,3,5-triisopropylbenzene cracking [314]. Catalyst deactivation was slower for the supported catalyst compared to bulk sulfated ZrO_2. In the condensation of *tert*-butanol and methanol over sulfated tetragonal ZrO_2 supported on SBA-15, the supported catalyst showed about 2 times higher yield of MTBE than bulk zirconia [226]. ZrO_2/SBA-15 also shows high activity in dehydration of 2-propanol, the conversion of 2-propanol were 9.2% and 13.2% at 48 and 60 wt% loading, respectively, whereas that of bulk zirconia was only up to about 6%. Also heteropoly acids can be supported on MCM-41 type materials. The catalytic activity of MCM-41 ($S_{BET} = 939\,m^2/g$, $V_p = 0.60\,cm^3/g$, $D_p = 2.60\,nm$), supported heteropoly acid, $H_3PW_{12}O_{40}$, in the cracking of 1,3,5-triisopropylbenzene initially increased with increasing heteropoly acid loading, and reached a maximum at around 23 wt% loading [243]. The high dispersion of the heteropoly acid and its strong interaction with the MCM-41 surface is assumed to be the origin for the high catalytic activity. At higher loading level, the regular structure of MCM-41 was lost and the activity decreased to approach that of bulk heteropoly acid. Similar catalysts (33 wt% loading) are also active in liquid phase and vapor phase esterification reactions [242]. XRD and TEM studies on these materials revealed that the initially highly dispersed polyoxometalates became mobile and migrated to form large clusters (~10 nm) on the outer surface after reaction. Fluorinated MCM-41 ($S_{BET} = 1311\,m^2/g$, $Vp = 1.03\,cm^3/g$, $Dp = 3.14\,nm$) improves the stability for heteropoly acid loading and incorporates heteropoly acid up to 50 wt% [244]. The catalyst with 50 wt% loading shows an excellent gas-phase MTBE synthesis activity. The conversion of *tert*-butanol and the selectivity at 100 °C were 98% and 100%, respectively, which are comparable to a commercial Amberlyst-15. The strong Brønsted acid sites are attributed to the presence of small clusters of heteropoly acid.

Oligomerization of butene at 150 °C and 1.5–2 MPa has been investigated over zeolites, amorphous silica–alumina, and ordered mesoporous aluminosilicates. The mesoporous catalyst exhibited high selectivity and good stability with time for the production of branched dimers, while strongly adsorbed residue was formed over microporous zeolites and amorphous silica–alumina, and fast deactivation occurred over these materials [315]. In 1-hexene dimerization, monobranched C_{12} isomers are the main products, and the activity of Al-MCM-41 is very similar to that of amorphous silica–alumina [310]. Selectivity to cracking products of saturated C_6 compounds is very low as compared to US-Y or Beta zeolites.

The pore diameter of mesoporous materials is too large to expect any shape selectivity in conversions of small hydrocarbons [311]. Conversion of 1-butene over mesoporous materials increases with increasing aluminum content, while the selectivity for isobutene decreases. Ammonia TPD, IR analysis, and TG analysis were performed to confirm that the higher concentration of activated 1-butene molecules on the mesoporous material with high aluminum content accelerates the mutimolecular oligomerization, and, thus, reduces the selectivity. For very large substrates, however, one may expect shape selectivity in certain conversions. For example, in benzene alkylation with linear 1-olefins with a chain length of C_6 to C_{16} by $AlCl_3$-grafted MCM-41 (pore diameter of 3.34 nm), selectivity to mono-substituted alkyl benzene was increased and the formation of multi-substituted products was decreased with increasing alkyl chain length of the olefin (Table 5) [316]. If 1-octene is used as the alkylation agent, the selectivity to the monoalkylated benzene is increased with decrease of the mesopore diameter of the catalyst.

5.1.2. Acidlbase reactions for fine chemicals synthesis

Although the inherent weakness of the acid sites in mesoporous materials restricts their applicability in many petrochemical reactions, there still is potential for their use in reactions which require a lower level of acidity, such as the Friedel–Crafts alkylation of electron rich aromatic compounds (Table 4). In addition, the rather large pore openings of mesoporous materials offer the advantage of effective diffusion of bulky substances as they are often found in fine chemicals synthesis. One of the earliest examples is that of a Friedel–Crafts alkylation with mesoporous aluminosilicates. The Al-MCM-41 with a pore diameter of 3.0 nm is active in the Friedel–Crafts alkylation of 2,4-di-*tert*-butylphenol with cinnamyl alcohol. The following acid catalyzed intramolecular ring closing reaction gives dihydrobenzopyran [317]. The yield over Al-MCM-41 (35%) was much higher than over HY zeolite (<1%), suggesting that diffusion restrictions of the bulky 2,4-di-*tert*-butylphenol exist in the zeolite. Somewhat more effective than the unmodified HY zeolite was USY zeolite (mesopore diameter of 2.0–6.0 nm resulting from the ultrastabilization treatment). However, the selectivity is very low (9%) compared to Al-MCM-41 because the acid site concentration decreases by the dealumination process. Furthermore, Al-MCM-41 gave a much higher yield of dihydrobenzopyran than conventional catalysts, such as H_2SO_4 (12%) and amorphous silica–alumina (6%) catalysts. These results clearly indicate the potentials offered by mesoporous materials in fine chemical synthesis with bulky substrates.

The catalytic activity in the alkylation of unsubstituted phenol with methanol over Al-MCM-41, which had been modified by grafting of an alumina-multilayer, was up to 2.3 times higher than that of a reference alumina catalyst [161]. In the Friedel–Crafts alkylation of

Table 4
Example of fine chemical reactions catalyzed over mesoporous catalysts

Reaction	Mesoporous catalysts	Substrates	Reference
Friedel–Crafts alkylation	$Al(OPr^i)_3$ grafted	Phenol + methanol	[161]
	Ga-substituted/impregnated	Benzene + benzyl chloride	[182]
	Al-substituted	2,4-Di-*tert*-butylphenol + cinnamyl alcohol	[317]
	Fe-impregnated	Benzene + benzyl chloride	[318]
Acetalization	Siliceous/Al-substituted	Heptanal, 2-phenylpropanal, diphenylacetaldehyde + trimethyl orthoformate	[319]
	Al-substituted	Heptanal + methanol	[320]
	siliceous	Cyclohexanone + methanol	[321]
Diels–Alder	$Al(OPr^i)_3$ grafted	Cyclopentadiene + crotonaldehyde	[323]
	Zn^{2+}-ion exchanged	Cyclopentadiene + methylacrylate	[173]
Beckmann rearrangement	Al-substituted	Cyclohexanone oxime	[324]
Aldol condensation	Al-substituted	Heptanal + benzaldehyde (→jasminaldehyde)	[320]
Prins condensation	Sn-substituted	β-Pinene + paraformaldehyde	[325]
MPV-reduction	Zr(OPr), $Al(OPr^i)_3$-grafted	4-*tert*-butylcyclohexanone + 2-propanol	[163]
Metathesis	Siliceous	Propene	[326]
(Esterification)	Cs^+-ion exchanged	Triolein + glycerol	[329]
(Etherification)	Cs-impregnated	Glycerol	[236]

Table 5
Selectivities for the alkylation of benzene with 1-alkenes over homogeneous (free $AlCl_3$) and heterogeneous ($AlCl_3$-grafted MCM-41) catalysts [316]

Alkene	Catalyst[a]	Selectivity toward alkylbenzenes[b]		
		Mono-[c]	Di-	Tri-
1-Hexene	Homog.	58.6	31.1	10.3
	Heterog.	79.9	20.1	–
1-Octene	Homog.	66.0	24.3	9.7
	Heterog.	79.7	20.3	–
1-Decene	Homog.	68.5	22.5	9.0
	Heterog.	91.1	8.9	–
1-Dodecene	Homog.	72.5	27.5	[d]
	Heterog.	96.2	3.8	–
1-Tetradecene	Homog.	70.1	29.9	[d]
	Heterog.	98.5	1.5	–
1-Hexadecene	Homog.	77.5	22.5	[d]
	Heterog.	>99.0	<1.0	–

[a] Homog.: homogeneous catalysis with $AlCl_3$ (0.15 mmol); heterog.: over $AlCl_3$-MCM-41 (D_p = 3.34 nm, 0.15 g of catalyst containing 0.15 mmol of $AlCl_x$).
[b] Determined by GC of the product mixture.
[c] Exclusively linear alkyl benzenes.
[d] Nonvolatile product, not analyzed by GC.

benzene with benzyl chloride in liquid phase, Ga impregnated MCM-41 exhibited higher activity than Ga substituted MCM-41 [182]. In series consisting of Fe-impregnated MCM-41, Al-MCM-41, La-MCM-41, and Fe-USY zeolite in the same reaction, the Fe-impregnated MCM-41 showed the highest activity [318].

Acetalization is an important reaction for the protection of carbonyl functional groups. This reaction does not require strong acid sites, and therefore, mesoporous silicas with weak to intermediate acid site strength are suitable catalysts in this reaction [319,320]. For example, acetalization of heptanal, 2-phenylpropanal or diphenylacetaldehyde with trimethyl orthoformate was carried out over siliceous and Al-substituted MCM-41 on the one hand and different zeolite catalysts on the other [319]. Zeolite Beta and zeolite Y catalysts were found to be more active than mesoporous materials, but they deactivated more rapidly. There was no difference in activity between siliceous MCM-41 and Al-MCM-41, indicating that the bridging hydroxyl groups (Si–OH–Al) are of minor importance in this reaction and that probably silanol groups are sufficient for catalysis in this case. Furthermore, it was found that when the size of the reactant increased, mesoporous molecular sieves had clear advantages over the zeolites, as was observed in many other reactions discussed in this contribution.

Acetalization is one of the reaction steps to produce jasminaldehyde. Al-MCM-41 having uniform mesopores (around 3.5 nm) is suitable for carrying out the three consecutive reactions in *one-pot* to produce α-*n*-amylcinnamaldehyde (jasminaldehyde) in good yield [320]. The reaction involves (1) the acetalization of hept-

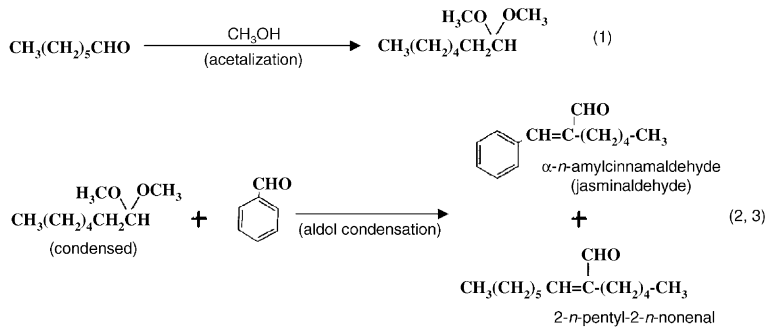

Scheme 4.

anal with methanol, (2) slow hydrolysis of the dimethylacetal, and (3) Aldol condensation of the two aldehydes (Scheme 4). From the comparison of several catalysts, including large pore zeolite (Beta) and mesoporous silica–alumina with various Si/Al ratios, it was concluded that a suitable catalysts should have mild acidity to avoid an excessive self-condensation of the aldehyde and undesired consecutive reaction. In addition, large and regular pores with a uniform pore diameter are also required, which enables fast diffusion of the products avoiding the side reactions.

Very recently, Iwamoto et al. [321] reported a pore size effect in the acetalization of cyclohexanone on MCM-41 (Fig. 12). The highest catalytic activity was obtained by MCM-41 with a pore diameter of 1.9 nm, and the reaction rate constant decreased when either narrower or wider pores were used. The high activity of the 1.9 nm pore size catalyst was attributed to the fact that the surface silanol groups are all oriented towards the center of pores, and they are thus assumed to work as an ensemble. Such an assembly might create very active sites for acid catalysis, the authors proposed. The decrease of activity in narrower pores was attributed to diffusion limitations. For wider pores, the co-operative action of different silanol groups is no longer operative.

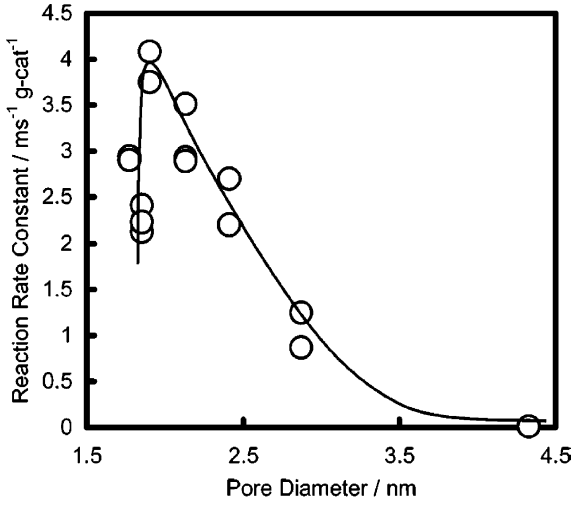

Fig. 12. Catalytic activity for the acetalization of cyclohexanone with methanol in dependence of the pore diameter of silica MCM-41 [321].

Aluminum substituted mesoporous silica exhibits better activity in Diels–Alder reactions with large organic molecules compared to conventional microporous zeolites (ZSM-5, HY) or ion exchange resins [322,323]. In the reaction of cyclopentadiene with crotonaldehyde, aluminum isopropoxide grafted MCM-41 shows the highest activity compared to directly prepared or template ion-exchanged Al-MCM-41. The activity increases with increasing amount of Al incorporated up to a level of Al/(Si + Al) = 0.04 mol/mol. Mesoporous aluminosilicate, ion-exchanged with $ZnCl_2$, was found to be effective in the Diels–Alder reaction of cyclopentadiene and methylacrylate [173]. The yield of products was as high as 90%, and the amount of polymerized side products was lower than with a homogeneous $BF_3 \cdot OEt_2$ Lewis catalyst. The mild acidity of the ordered mesoporous aluminosilicate is effectively used in these reactions.

The weak or intermediate strength acid sites are also effective for the Beckmann rearrangement of cyclohexanone oxime to give ε-caprolactam [324]. Mesoporous Al-MCM-41 exhibited higher activity and selectivity compared to amorphous silica–alumina in the vapor-phase reaction with 1-hexanol as a diluent.

Tin modified materials were found to be interesting catalysts for a number of important organic reactions. Sn-MCM-41 showed high activity in the Prins condensation of β-pinene and paraformaldehyde to nopol [325]. Conversion of β-pinene reached around 99% with good selectivity, whereas a reference amorphous silica catalyst only showed 37% conversion. No loss of activity was observed after five cycles.

The Meerwein–Ponndorf–Verley (MPV) reaction is a useful reduction of a carbonyl substrate with a secondary alcohol. Zirconium 1-propoxide grafted SBA-15 shows high activity in this reaction and the rate of reaction increased with increasing Zr loading level [163]. It seems that the pore system of the support material influences the catalytic activity. In the reduction of 4-*tert*-butylcyclohexanone with 2-propanol, the initial conversion

was in the order MCM-41 > MCM-48 > SBA-15. In addition, the selectivity to the corresponding *cis*-alcohol was increased with decrease of the mesopore diameter, suggesting a stereoselectivity due to the pore structure. A Zr-grafted SBA-15 had higher activity than $Al(OPr^i)_3$ grafted SBA-15, the conversion of the latter catalyst being about half of the former.

Siliceous mesoporous materials catalyze a propene photometathesis [326]. The relative activities of FSM-16, MCM-41, and amorphous silica, pre-evacuated at 800 °C under 133 mbar O_2, were roughly 4:2:1. The activity of each of the three catalysts increased with increasing the pre-treatment temperature in the range of 400–800 °C. The ESR and VUV–UV–vis spectra suggest the generation of nonbridging oxygen hole centers (NBOHC) during high temperature vacuum treatment. Therefore, the active center for this reaction was concluded to be a strained siloxane bridge [327,328].

Not many examples are known for base catalysis over modified ordered mesoporous materials (some more examples where grafted basic groups are used will be discussed below). Cesium ion exchanged Al-MCM-41 (Si/Al = 13) can catalyze transesterification reactions, such as the glycerolysis of triolein with glycerol, although bulk MgO or hydrotalcite which have higher basicity than Cs/Al-MCM-41 are more active [329]. Selective etherification of glycerol to obtain *di*- or *tri*-glycerol—these glycerol oligomers and their methyl esters are becoming more and more important in new products for surfactants, lubricants, cosmetics, food additives etc.—can be carried out over Cs-impregnated MCM-41 [236]. In La or Mg containing mesoporous catalysts, the glycerol dehydration to acrolein is very significant. Framework cerium substituted MCM-41 has an activity for vapor phase dehydration of cyclohexanol to cyclohexene [330].

5.1.3. Redox catalysis

There are numerous reports in the literature about redox reactions on framework modified ordered mesoporous materials or materials which had been altered by grafting of active species. In many cases it is very difficult to judge the performance of such materials, because the reaction conditions are often not comparable with each other and no proper benchmarks are analyzed.

Ti-zeolites, such as TS-1, TS-2, and Ti-β, are effective catalysts in the oxidation of a variety of organic compounds [331–333]. Such materials are known since the early 1980s. Ti containing mesoporous materials as well as those modified with early transition metals, such as Zr, V, Cr, Mn, or Fe, were expected to be promising oxidation catalysts as well. Titanium modified MCM-41 was therefore already very early in the research on ordered mesoporous materials studied as selective oxidation catalyst [184,334]. Such mesoporous materials present the clear advantage of a large pore system, enabling the oxidation of much larger hydrocarbons. Up to the discovery of modified ordered mesoporous materials, only Ti-β, a large pore zeolite, allowed relatively bulky peroxides to be used as oxidants and to process sterically demanding substrates.

Leaching is a particular problem of solid catalysts in liquid-phase processes, and especially in oxidation reactions with peroxides, which is attributed to the strong complexing and solvolytic properties of oxidants and products [335]. Significant Ti-leaching has been reported for the liquid-phase oxidation of crotylalcohol using Ti-β and Ti-MCM-41 (Table 6) [336]. Ti-leaching was ob-

Table 6
Oxidation of crotylalcohol with hydrogen peroxide and *tert*-butyl hydroperoxide at 50 °C[a] [336]

Catalyst	Oxidant	Time (h)	Crotylalcohol conversion (%)	Yield (%)			Ti-leaching (ppm)[b]
				Epoxide	Triol	Ether diols	
TS-1	H_2O_2	217.1	89.7	0	80.4	9.3	0.2
Ti–Alβ		189.6	87.9	0.8	70.7	16.4	26.8
Ti-β		168.9	23.7	7.7	10.1	5.9	7.9
Ti-MCM-41		1.7	0	0	0	0	2.9
		169.1	83.9	1.0	67.0	15.9	18.0
Cp_2TiCl_2-grafted MCM-41		1.4	3.6	3.6	0	0	8.3
		169.3	45.1	5.3	29.8	10.0	24.0
Ti–Al-MCM-41		62.3	10.5	5	0	10.5	4.7
		168.9	73.1	1.6	55.4	16.2	10.0
TS-1	TBHP	198	0	0	0	0	0
Ti–Alβ		104.7	63.2	0	54.8	8.4	1.3
Ti-β		194.1	10.3	10.3	0	0	3.0
Ti-MCM-41		48.0	1.6	1.6	0	0	n.a.
		191.7	3.4	3.4	0	0	2.0
Cp_2TiCl_2-grafted MCM-41		198	0	0	0	0	0
$TiCl_4$ grafted Al-MCM-41		198	0	0	0	0	0

[a] Reaction conditions: 0.1 g Catalyst; 0.72 g crotylalcohol, 1.35 g of 30 vol.% of H_2O_2, 50 °C. Titanium content of fresh catalyst used is in the range 0.940–2.206%. Caution, the amount of TBHP was not available in Ref. [336].

[b] Experimental error on ICP-MS analysis is ±0.5 ppm.

served in all samples with the exception of TS-1, and the order of leaching was Ti-Alβ > Cp_2TiCl_2-grafted MCM-41 > Ti-MCM-41 > Ti-Al-MCM-41 ≫ TS-1, when hydrogen peroxide was used as an oxidant. If hydrogen peroxide was replaced with *tert*-butyl hydroperoxide (TBHP) as an oxidant, Ti-leaching was minimized and the selective epoxide formation was observed with Ti-β and Ti-MCM-41.

Nevertheless, the advent of Ti-MCM-41 certainly widened the range of catalysts available for selective oxidation reactions with hydrogen peroxide or organic hydroperoxides as oxidants. When alkylhydroperoxides are used, a better hydrophobic interaction with the substrates, competing with water, is expected. Moreover, in Ti-MCM-41, the alkylhydroperoxide can easily penetrate the mesopore system, avoiding diffusion limitations or steric hindrance. For example, the oxidation of α-terpineol using TBHP as an oxidant, Ti-MCM-41 gave higher alkene conversion (62.2 mol%) and epoxide selectivity (30.2%) than Ti-β zeolite (32.7 and 12.8 mol%, respectively) [337].

Organically modified Ti-MCM-41 materials are even more efficient catalysts in epoxidation and oxidative cyclization using TBHP [115–117]. More hydrophobic materials exhibited high activity in catalytic epoxidation of unsaturated alcohols followed by cyclization to cyclic ethers. The oxidation activity increased extremely when TBHP was used instead of H_2O_2 [115]. This can be attributed to the preferred uptake of the reagents in the hydrophobic pore system.

The most active and selective sites in Ti-based epoxidation catalysts have isolated and 4-co-ordinated Ti(IV) centers. Aqueous synthesis conditions, however, for example direct synthesis of Ti-mesoporous materials, often promote the agglomeration of metal oxide species. Therefore, grafting of the active component with a precise structure and composition is in many cases superior. A site-isolated, mononuclear Ti catalyst has recently been reported by Jarupatrakorn and Tilley [143]. Different (*tert*-butoxy)siloxy titanium compounds, such as $Ti[OSi(O^tBu)_3]_4$ (denoted TiSi4), $(^iPrO)Ti[OSi(O^tBu)_3]_3$ (TiSi3) and $(^tBuO)_3TiOSi(O^tBu)_3$ (TiSi), were grafted on the surface of MCM-41 and SBA-15. The titanium species exist mainly in isolated and tetrahedrally co-ordinated environments, although TiSi4 shows low loading due to the low reactivity towards silanol groups. SBA-15 supported TiSi3 (0.25–1.77 wt% Ti loading) exhibits high activity in cyclohexene epoxidation; the yield of cyclohexene oxide, after 2 h, was 61% and 98% using TBHP or cumene hydroperoxide (CHP) as oxidant, respectively. Initial turnover frequencies decreased as Ti content increased, indicating that the more isolated sites are the most active ones. TiSi3/SBA-15 and TiSi3/MCM-41 catalysts, with a similar Ti loading, exhibit a higher activity than TiSi3/Aerosil, due to the high surface area and a greater dispersion of the Ti active centers.

Grafting of $Fe[OSi(O^tBu)_3]_3$ onto SBA-15, analogous to the titanium species mentioned above, gave isolated Fe centers [144]. The calcined Fe/SBA-15 catalysts obtained, in which only small amounts of octahedral Fe^{3+} were detected, showed good selectivity in oxidation reactions of alkanes, alkenes and arenes with H_2O_2 as an oxidant. When Fe/SBA-15 with 0.5 wt% Fe loading was used, benzene oxidation to phenol shows 7.5% of benzene conversion (corresponds to 42% conversion of H_2O_2) with close to 100% selectivity at 60 °C.

MCM-41 supported Mn catalysts, prepared by the template ion exchange method, shows high activity for the epoxidation of stilbene [194]. Gas-phase grafted Mn species provide higher activity in stilbene oxidation than impregnated Mn-MCM-41 when TBHP was used as an oxidant [200]. In contrast, Mn-impregnated MCM-41 showed higher activity than gas-phase grafted Mn-MCM-41 in diphenylmethane oxidation using air as an oxidant. The differences are attributed to the nature of the Mn centers: Isolated and electrophilic Mn species which are generated via gas-phase deposition are active for the oxygen transfer reaction in the stilbene oxidation, whereas bulky Mn oxides prepared via the impregnation method which has nucleophilic lattice oxygen is responsible for the hydrogen abstraction in diphenylmethane, the authors concluded [200].

Nb- or NbCo-substituted mesoporous MCM-41 are active in liquid phase oxidation of aromatic hydrocarbons such as styrene, benzene or toluene to benzaldehyde, phenol or benzalcohol, respectively, with H_2O_2 [338]. Liquid phase oxidation of cyclohexane with aqueous H_2O_2 or TBHP can be catalyzed by Fe [339], Cr [340], Co [341] and Mo [342] containing MCM-41. In the oxidation of cyclohexane with Mo-MCM-41 (Mo:0.05 wt%), the selectivity to cyclohexanol and cyclohexanone were 14.38 and 85.62 mol%, respectively [342]. The values are comparable to those for Ti-MCM-41 (0.06 wt%). The activity was slightly lower if post-impregnated Mo-MCM-41 catalysts were used. High catechol selectivity was observed in phenol oxidation with H_2O_2 over Cu-nitrate impregnated MCM-41, while Cu-acetate impregnated MCM-41 was selective to hydroquinone and benzoquinone [343].

Co-MCM-41 and Ni-MCM-41 are active for benzene or styrene oxidation in liquid phase to give phenol or benzaldehyde, respectively, with H_2O_2 as an oxidant [344,345]. Conversion, selectivity and efficiency of H_2O_2 are increased with increase of Co loading. Liquid phase hydroxylation of benzene to phenol by H_2O_2 was also studied for the case of MCM-41 supported VO_x catalysts, although the highest activity was obtained over the amorphous SiO_2 supported catalyst, i.e. the ordered mesoporous material did not have an advantage over amorphous silica [346]. The liquid phase oxidation of benzene to phenol can also be carried out with molecular oxygen. Cu-MCM-41 catalysts, synthesized by

impregnation and by ion exchange and then reduced with ascorbic acid, were more active than Cu supported on SiO_2, TiO_2, MgO, Na-ZSM-5, or K-L zeolite catalysts [347].

Sn(IV) containing MCM-41 has a good activity in the catalytic Bayer–Villiger oxidation which is normally carried out stoichiometrically with correspondingly high production of waste. In the oxidation of adamantanone, the conversion and selectivity to the corresponding lactone was 71% and 98%, respectively, when H_2O_2 was used as an oxidant [146,348]. However, the catalytic activity of Sn-β zeolite is even superior. No significant difference for catalytic activity was observed between the directly prepared and post-synthesis grafted Sn-MCM-41. Catalytic activity could be regenerated by calcination of the spent catalyst.

One of the big disadvantages of the hydroperoxide process for epoxidation reactions is the production of equimolar amounts of the co-product, *tert*-butanol or styrene, depending on which variant of hydroperoxide is used in the process. Direct olefin epoxidation in the vapor phase using both atoms of oxygen or in situ formation of (hydro)peroxy species from H_2/O_2 would be of tremendous industrial significance. Nitrate impregnation of Ti-MCM-41 improves the peroxide selectivity in the gas phase oxidation of propylene [349]. Homogeneously dispersed gold particles on Ti-MCM-41 and Ti-MCM-48 catalyze the vapor-phase epoxidation of propene using H_2/O_2-mixtures [350–353]. Initial conversion and propene oxide selectivity at 150 °C were 5.1% and 88% for Au/Ti-MCM-41 and 5.6% and 92% for Au–Ti/MCM-48, respectively, when a feed gas containing 10 vol% each C_3H_6, H_2 and O_2 diluted with Ar at a space velocity of 4000 $h^{-1}cm^{-3}$/g-catalyst was used [352]. From the theoretical prediction that the gold surface is capable of generating H_2O_2 [354], the authors have proposed a reaction mechanism as shown in Scheme 5 [352]. Hydrogen peroxide formed on the surface of gold (ii) would form hydroperoxo-like species on isolated tetrahedral titanium sites on Ti-MCM catalysts (iii). The resultant hydroperoxo-like species react with propene (iv), which have previously been adsorbed on the Ti-MCM (i), giving propylene oxide by the same mechanism as reported for the liquid-phase epoxidation of propene with H_2O_2. Silylation of mesoporous titanosilicate helps to improve propene oxide selectivity and H_2 efficiency due to an increase in the hydrophobicity [350,352]. Very recently, this group reported an enhanced activity in this reaction by use of 3D mesoporous titanosilicate supported gold catalyst [355]. Addition of 1 wt% of $Ba(NO_3)_2$ as a promoter to Au/titanosilicate catalyst (Au, 0.3–0.4 wt%; Ti, 3 mol%) improves an initial C_3H_6 conversion to 9.8% keeping a high PO selectivity (90.3%) under the same feed-gas condition at 160 °C. While the conversion decreases with time on stream, the activity of the catalyst in terms of space-time yield is in the range of 130–150 $g l^{-1} h^{-1}$. This enhanced activity by addition of $Ba(NO_3)_2$ is probably due to promoting the formation of hydroperoxide-like species from H_2 and O_2, as well as to lowering the acidity of the catalyst, the authors supposed. In addition, the larger pore size and 3D mesoporosity of the support, which allows easy diffusion of reactants and products, may also be responsible for this improvement.

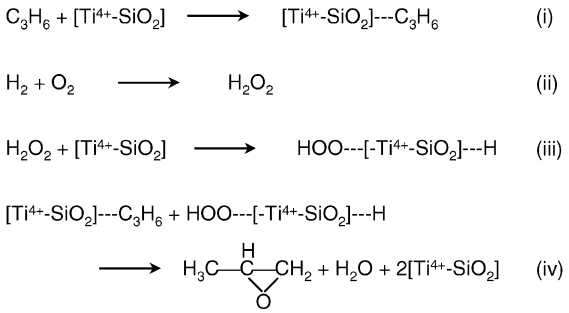

Scheme 5.

Oxidative dehydrogenation (ODH) of alkanes to obtain alkenes over V-MCM-41 has been reported [195,356,357]. The template ion exchange method was found to be effective for this purpose, and the resulting catalysts show good selectivity for oxidation of ethane and propane [195]. The turn-over-frequency (TOF) for propane ODH decreased with increase of the V-loading, which is consistent with the appearance of the V_2O_5 crystalline phase in the materials [356]. The highest selectivity in isobutane ODH was observed for a V-MCM-41 catalyst with a Si/V ratio of 30 as compared to MCM-41 and amorphous V-silica (He:*i*-C_4H_{10}:O_2 = 82:12:6, W/F = 3.54 g h/mol *i*-C_4) [357]. The isobutene selectivities were 59 and 52% at 5 and 10% of isobutane conversion, respectively. The *cis*-/*trans*-ratio of 2-butene was close to unity, indicating that no secondary isomerization of butenes was taking place.

Methane partial oxidation by air over V-MCM-41 and -48 catalysts containing isolated V=O species (V content, 2.8 wt%) has been reported by Berndt et al. [358]. The space–time-yield of formaldehyde and methanol over the V-MCM-41 catalyst were 75 and 1.25 mol $kg_{cat}^{-1} h^{-1}$, respectively, at a GHSV of 280,0001 $kg^{-1} h^{-1}$ and 622 °C (CH_4/air = 1.13). Recently, it was revealed that larger pore mesoporous catalyst, V-impregnated SBA-15, was even preferable in this reaction [359]. The V-SBA-15 with 3 wt% V-loading exhibits CH_4 conversion and HCHO selectivity of 1.6% and 94%, respectively, at a GHSV of 144,0001 $kg^{-1} h^{-1}$, corresponding to a formaldehyde space–time-yield of 93 mol $kg_{cat}^{-1} h^{-1}$ (CH_4/O_2 = 23.1 at 625 °C). Molybdosilicates are also active in this reaction. Directly prepared Mo-SBA-1 (8.8 wt%) showed a slightly higher HCHO selectivity and yield than Mo post-impregnated SBA-1 (9.0 wt%) [360].

Methanol oxidation with Nb-doped MCM-41 was investigated by Gao et al. [361]. Nb-MCM-41 (3.5 wt% Nb doped) and Nb_2O_5 supported on amorphous silica (1 wt%) have similar activity. The FT-Raman and UV–vis studies of these dehydrated samples revealed the presence of highly dispersed isolated NbO_4 units. The TOF, based on the total number of Nb atoms in the catalysts, were 20 and 29 (10^{-3} s^{-1}), respectively. Comparison of activity based on a unit mass catalyst, on the other hand, were 27 and 8 mmol/g h, respectively, indicating a higher overall activity of Nb-MCM-41 catalyst. The selectivity to formaldehyde, methylformate, and dimethyoxy methane were 52%, 44% and 4% in Nb-MCM-41, respectively, while they were 27%, 67% and 6% in the Nb_2O_5/SiO_2 catalyst.

5.2. Catalysis by supported nanoparticles

The pore system of ordered mesoporous materials with the narrow pore size distribution and in many cases rather long pores, is ideally suited to stabilize nanoparticles in high dispersion. Accordingly, many different catalytically active materials have been supported on these materials, not only small noble metal particles, but also bulk base metal oxides and sulfides. Depending on the strength of the interaction between the support and the supported phase, thin coatings on the walls or particles in the pore system may form.

The influence of the acidity of support materials on basic oxides, such as Ga_2O_3 and In_2O_3, was investigated by use of MCM-41, silica–alumina, γ-Al_2O_3, ZrO_2, and zeolites as a support [234]. In the benzylation of benzene with benzyl chloride, the activity of Ga_2O_3 and In_2O_3 supported on nonacidic supports (Si-MCM-41, silica–alumina with low surface area, silicalite–I, and silica gel) is comparable or even much higher than over catalysts supported on acidic supports (Al-MCM-41, silica–alumina with high surface area, H-ZSM-5, and γ-alumina). However, the study comes to the conclusion that the acidity of the support material does not play a significant role in this reaction. The In_2O_3 supported on Si-MCM-41 shows the best performance; time required for 50% of conversion of benzyl chloride was 2.4 min with 20 wt% loading, whereas over the 20 wt% Ga_2O_3/Si-MCM-41 or bulk In_2O_3 the times were 2.5 and 12.8 min, respectively. The authors also reported that these systems catalyze Friedel–Crafts type benzene benzylation or acylation reactions in the presence of moisture. The presence of moisture prolongs the induction period. After the induction period, however, the reaction proceeds at almost the same or even higher activity than in the absence of moisture.

Hydrotreatment of petroleum fractions which involves hydrodesulfurization (HDS), hydrodenitrogenation (HDN), or mild cracking of heavy feeds and aromatics in different distillates is an example of a process for which a need for converting large molecules is obvious. MCM-41 supported MoS_2 shows a higher rate constant for HDS of dibenzothiophene than MoS_2 supported on amorphous SiO_2 [253]. SBA-15 supported Ni–WS_2 shows 1.4 and 7.3 times higher catalytic activities than a commercial Co–Mo/Al_2O_3 catalyst for HDS of dibenzothiophene and hydrogenation of toluene, respectively [119].

Isopolyoxide of $(NH_4)_6Mo_7O_{24}$ and $Co(NO_3)_2 \cdot 6H_2O$ were co-impregnated in Al-MCM-41 and following calcination yielded a good HDS catalyst [250,251]. At 350–375 °C and a H_2 pressure of 6.9 MPa, the sulfided Co–Mo/Al-MCM-41 catalysts show higher hydrogenation and hydrocracking activities than conventional Co–Mo/γ-Al_2O_3 catalysts in HDS of a model fuel containing 3.5 wt% of sulfur as dibenzothiophene in *n*-tridecane [251]. In the desulfurization of a petroleum residue, however, a commercial Co–Mo/Al_2O_3 (criterion 344TL) had better performance than the MCM-41-based catalyst [250].

Iron oxide supported on MCM-41 has high catalytic activity in the oxidation of SO_2 in highly concentrated gas streams, as they are present at smelters using oxygen instead of air for roasting of oxidic ores (Fig. 13) [362]. Although the activity at low temperature is lower than that of commercial vanadium-based catalysts (which can, however, not be used under commercial conditions in these highly concentrated gases), it is substantially higher than that of iron oxide supported on a commercial high surface area amorphous silica support. The catalytic activity was rather independent of the preparation procedure (incipient wetness, solid–solid impregnation

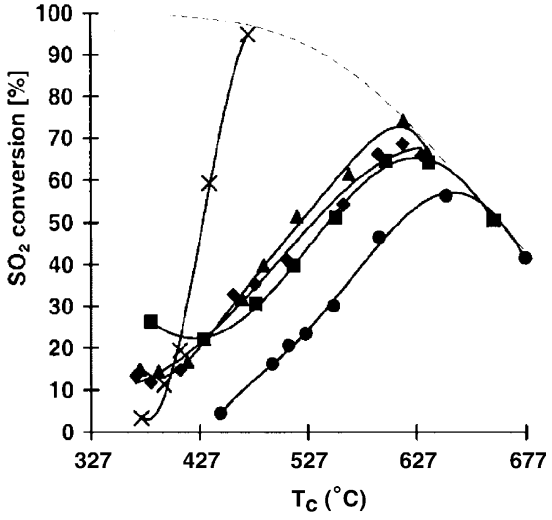

Fig. 13. SO_2 conversion vs. T: (▲) incipient wetness impregnation; (♦) solid-state impregnation: (■) in situ synthesis; (●) iron on a commercial silica support (BASF V1605); (×) a vanadium-based commercial catalyst (BASF V4-111). The connecting lines are just a guide for the eyes. The dotted line shows the equilibrium conversion [362].

or direct synthesis). In addition, these catalysts show remarkable thermal and long term stability up to 750 °C.

Mesoporous silica supported Ni, Pt, Rh, Ir, Ru or metal alloys have been widely studied as hydrogenation or hydrocracking catalysts for bulky substrates and were shown to be very efficient catalysts. For example, hydrogenation of aromatics in diesel [363], hydrocracking of 1,3,5-triisopropylbenzene [364] or naphthalene [221,365] have been reported.

Hydrogenation of unsaturated carbonyl compounds to saturated ketones or aldehydes is easily achieved over most platinum group metal catalysts under mild conditions and in different solvents. However, the selective hydrogenation of unsaturated carbonyl compounds to unsaturated alcohols still remains an important challenge in heterogeneous catalysis. Because of the wide pore opening of mesoporous silica, bulky substances, like prostaglandin intermediate ketones, can successfully be reduced to the corresponding secondary allylic alcohols over mesoporous silica supported Ru or Pt–Sn [366,367].

In the hydrogenation of benzoic acid to cyclohexane carboxylic acid over MCM-41 supported Ru-containing bimetallic catalysts (Ru_5Pt, $Ru_{10}Pt_2$, Ru_6Sn, Pd_6Ru_6 or Cu_4Ru_{12}), the Ru–Pt catalysts are the most active catalysts (Fig. 5) [221]. The $Ru_{10}Pt_2$ showed a higher activity and selectivity to cyclohexane carboxylic acid than Ru_5Pt, although both catalysts have the same Ru/Pt ratio. Hydrogenation of 1,5,9-cyclododecatriene took place at temperatures as low as 80 °C over bimetallic Ru_6Sn catalysts ($[Ru_6C(CO)_{16}SnCl_3]^-$ as a precursor) on MCM-41 without any solvent [220]. Selectivity to cyclododecene at this temperature is 68.2%, and increases to 91.3% at 100 °C. The same catalyst shows 100% selectivity to cyclooctene in 1,5-cyclooctadiene hydrogenation at 40 °C. From the comparison of several MCM-41 supported bimetallic catalysts, such as Cu_4Ru_{12}, Ag_4Ru_{12}, Pd_6Ru_6, the authors concluded that Ru_6Sn is the best catalyst for selective hydrogenation of one or two double bonds.

The application of MCM-41 supported palladium catalysts in the hydrodehalogenation of chlorinated hydrocarbons in polluted groundwater under ambient conditions has also been explored. The catalysts based on MCM-41 have superior activity compared to dealuminated zeolite Y-based systems. However, deactivation is much more rapid in the case of MCM-41, since hydrophilic catalyst poisons, such as sulfur containing compounds, penetrate the pore system easier than in case of the hydrophobic Y-zeolite [368].

Palladium catalyzed carbon–carbon coupling (Heck reaction) is an important reaction in modern organic synthesis. Palladium grafted mesoporous silica, prepared by vapor phase grafting and subsequent reduction with hydrogen, shows remarkable activity in the Heck-type carbon–carbon bond formation [369,370]. For example, 99% yield at 100% conversion was obtained after only 1 h in the reaction of 4-bromoacetophenone and *n*-butylacrylate in air. The large pore opening of the support material and the highly dispersed active site (30%) provide an easy access for large substrate molecules, and consequently lead to an excellent activity for this reaction, the authors concluded.

The extremely high surface area of mesoporous silica (1000 m^2/g) is especially attractive in reactions, in which the activity is insensitive to the structure of active sites, such as CO hydrogenation on Co/SiO_2 [371,372]. Highly dispersed Co metal supported on MCM-41 shows significant increase of CO hydrogenation activity in comparison to an amorphous SiO_2 supported catalyst. Khodakov et al. [373] reported pore size effects on Fischer–Tropsch reaction rates and selectivity for mesoporous silica supported Co catalysts. The fraction of C_{5+} species increased with the pore diameter, and reaction rate was improved when SBA-15 with a pore diameter lager than 3 nm was used. CoRu/MCM-41 prepared by impregnation has also been used in this reaction [374–376]. Highly dispersed Ni nanoparticles in mesoporous silica present good benzene hydrogenation activity from 150 to 200 °C [377]. Incorporation of Al or Nb in the mesoporous framework increases the interaction between the Ni particles and support oxides for the Ni stabilization.

Gold nanoparticles, deposited on MCM-41 by chemical vapor deposition of dimethyl gold acetylacetonate, exhibit high catalytic activities for the oxidation of CO and of H_2, below and above 0 °C, respectively [378]. Active gold catalysts could also be prepared by a solution-based synthesis, after the normally negative surface of SBA-15 had first been charge inverted by grafting of alkylammonium groups [211], subsequent impregnation with $HAuCl_4$ and reduction with $NaBH_4$ [213]. Metal clusters like Pd_{561} and Au_{55}, stabilized by hydrophobic ligands, have been used as precursors in the in situ synthesis of MCM-41 [379]. Both surfactant and ligands can be removed by calcination resulting in highly dispersed metal clusters on the inner and outer surface. FSM-16 supported Pt particles prepared from supercritical CO_2 as solvent also showed high CO oxidation activity [209]. In the water–gas-shift reaction, Pt-nanowires encapsulated in FSM-16 is more active than the corresponding Pt-nanoparticle catalyst [380,381].

Pt and Pd supported mesoporous carbon (CMK-1) is active in the liquid phase hydrogenation of nitrobenzene, 2-ethylanthraquinone or 4-isobutylacetophenone to *p*-aminophenol, 2-ethylanthrahydroquinone or 1-(4-isobutylphenyl)ethanol, respectively [382]. Compared with commercial carbon supported precious metal catalysts, mesoporous catalysts gave better conversion and selectivity at the same loading level (5 wt%). Generally, 2 wt% metal loaded CMK-1 exhibited similar catalytic performance as 5 wt% of loading in commercial carbon.

Mesoporous carbon (CMK-5) supported Pt has very interesting catalytic properties for O_2 reduction in a fuel cell setup [290]. Details of this new electrocatalyst will be described later.

The surface area of Pd/SBA-15 does not change very much before (730 m^2/g) and after (690 m^2/g) methane total oxidation under reaction conditions (520 °C, GHSV = 30 $m^3_{CH_4}\,h^{-1}\,kg^{-1}_{Pd}$) [383]. A kinetic study of methane oxidation over mesoporous silica (D_p = 3.4 nm) supported $LaCoO_3$ was presented by Nguyen et al. [239]. Independent of the loading with $LaCoO_3$ up to 38.5 wt%, mass transfer limitations appeared at reaction temperatures above 380 °C. Even though this negatively influenced the apparent rate, the supported catalysts still show higher conversion and a lowering of the onset temperature compared to bulk $LaCoO_3$. The supported catalyst maintains its high activity also in the presence of SO_2, whereas the non-supported catalysts were rapidly deactivated. Highly dispersed MnO_x, which was prepared by vapor phase grafting of $Mn_2(CO)_{10}$ on MCM-41 and subsequent calcination, had superior catalytic activity in the total oxidation of propene [384]. The onset temperature was ca. 100 °C lower than for the catalyst obtained on amorphous silica as a support.

The catalytic activity of Fe^{3+} ion exchanged mesoporous silica for selective catalytic reduction of NO with NH_3 has been reported [174]. The Fe/Al-MCM-41 and Fe/Al-HMS showed a wider temperature window compared with V_2O_5-based catalysts such as V_2O_5/TiO_2 and V_2O_5–WO_3/TiO_2. Ruthenium-based catalysts were active in the decomposition of N_2O. Among $RuCl_3$, $Ru(OH)_3$ and $Ru_3(CO_{12})$, the $Ru(OH)_3$ impregnated catalysts present highly dispersed Ru species and thus the hydroxide is the most suitable precursor [385]. Complete decomposition of N_2O took place at 400 °C when Ru/MCM-41 (5.0 wt%) was used. Addition of small traces of CO leads to a decrease in the decomposition temperature.

Polyoxometalate units are borderline cases between supported oxides and supported molecular species. However, in many cases it is not fully clear in which state the polyoxometalates are present after impregnation and during reaction; such systems shall be discussed in the last paragraph of this section. Mesoporous silica loaded with ammonium heptamolybdate, $(NH_4)_6Mo_7O_{24}$, has a remarkable activity in olefin methathesis [249]. Conversion of oct-1-ene and the yield of tetradec-7-ene in the early stages of the reaction increase with the pore diameter of the HMS used. The conversion reached the highest value within 5 h in large pore catalysts (d_{100} = 3.4 and 3.5 nm) and the yield and selectivity to tetradec-7-ene decreased after this stage, owing to the deactivation of catalysts. In contrast, on smaller pore catalyst (d_{100} = 3.0 nm), the yield of tetradec-7-ene steadily increased up to 44% (at 16 h) with high selectivity (77%). HMS supported $CuH_3[PMo_{10}V_2O_{40}]$ is active in propylene oxidation to acetone [386]. The low conversion of $CuH_3[PMo_{10}V_2O_{40}]$ (1.3%) without silica support increased to 9.2% and 17.2% by supporting it on amorphous silica (164 m^2/g) and HMS (1100 m^2/g), respectively. This result indicates that polyoxometalates can be highly dispersed on the HMS surface and have many exposed surface sites. Finally, Maldotti et al. [248] also reported photocatalytic oxidation activity for the reaction of cyclohexene or cyclododecane to the corresponding alcohol and ketones for MCM-41 supported $(n\text{-}Bu_4N)_4W_{10}O_{32}$.

5.3. Grafted active sites with defined and well-characterized structure

Ordered mesoporous materials are well suited for the immobilization of molecular catalysts including enzymes, basic molecules, or chiral/non-chiral organometallic complexes, since they provide a very homogeneous environment and thus allow the creation of rather similar sites in the material. There are many strategies for immobilization of active components on mesoporous materials, as discussed above. One of the most reliable ways is grafting of the active species with a precise structure, such as present in defined metal complexes and enzymes. These species can be immobilized via ion exchange, condensation, and co-valent attachment of organic ligands.

One of the most widely used methods for immobilizing enzymes is encapsulation inside sol–gel silica. However, due to small pore sizes and partially closed pore structures, most studies on such immobilized enzymes reported much lower specific activity than for the free enzymes in solution. Mesoporous silicas with wide, fully accessible mesopores, therefore, have attractive features for enzyme immobilization.

Immobilization of trypsin on MCM-41, MCM-48 and SBA-15 was reported by Yiu et al. [262]. However, there was significant leaching (35–72%) observed from the support in buffer solution (pH = 8) [262]. Surface functionalized silica can increase the interaction between the enzyme molecule and the support surface, and prevent leaching of the enzyme. Thus, trypsin adsorbed on thiol-fuctionalized SBA-15 shows negligible leaching, and achieves 84% of the catalytic activity in hydrolysis of *N*-α-benzoyl-DL-arginine-4-nitroanilide as compared to free trypsin [266]. Lei et al. [263] reported the immobilization of organophosphorus hydrolase (OPH) on surface functionalized SBA-15. Positively charged OPH is more likely to be entrapped in a material functionalized with carboxylic groups than in those modified with amine groups. High specific activity was observed for hydrolysis of paraoxon (4182 units/mg) which was twice as high as that of the free enzyme (1928 units/mg).

Due to the pore size of mesoporous materials, grafting of complete metal complexes and organometallic

moieties is possible, enabling the formation of selective catalysts with a large concentration of accessible and well-spaced active sites. Species known to be active in homogeneous catalysis can, if used in this manner, utilize the advantages of heterogeneous catalysis. Therefore, most of the studies using such immobilized species were carried out under mild conditions in order not to affect the grafted complex.

The simplest procedure for immobilization of molecular species is impregnation or ion exchange. However, this results in a rather weak interaction between support and metal complex, which means that the active complex is easily leached. Although in fortunate cases immobilization is possible by simple impregnation [387], complexes are mostly co-valently anchored to the mesoporous support via silylation of silanol groups [22]. In this way, leaching of the complexes is less of a problem, although it still may occur, if either the bond to silica is cleaved under reaction conditions or one of the other bonds in the linker.

MCM-41 ion-exchanged with [Fe(phenanthroline)$_3$]Cl$_2$ [175] or [Fe(8-quinolinol)$_3$]Cl$_2$ [176] showed activity in phenol hydroxylation with H_2O_2. Ion-exchange of Al-MCM-41 with [Mn(2,2′-bipyridine)$_2$]NO$_3$ led to a catalyst exhibiting higher activity for the oxidation of styrene than the corresponding homogeneous catalyst [177]. However, leaching of active components (several% in each run) has been reported for these catalysts.

Epoxidation catalysts can also be designed to be enantioselective: Al-MCM-41, ion exchanged with Mn(OAc)$_2$ and subsequently modified with a chiral salen, (*R*,*R*)-(−)-*N*,*N*′-bis(3,5-di-*tert*-butylsalicylidene)-1,2-cyclohexadiamine, is an effective enantioselective solid epoxidation catalyst for *cis*-stilbene [388]. This modification leads to an enhancement in *cis*-epoxide selectivity from 29% in the homogeneous reaction to 58%, if iodosylbenzene is used as oxidant. The turnover rates, based on the amount of Mn-salen, for the solid catalyst were found to be higher than those for the homogeneously catalyzed reaction. Although leaching of some salene ligand was observed, no Mn^{3+} leaching was observed during the reaction. The conversion of styrene and stilbene over mesoporous silica immobilized Mn(III) salene complex was improved by replacing the regular MCM-41-type silica with disordered mesoporous silica [118].

By tuning the ligand environment, the catalytic activity can be modified for the immobilized systems in a manner analogous to homogeneous catalysis. With the purely nitrogen donor ligand 1,11-bis(2-pyridyl)-2,6,10-triazaundec-1,10-diene Mn(III), [NNNN] liganded, the complex shows significantly higher catalytic activity than the above mentioned system of the Schiff base analogue complex with 3-[*N*,*N*′-bis-3-(salicylidenamino)propyl]amine, [NNOO] liganded [389]. The

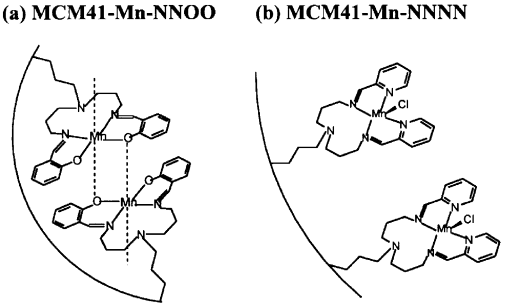

Scheme 6.

cyclohexane conversion was 99.8% with the [NNNN] ligand, while only 60.1% were observed for the [NNOO] ligand. The higher activity of the nitrogen donor ligand can be explained by the prevention of μ-phenoxyl intermolecular interaction (Scheme 6).

Epoxidation is also possible over molybdenum-based catalysts. The oxodiperoxo molybdenum complex, [(L–L)MoO(O$_2$)$_2$] (L–L = (3-triethoxysilylpropyl)[3-(2-pyridyl)-1-pyrazolylacetamide]) grafted on MCM-41 or Al-MCM-41 shows cyclooctene epoxidation activity already at 60 °C [113]. When TBHP was used as an oxidant, the cyclooctene epoxide selectivity was close to 100%. Surface silylation of the MCM-41 or Al-MCM-41 prevents leaching of the molybdenum complex and results in superior catalyst re-cyclability.

Ruthenium perfluorophthalocyanine complexes in the mesopore channels of MCM-41 show activity for cyclohexane oxidation with TBHP in the liquid phase under ambient conditions [390]. The catalyst which had been prepared via ligand exchange of a ruthenium carbonyl complex by ship-in-the-bottle synthesis (0.6 wt% loading) showed a higher activity than the catalyst which had been grafted by linking to aminopropyl functionalized MCM-41 (5 wt% loading). The low activity of the grafted material is due to the relatively high loading of complex which would lead to a pore blockage, or co-ordination change of ruthenium by a Ru-N bond, the authors claimed. A perruthenate immobilized within amine- or tetraalkylammonium modified MCM-41 has been used in alcohol oxidation with molecular oxygen [268]. In oxidation of various allylic alcohols, for example 1-phenylethanol, the corresponding aldehydes were obtained quantitatively within several hours without over-oxidation. The reaction also took place when silica aerogel was used as a support, however, significantly longer reaction time was needed.

Homogeneous reduction catalysts have also been immobilized on the surface of ordered mesoporous silicas. Dichlorobis(benzylcyano)palladium(II) grafted on MCM-41, which had been pretreated with 3-trimethoxysilylpropyl amine, was used in the reduction of aromatic nitro compounds to the corresponding amino compounds, and for the hydrodehalogenation of 1-bromonaphthalene by molecular hydrogen [391,392].

Silylamides are used as reactive precursors in order to design Lewis acidic complexes based on aluminum or lanthanides (Fig. 10) [273,275]. These immobilized Lewis acid catalysts exhibit markedly increased catalytic activity in the hetero Diels–Alder cyclization of *trans*-1-methoxy-3-trimethylsiloxy-1,3-butadiene and benzaldehyde compared to their molecular counterparts in solution [273]. One could expect an extension of the applicability of these kinds of catalysts towards asymmetric reactions by use of chiral ligands instead of fod (1,1,1,2,2,3,3-heptafluoro-7,7-dimethyl-4,6-octanedionate).

For the hydrogenation of olefins, the hydrido chlorocarbonyl tris-(triphenylphosphine) ruthenium complex ($[RuHCl(CO)(PPh_3)_3]$) has been immobilized on the surface of aminopropyl functionalized mesoporous silica via ligand exchange [393]. For all the substrates tested, including styrene, *trans*- and *cis*-stilbene, α-methyl styrene and limonene, conversion and turnover frequency were considerably higher with MCM-41 and SBA-15 catalysts than with the unsupported complex. SBA-15 was superior to MCM-41 as support which was attributed to the easier access of substrate molecules to the active sites in SBA-15.

An anchored rhodium phosphine complex can simply be prepared via ligand exchange by treating MCM-41 with $(EtO)_3Si–(CH_2)_3–PPh$ and $Rh(PPh_3)_3Cl$ [394]. The resultant solid catalysts are active in cyclohexene hydrogenation for more than 15 cycles which shows the effective immobilization achieved via this simple procedure. In order to use bidentate phosphine ligand and to prevent the dimerization of the rhodium centers through chloro bridges, a cationic $[Rh(cyclooctadiene)(THF)_2]^+BF_4^-$ was used to introduce an active site in previously grafted diphenyl-functionalized mesoporous silica [395]. The turnover frequency in isosafrol hydrogenation exceeds the result of homogeneous catalysts.

A platinum–phosphine complex, $[PtCl_2\{PhP(CH_2)_2Si(OEt)_3\}_3]$, grafted on MCM-41 was used as a hydroformylation catalyst in supercritical CO_2 with $SnCl_2\cdot 2H_2O$ as a co-catalyst [396]. In the hydroformylation of 1-hexene, the MCM-41 catalyst gave higher yield (20,500 mol of aldehydes per mole of Pt) than the same catalyst grafted on amorphous SiO_2. The former catalyst showed also higher regioselectivity to the linear heptanal than the latter. The narrow pore size, surface interactions with the catalyst, or better retention of the Sn co-catalyst may lead to the difference in regioselectivity.

Dirhodium(II) tetrakis (methyl-2-oxopyrrolidine-5-carboxylates) and dirhodium(II) tetrakis (4-benzyl-2-oxazolidinones), attached to the MCM-41 surface through ligand exchange with carboxylic acid functionalized tethers catalyze cyclopropanation of styrene with diazoacetates (*tert*-butyl diazoacetate or ethyl diazoacetate) [269]. The relatively small ligand of the complex does not significantly restrict the substrates, the *trans*/*cis* ratio in the products are thus not very high in the homogeneously catalyzed reaction. In the heterogeneous raction, more trans-compound is formed due to the steric limitations caused by the support surface. This effect is more pronounced if the bulky *tert*-butyl diazoacetate is used instead of ethyl diazoacetate. The authors also attempted a Si–H insertion reaction of methyl phenyldiazoacetate with dimethylphenylsilane. However, due to the small pore of MCM-41 (1.9 nm), only traces of the product were obtained.

The large pore diameter of mesoporous silica permits the direct grafting of complete chiral metal complexes and organometallic moieties onto the inner walls of these high surface area solids by a variety of different routes, including tethering to a surface functionalized with organic groups, such as alkylhalides, amines, carboxyls and phosphines [276,397]. MCM-41 and other members of the family of ordered mesoporous silicas have proven to be good supports for metals or anchored organometallic complexes with a good activity and selectivity in various reactions.

Tethered palladium phosphine (Fig. 9, pathway (B)) on the surface of MCM-41 can catalyze a one-step asymmetric hydrogenation of ethyl nicotinate to ethyl nipecotinate with a 17%ee and conversions in excess of 50% [271]. The result is superior to the usual two-step hydrogenation using Pd/C and cinchonidine modified Pd/C catalysts (19%ee with 12% conversion).

Non-co-valently immobilized rhodium diphosphine catalysts also exhibit excellent hydrogenation activities. The $[(1,5\text{-COD})Rh(Duphos)]^+Cl^-$ (Scheme 7, COD = cyclooctadiene, Duphos = (1,2-bis((2S,5S)-2,5-dimethylphospholano)benzene)) immobilized on Al-MCM-41 showed high activity in the hydrogenation of dimethylitaconate with 99% selectivity and 92% enantioselectivity in dichloromethane as a solvent [256]. The catalyst was reusable at least four times without any loss in activity; after 8–10 consecutive runs, however, a decrease in catalytic performance was observed. In the hydrogenation of an α-enamide ester dissolved in dichloromethane, [(R,R)-Me-(DuPHOS)Rh(COD)]OTf (Me-DuPHOS = 1,2-bis(2,5-dimethylphosphacyclopentyl)ethane) on MCM-41 allows comparable conversion and higher enantioselectivity than homogeneous catalysts [257].

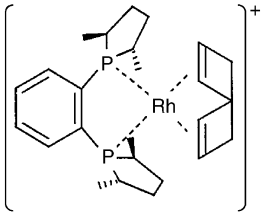

Scheme 7.

However, since the interaction is normally relatively weak in these cases, leaching easily occurs if a polar or protic solvent such as methanol or ethanol is used.

Immobilized Ru-BINAP (BINAP = (R)-(+)-2, 2′-bis(diphenylphosphino)-1,1′-binaphtyl) and Rh-BPPM (BPPM=(2S,4S)-N-(*tert*-butoxycarbonyl)-4-(diphenylphosphino)-2-[(diphenylphosphino)methyl] pyrrolidine), attached to the support by direct impregnation, work as hydrogenation catalysts in aqueous media [258]. In the hydrogenation of α-acetamidocinnamate, Ru-BINAP and Rh-BPPM show 81% and 100% conversion, respectively, and 48% and 49%ee. Since there are no benchmark experiments, it is difficult to judge the activity of these complexes. However, the catalytic activity was significantly reduced by re-cycling; nearly 90% of Rh was lost in the recovered catalyst. Tethering these complexes with amino- or carboxyl groups in MCM-41 did not improve the catalytic performance [398].

Palladium–phosphine complexes catalyze regioselective allylic amination reactions [270]. Immobilized Pd(II)-1,1′-bis(diphenyl phosphino) ferrocene complex tethered to MCM-41 promotes a dramatic change of the regioselectivity in the reaction between cinnamyl acetate and benzylamine. Due to the pore confinement effect, the branched product with 51% regioselectivity and close to 100% enantioselectivity was obtained, while the homogeneous catalyst directs the conversion towards the straight chain product (Scheme 2). The performance of the MCM-41 supported catalyst is also drastically improved compared to the amorphous silica supported catalysts (2% regioselectivity with 43%ee).

Besides the phosphine complexes, asymmetric hydrogenations catalyzed by diamine complexes have become more interesting because phosphines are generally air sensitive, toxic and favor deactivation of the catalytic complex. Recently, heterogenized diamino Ru [399], Rh and Pd [400] complexes were reported.

Immobilized dichloro-(*S*)-6,6′-dimethyl-2,2′-diaminobiphenyl–ruthenium complex ((*S*)-MAB-MCM-Ru) has been prepared via grafting of (*S*)-6-(3-aminopropylentrimethyoxysilanemethylen)-6′-methyl-2,2′-diacetamidobiphenyl onto MCM-41. The cleavage of the amide groups to give an amine ligand allowed to introduce an active component, dichloro-cycloocta-1,5-dienyl–ruthenium (Scheme 8) [399]. The supported catalyst gave an excellent performance in hydrogenation of α-acetamidocinnamic acid; the enantiomeric selectivity to the (R)-isomer in the heterogenized and homogeneous catalysts were 96.8 ± 1.2 and 69.8 ± 0.3%ee, respectively. The catalysts are reusable without any loss of product yield, only the enantioselectivity decreased slightly from 97% to 94% after three runs. Improved enantioselectivity was also observable in the hydrogenation of itaconic acid. Increase of enantioselectivity is caused by the increased rigidity of the anchored structure, the authors supposed, in which the anchored structure would hamper the rotation of the transition state during insertion of the hydrogen atoms to the double bonds of the acids and thus favor the (R)-isomer.

Jones et al. [400] reported the enhancement of the enantioselectivity of rhodium(I) and palladium(II) hydrogenation catalysts, compared with the corresponding homogeneous systems or such complexes immobilized on convex surfaces, such as spherical silica particles as present in a silica gel. This improved performance was attributed to the anchoring of the active site on the concave inner surface of the channels in the ordered mesoporous materials [400]. For example, MCM-41 supported Rh(I) catalysts showed 93%ee for hydrogenation of α-phenyl cinnamic acid, whereas only 81%ee and 79%ee were observed in the corresponding homogeneous or Cabosil supported catalysts, respectively. The access of the bulky substrate to the active metal center is favored only when the reactant approaches along the pore axis (Fig. 14). The immobilization on the convex silica surface (Cabosil) or a homogeneous phase

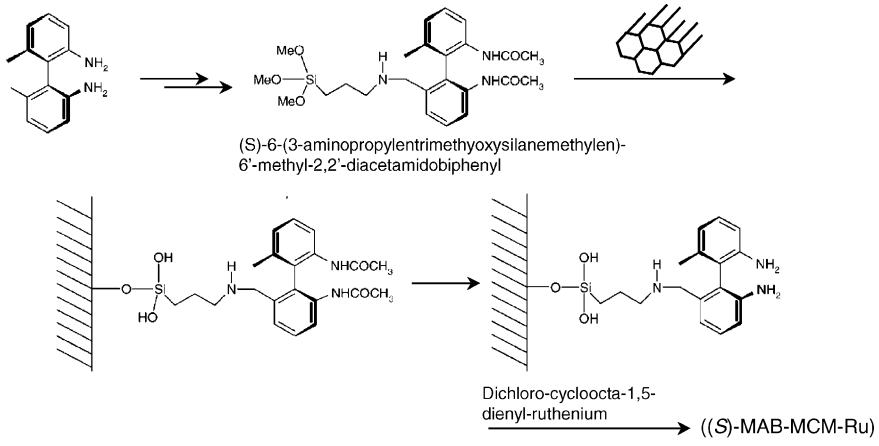

Scheme 8.

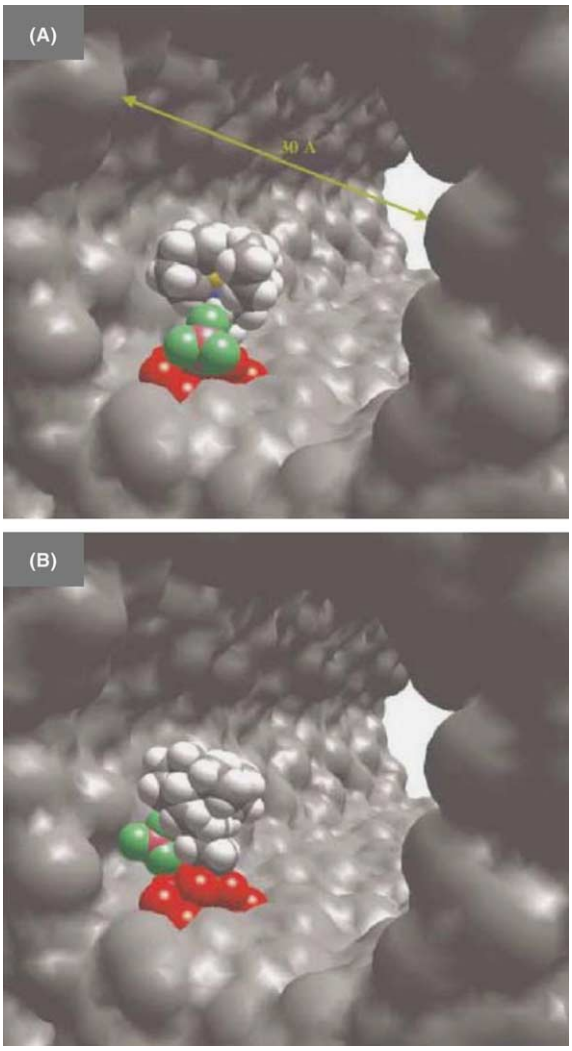

Fig. 14. Postulated computer graphic models of MCM-41 supported (*S*)-(−)-2-aminomethyl-1-ethyl pyrrolidine co-ordinated Rh-1,5-cyclo-octadiene. (A) Substrates can access along to the pore in this conformation. (B) The C–C bond rotation of the tether leads to a restriction of access to the active site [400].

reaction does not help such a beneficial restriction for these amine-bidentated complexes.

A chiral copper(II) bisoxazoline co-valently anchored to MCM-41 catalyzes asymmetric Diels–Alder or Friedel–Crafts reactions [401,402]. In the asymmetric Diels–Alder reaction between cyclopentadiene and 3-(2-propenoyl)-2-oxazolidimone, the heterogenized catalyst has good enantioselectivity of 78%ee and an endo/exo-selectivity (17:1) which was better than in the corresponding homogeneous reaction [401]. Also in the Friedel–Crafts hydroxyalkylation of 1,3-dimethoxybenzene with 3,3,3-trifluoropyruvate the conversion (77%) and the enantioselectivity (82%) over the MCM-41 immobilized complex (Scheme 9) exceed the performance in homogeneous phase (44% and 72%, respectively) [402]. The MCM-41 catalyst is reusable without loss of enantioselectivity, though the conversion decreases slightly. In this report, amorphous silica grafted catalysts exhibited the highest ee (92%). The lower ee values achieved using MCM-41 compared with amorphous silica reflect the negative influence of the residual free silanol groups, observed with FT-IR in the MCM-41 catalyst, as the authors supposed. The heterogenized copper bisoxazoline catalyst catalyzes the enantioselective cyclopropanation of styrene with ethyl diazoacetate [403]. Here the immobilized catalyst exhibits almost the same yield and enantioselectivity with only one-tenth of the amount of Cu than in the homogeneous system. A slight decrease of the yield was observed, however, in a repeated run, while the enantioselectivity remained almost the same.

Carbon–carbon coupling reactions (Suzuki reaction) have already been discussed in the section on supported small metal particles as catalysts. Such reactions have also been performed with immobilized homogeneous catalysts. A palladium–phosphine complex, $PdCl_2[Ph_2P(CH_2)_2S(CH_2)_3SO_3Na]_2$, immobilized on alkylsilylsulfonic acid silylated Al-MCM-41 gave a (4′4)-methoxymethylbiphenyle from *p*-iodanisole and *p*-toluneborone acid [404]. A long induction period, in which the reduction of Pd(II) to Pd(0) is taking place, is observed in this reaction. Interestingly, the re-cycled catalysts showed an enhanced activity which was comparable to the homogeneous system. A catalyst prepared by stirring an alkylsilylsulfonic acid modified Al-MCM-41 in CTAB solution, and following ligand exchange of Pd–phosphine complex is applicable also in a two-phase reaction between *p*-iodoanisole (in toluene) and phenylboronic acid (in ethanol) [405].

A Grubbs' type Ru-alkylidene complex, $(Ph_3P)_2Cl_2Ru{=}CHPh$, anchored on MCM-41, using a

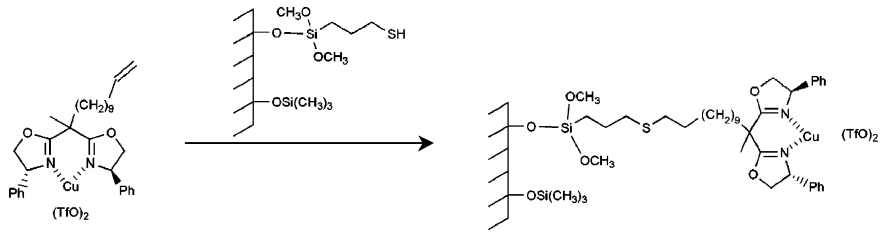

Scheme 9.

previously grafted diphenylphosphinoethyltriethoxysilane ($(EtO)_3Si(SH_2)_2PPh_2$) as a tether and subsequent ligand exchange of phenylphosphine between complex and that in tether, showed a good activity in ring-closing metathesis of diallylamine [406]. The activity is comparable with the homogeneous catalysts. However, the authors claimed a mass transfer limitation when a bulky substrate such as diethyldiallylmalonate was used. A similar catalyst, but using cyclohexylphosphine instead of phenylphosphine ($(Cy_3P)_2Cl_2Ru{=}CHPh$), exhibits activity for ring-opening metathesis polymerization of norbornene, even in an aqueous environment.

Highly interesting are heterogenized single site olefin polymerization catalysts. Such systems were obtained with supported Mo [407] or Cr [408,409] active sites or metallocene complexes on methylalumoxane (MAO) modified MCM-41 [410–413].

Ordered mesoporous silica has also been used as support for polymerization catalysts in several studies. Tetravalent binuclear molybdenum compounds act as initiators for the cationic polymerization of cyclopentadiene and methylcyclopentadiene. The MCM-41 grafted $[Mo_2(\mu\text{-}O_2CCH_3)_2(CH_3CN)_{10}](BF)_4$ shows a comparable polymerization activity as in the homogeneous case; polymethylcyclopentadiene with a molecular mass of 96000 $g\,mol^{-1}$ and polydispersity index of 1.9 was obtained [407].

Weckhuysen et al. [408,409] showed that the chromium acetyl acetonate complex, [Cr(acac)$_3$], grafted onto Si-MCM-41 or Al-MCM-41 were effective catalysts for the gas-phase and slurry phase polymerization of ethene. The activity of the catalysts, Cr/MCM-41 and Cr/Al-MCM-41 (1 wt% [Cr(acac)]$_3$ loaded), used after calcination at 650 °C were 6300 and 14,000 $g_{PE}/g_{Cr}\,h$, respectively, in the slurry phase reaction under 31.4 bar of ethene at 104 °C. The activity of Cr/Al-MCM-41 is comparable with that of a commercial Cr/SiO_2 catalyst. The high load melt flow index (HLMI) of the polymers obtained over Cr–Al-MCM-41 was 1.38, indicating a polymer with a high molecular weight. The catalytic activity increased with increase of Cr loading up to 1 wt%, while higher loadings decreased the activity again. Increase of the calcination temperature also leads to the increase of the activity because of the effective removal of surface silanol groups.

Isotactic polypropylene can be prepared by the use of *rac*-ethenebis(indenyl)zirconium dichloride grafted on MCM-41 [410,411]. The number average molecular masses (M_n) showed an approximate fourfold increase relative to the homogeneous system. With respect to activity (1163 $kg/mol_{Zr}\,h$), however, the homogeneous system proves to be superior (4941 $kg/mol_{Zr}\,h$). In ethene polymerization with zirconocene chloride (Cp_2ZrCl_2), Al-MCM-41 is preferable to silica MCM-41 as a support; the activities were 15800 and 6100 $kg_{PE}/mol_{Zr}\,h$, respectively [412]. The *Mn* value in Cp_2ZrCl_2/Al-MCM-41, Cp_2ZrCl_2/MCM-41 and homogeneous Cp_2ZrCl_2 were comparable (451,000, 431,000 and 476,000, respectively), however, the activity of the homogeneous catalysts is two- to threefold higher than that of supported catalysts.

Tethering of a zirconium polymerization catalyst, η^5-cyclopentadienyltris(dimethylamido) zirconium, $CpZr(NMe_2)_3$, has been reported by Schneider et al. [414]. The $CpZr(NMe_2)_3$ was immobilized via ligand exchange between the (NMe_2) groups and previously immobilized indenyl groups on the silica surface. The ethene and propene polymerization activities, however, were far below those over the homogeneous catalyst. The authors concluded that the reaction between $CpZr(NMe_2)_3$ and the residual surface silanol leads to the formation of various zirconium species which are more or less inactive. Surface silylation with hexamethyldisilazane slightly improves the catalytic performance, supporting this conclusion.

A remarkable reaction was reported to lead to polymers with unusual properties: crystalline polyethylene fibers with a diameter of 30–50 nm were described to be formed by the polymerization of ethene with Cp_2TiCl_2 grafted on mesoporous silica-fiber and MAO [methyl aluminooxane] as a co-catalyst. The mesoporous silica fibers with mesopores supposed to be arranged in a parallel direction to the fiber axis are believed to act as "nano-extruders" in this template-assisted extrusion polymerization [415,416]. However, in most of the fibers the pores are not oriented parallel to the fiber axis which sheds some doubt on the proposed mechanism [128,129,417].

Changing the microenvironment of Lewis acidic complexes grafted via the silylamide route allows to extend this new material to excellent polymerization catalysts (Fig. 10). Recently, polymerization of methyl methacrylate (MMA) catalyzed by surface grafted Sm(II) was reported [418]. Ligand exchange of tetramethyldisilazane [$N(SiHMe_2)_2$] on Sm(II) [274] with methanol, dimethylindenylsilane or MAO was found to improve the activity; the smaller ligand methanol is more effective than larger dimethylindenylsilane. From the nitrogen sorption and SEM studies, the PMMA-MCM-41 composite formed had completely filled pores or at least fully blocked pore entrances by the polymer. By activation of surface grafted $Nd(AlMe_4)_3$ via ligand exchange with diethylaluminum chloride (Et_2AlCl), on the other hand, heterogeneous isoprene-polymerization catalysts can be obtained [419]. Both the homogeneous and heterogeneous Nd–Et_2AlCl catalysts have a high activity (yield, >99%) with high *cis*-1,4-polyisoprene stereospecificity (>99%). In comparison to the homogeneous system, the immobilized variant produced polymer with higher molecular weights (*Mw*) and smaller polydispersity index (PDI); values of 1.026×10^6 and 1.60, respectively, for immobilized catalyst instead of 3.26×10^5 and 2.78

in homogeneous reaction. The narrow molecular-weight distribution of the polymer obtained from the solid catalyst can be attributed to the absence of any organo-aluminum co-catalyst dissociation/re-association processes at the active Nd center, the authors concluded.

Surface functionalization by organic molecules imparts new functions to these mesoporous silicas, and, as shown, many organometallic complexes can be immobilized following this pathway. However, even functionalization with non-metal containing groups can lead to interesting properties. For example, thiol-functionalized mesoporous silica works as a good adsorbent of heavy metal ions from water [420,421]. With respect to catalytic applications, functionalized silicas have been used for base or oxidation catalyses [422]. Knoevenagel condensations, Michael addition and condensation reactions over alkylammonium grafted MCM-41 or aminopropylated mesoporous silica via one-pot synthesis have been reported [284,423].

It has also been achieved to immobilize 1,8-bis(dimethylamino)naphthalene (DMAN), a so-called "proton sponge", which is highly basic and therefore widely used for proton abstraction reactions, in mesoporous silica (Scheme 10) [424,425]. The functionalized DMAN, 4-[(triethoxysilyl)propylaminocarbonylamino]-1,8-bis(dimethylamino)naphthalene, was grafted on pure silica MCM-41 (denoted PS-MCM-41), and this material is active as a catalyst in the Knoevenagel condensation of benzaldehyde and ethyl cyanoacetate, and a Claisen–Schmidt condensation between benzaldehyde and 2′-hydroxyacetophenone. When using homogeneous DMAN and DMAN supported on amorphous silica, the polarity of the solvent has a strong effect on the reaction; the reaction rate increases with the solvent polarity. However, PS-MCM-41 has better intrinsic activity both in polar and non-polar solvent. This means that the support MCM-41 can act like a polar solvent environment and stabilize the transition state of the intermediate complex, due to the polarity of the amino-propyl-functionalized MCM-41 [426,427]. Claisen–Schmidt condensation between benzaldehyde and 2′-hydroxyacetophenone—on first sight surprisingly—takes place over PS-MCM-41, even though the pK_a of 2′-hydroxyacetophenone (15.8) is higher than that of DMAN (12.1). The interaction of the carbonyl group and residual surface silanols of MCM-41 obviously allows PS-MCM-41 to abstract protons with a higher pK_a than that of the DMAN.

Immobilization of TEMPO (2,2,6,6-tetramethyl-1-piperidinyloxy), which has been known as a stable radical or radical trapping agent, on the MCM-41 surface is interesting for designing new organic–inorganic heterogeneous oxidation catalysts. Selective oxidation of primary alcohols to either carboxylates or aldehydes has been reported by Brunel et al. (Scheme 10) [428]. In the oxidation of α-methyl glucoside, 1-*O*-methyl glucuronate was obtained with high selectivity within 20 min when NaOCl was used as a primary oxidant at 0 °C. Conversion and selectivity in 1,3-pentanediol oxidation to γ-valerolactone was reported to be 50% and >95%, respectively. If an amide-tether was used instead of an ether-tether, the conversion increased to 99% with the same selectivity.

5.4. Catalysis by non-siliceous ordered mesoporous materials

Organically modified mesoporous silicas provide more hydrophobic environments, and therefore, hydrothermal stability or catalytic selectivity could be improved, as described for several examples in the preceding sections.

Novel options in catalysis are available with such organically modified materials, where the organic groups are integral parts of the framework. Ethane bridged hybrid mesoporous silsesquioxane with titanium incorporated into the framework, prepared from a mixture of TEOS, 1,2-bis(trimethoxysilyl)ethane, TBOT, TMAOH,

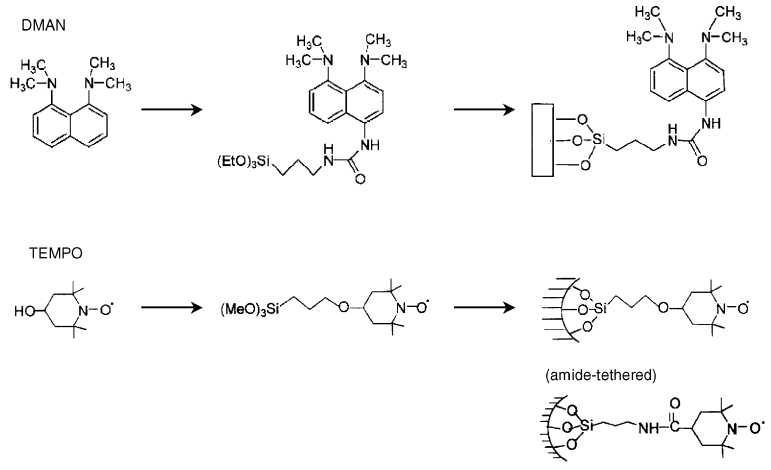

Scheme 10.

octadecyltrimethylammonium chloride, and H_2O, provide a high hydrophobicity, and as predicted, is a good epoxidation catalysts with high hydroperoxide efficiency [429]. The same catalyst shows ammoximation of ketone in the presence of H_2O_2 and ammonia [288]. The conversion of cyclohexanone and cyclododecanone were 63.2 and 42.0 mol% at 80 °C with selectivity towards the corresponding oxime of 100 mol% in both cases. Interestingly, catalysts still showed high activity after removal of the ethylene groups upon calcination at 550 °C. The conversions were 90 and 72.5 mol% for each substrate, respectively, with almost comparable selectivity (>95 mol%), while conventional Ti-MCM-41 showed no catalytic activity in this reaction.

Surfactant templating has provided a breakthrough methodology for the preparation of non-siliceous mesoporous materials. Among these, not only oxides but also phosphates, sulfides, [430], selenides [431], metals and many other compounds may be of interest as catalysts or catalyst support, although—as for the ordered mesoporous silicas—their prices could be a serious obstacle for commercialization. Several of these non-silica mesoporous materials have catalytic activity for certain reactions. For example, hexagonal and cubic mesoporous tin(IV) phosphates were used for NO removal in the presence of C_2H_4 and O_2 [432]. Hexagonal tin phosphate was found to be more active than the cubic one. The difference in the co-ordination state of tin(IV) centers and/or the number of surface tin(IV) species may cause the different activity, the authors supposed. Rhenium oxide supported on mesoporous alumina is a good catalyst for an olefin metathesis in the liquid phase and was found to be superior to γ-alumina [433]. Titanium phosphate was used for liquid-phase oxidation of cyclohexene. Conversion to 1,2-cyclohexanediol and selectivity to this product were 76% and 88%, respectively, when H_2O_2 was used as an oxidant [434]. However, no benchmark catalyst was used in this study, and thus the reported performance is difficult to judge.

Cerium oxide and zirconium oxide are interesting as support materials. Mesoporous CeO_2 and ZrO_2 were found to be good catalyst supports in vapor phase phenol hydrogenation [435]. The hydrogenation catalyst was palladium, which was loaded by a deposition–precipitation method into the mesopores of CeO_2 and ZrO_2. Hydrogen sorption experiments confirmed that palladium was present in the catalyst in form of nanoparticles. The resulting Pd/CeO_2 (3 wt%) showed a phenol conversion of 81.4% at 180 °C with a selectivity to cyclohexanone, cyclohexanol and cyclohexane of 46.2%, 34.8% and 19.0%, respectively. The Pd/ZrO_2 (3 wt%) had very high selectivity for cyclohexanone (93.0%), however, on expense of conversion, which decreased to 62.9%. The reported activities were higher than for non-porous oxide supports, due to the higher dispersion and smaller particle size of Pd.

Very interesting for catalytic applications could be (semi)conducting mesoporous transition metal oxides. Several reports concerning photocatalysis have been published. An oxidative dehydrogenation of 2-propanol to acetone was studied by use of mesoporous titania catalyst [436]. The observed quantum yield of the reaction was, however, extremely low (0.0026) as compared to the standard titania catalyst, Degussa P25 (0.45). Similarly, very low quantum yield was also found for mesoporous Nb-TMS (0.0041). Low activities of these mesoporous materials are due to their poor crystallinity, where defect sites act as electron–hole traps. By loading a NiO on Ta-TMS, although the wall of Ta-TMS was amorphous, the photocatalytic activity for the water decomposition was improved [437]. The large band gaps of Ta_2O_5 (4.0 eV) as compared to TiO_2 (3.0 eV), in which the excited electrons in the conduction band of Ta_2O_5 have higher potentials than those in TiO_2, are responsible for this high activity. The activity of NiO (4.0 wt%) loaded Ta-TMS was 150 μmol h^{-1} and 73 μmol h^{-1} for H_2 and O_2, respectively. The amount of H_2 and O_2 evolution in NiO (4.0 wt%) loaded Ta-TMS was 1.5 times higher than over NiO (1.0 wt%) loaded crystalline bulk Ta_2O_5. The small wall thickness of mesoporous Ta-HMS, ca. 1.8 nm corresponding to nine Ta–O bonds, makes the material effective for migration of excited electrons, the authors claimed. This group also reported photocatalysis activity of mesoporous Mg–Ta mixed oxide which was prepared by use of Pluronic-123 as template [438]. The activity in water decomposition reaction was 100 μmol h^{-1} and 50 μmol h^{-1} for H_2 and O_2, respectively, in the absence of NiO.

It was observed that mesoporous low-valent niobium oxide [72] coated with niobium by the deposition of bis(toluene) niobium could react with molecular nitrogen and form nitride species at room temperature [439]. In similar materials, based on mesoporous titanium oxide, it was confirmed by experiments with isotope labeled nitrogen that the source of nitrogen was the reaction atmosphere [440]. Moreover, the authors revealed that the surface nitride species could react with moisture imbedded in the walls, and generate ammonia. These results suggest that activation of nitrogen from the atmosphere could be possible and ammonia may be generated in such a process.

Silicon imido nitride, the pore size of which is controllable by the addition of alkylamines with different chain length during the condensation, shows shape selective alkylation of toluene with styrene and in the isomerization of 1-hexadecene [441]. The mesoporous (d_{av} = 5.6 nm) silicon imido nitride gives 100% and 80.8% of conversion, respectively, for the different reactions within minutes at 22 °C, whereas over microporous catalysts (d_{av} = 1.7 nm) no reaction occurs over times up to several tens hours. Smaller substrates, on the other hand, are converted over both types of catalysts. How-

ever, it should be mentioned, that the micro- and mesoporous silicon imido nitrides are not surfactant templated, although the pore size distribution is rather narrow.

Very interesting for catalytic applications seem to be the ordered mesoporous carbon materials. Carbons are used in various applications as support materials, and the extremely high surface areas and tailored pore sizes of the ordered mesoporous carbons give an added value which can be exploited in catalysis. CMK-5 was found to support very high loadings of platinum in a highly dispersed state [290]. Even for a Pt loading level of 50 wt%, particle sizes of 2.5 nm could be maintained, which is much smaller than in reference carbon catalyst supports. This highly dispersed Pt/CMK-5 material led to superior performance in the O_2 reduction in a fuel cell setup, the peak activity at a reduction potential of +0.900 V was 100 A g^{-1}(Pt) at a loading level 33 wt%, whereas the standard Pt/carbon electrode (Vulcan-carbon) showed very poor activity (<10 A g^{-1}(Pt)) (Fig. 15). This is attributed to the fact that the reduction potential of the Pt/CMK electrode is shifted to a more positive value and the catalytic current increased sharper than with the standard electrode. These properties are useful for the construction of fuel cell anodes.

Some interesting electrochemical properties, high electric double-layer capacitance (EDLC) [442,443] or specific lithium capacitance [444], of other ordered mesoporous carbon (CMK-3) have also been reported. The EDLC of mesoporous carbon (surface area = 1257 m^2/g and pore diameter = 2.3 nm) was reported to be 120 Fg^{-1}. Although the value is lower than for the reference carbon material (MSC25, 200 Fg^{-1} with 1970 m^2/g and <2.0 nm), the mesoporous carbon exhibited a higher critical scan rate than the MSC25 [442]. In another report, it was described that the CMK-3 modified electrode showed an EDLC of 60–90 F/g at a scan rate from 5×10^{-4} to 5×10^{-2} V/s in the range of 1.5 and 3.4 V (Li/Li^+). The specific capacitance was estimated to 10 μF/cm^2, although the capacity decreased to 20% of the initial value after 100 cycles [443]. High lithium intercalation/de-intercalation capacity, which is closely linked to the negative electrode in the re-chargeable lithium battery, has been reported by Zhou et al. [444]. The reversible storage capacity of 850–1100 mAh/g over up to 20 cycles of the CMK-3 electrode is appreciably higher than that for pyrolyzed poly(vinyl chloride) (710 mAh/g) or densely packed bundles of single-wall nanotubes, SWNTs, (595.2 mAh/g). Because of the fact that the porous SWNTs electrode gave a lower value than CMK-3, the authors suggested that the 3D ordered structure of CMK-3 perhaps plays a key role in this phenomenon.

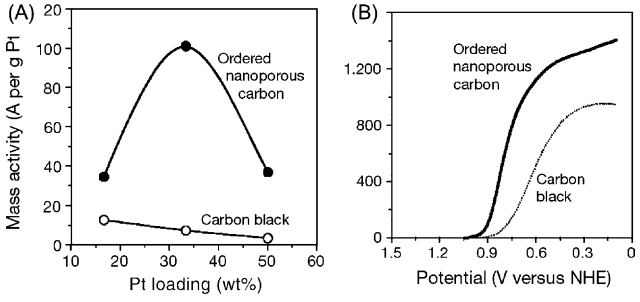

Fig. 15. Electrocatalytic mass activities of Pt/CMK-5 and Pt/carbon (Vulcan) for the O_2 reduction. (A) Catalytic activity in amperes per gram of Pt measured at a potential of +0.900 V with respect to the normal hydrogen electrode. (B) Activity-potential relation for 33 wt% of Pt/CMK-5 and Pt/carbon at a scan rate of 50 mV s^{-1}. The activities were measured on a rotating disk electrode coated with carbon catalysts and rotating at 10,000 r.p.m in 0.1 M $HClO_4$ saturated with O_2 [290].

Very recently, Choi and Ryoo reported a surface-polymer coated mesoporous carbon [445]. The resultant polymer–carbon composite material shows extremely high mechanical strength simultaneously with high electric conductivity, suggesting new application fields for such materials as fuel-cell electrode.

Recently an ordered mesoporous carbon has been used for the assembly of a magnetically separable hydrogenation catalyst [446]. To achieve this goal, the first steps up to the carbonization of the polymer are identical as in the synthesis of CMK-3 type carbon. However, before removal of the silica, magnetic nanoparticles are deposited, which are located exclusively on the external surface, since the pore system is still blocked. After protecting the magnetic particles by a thin carbon shell and removal of the silica by HF or NaOH, a magnetic, highly porous carbon is achieved. Such a magnetic carbon loaded with palladium as hydrogenation catalyst could be completely removed by a magnet from the reaction solution in the test case of the hydrogenation of octene.

It should be added, that non-silica mesoporous materials are not only useful in catalysis, but also, for example, as ion exchangers [434] or as adsorbents [447].

6. Conclusion

There are many strategies for the design and the preparation of mesoporous catalysts. The narrow and uniform pore size of mesoporous materials with extremely high surface area holds much promise for the development of novel solid catalysts. Substitution of elements in the framework, impregnation of active components, and immobilization of active species with pre-determined structure can create well-isolated sites with uniform properties. Varying wall components, as well as surface coating or treatment with hydrophobic organic compounds can result in the formation of new functions. As far as we are aware, there are no other examples in which the same type of material can be modified

by so many different means as schematically shown in Fig. 2. This fact also highlights the high potential of these mesoporous materials. However, one should keep in mind that the large number of different modifications of these materials is also triggered by the many reports already available in the literature and the fascination these highly regular materials create.

Attempts of strong acid catalysis by mesoporous catalysts to extend the range of applications of microporous catalysts failed so far. However, the mild acidity of the ordered mesoporous materials themselves is very attractive in fine chemicals synthesis as the many studies report. The wide pore openings of the mesoporous catalysts minimize mass transfer problems of bulky reactants and products which may be encountered in zeolitic catalyst. Also, the large pores allow the use bulky oxidants in fine chemical oxidation. Such oxidation reactions are very important in fine chemicals synthesis, and since the resulting compounds are often high value added products, these rather expensive oxidants can be tolerated. The inorganic materials with their high surface area and rather wide pores are also highly suitable for immobilization of space-active homogeneous catalysts. In most of the cases, the immobilized catalytic species worked well in the immobilized state, often actually better than expected.

There are several studies which report characteristic phenomena attributed to the regular mesopore system, which seem to influence the catalytic activity. Detailed studies of these phenomena are in progress in many laboratories, as in most cases satisfying explanations why the ordered mesoporous materials are superior to less ordered catalysts are still lacking. If in the future the effects of the pore system are understood and rationalized, the way to better control the catalytic activity of complex catalyst systems will be more clearly visible and catalysts improved by design on different length scales will become accessible.

Acknowledgment

We would like to thank for the generous continuous funding of the DFG and the FCI over the years we have worked on ordered mesoporous materials, in addition to the basic funding provided by the MPI für Kohlenforschung.

References

[1] K.S.W. Sing, D.H. Everett, R.A.W. Haul, L. Moscou, R.A. Pierotti, J. Rouquerol, T. Siemieniewska, Pure Appl. Chem. 57 (1985) 603.
[2] An exhaustive treatment can be found in F. Schüth, K. Sing, J. WeitkampHandbook of Porous Solids, vol. I–V, Wiley-VCH, Weinheim, 2002.
[3] M.E. Davis, C. Saldarriaga, C. Montes, J. Garces, C. Crowder, Nature 331 (1988) 698.
[4] B.J. Schoeman, J. Sterte, J.-E. Otterstedt, J. Chem. Soc. Chem. Commun. (1993) 994.
[5] A.H. Janssen, A.J. Koster, K.P. de Jong, Angew. Chem. Int. Ed. 40 (2001) 1102.
[6] I. Schmidt, A. Boisen, E. Gustavsson, K. Ståhl, S. Pehrson, S. Dahl, A. Carlsson, C.J.H. Jacobsen, Chem. Mater. 13 (2001) 4416.
[7] V. Chiola, J.E. Ritsko, C.D. Vanderpool, US Patent No. 3 556 725, 1971.
[8] F. Di Renzo, H. Cambon, R. Dutartre, Micropor. Mater. 10 (1997) 283.
[9] J.S. Beck, C.T.-W. Chu, I.D. Johnson, C.T. Kresge, M.E. Leonowicz, W.J. Roth, J.W. Vartuli, WO Patent 91/11390, 1991.
[10] C.T. Kresge, M.E. Leonowicz, W.J. Roth, J.C. Vartuli, J.S. Beck, Nature 359 (1992) 710.
[11] J.S. Beck, J.C. Vartuli, W.J. Roth, M.E. Leonowicz, C.T. Kresge, K.D. Schmitt, C.T.W. Chu, D.H. Olson, E.W. Sheppard, S.B. McCullen, J.B. Higgins, J.L. Schlenker, J. Am. Chem. Soc. 114 (1992) 10834.
[12] T. Yanagisawa, T. Shimizu, K. Kuroda, C. Kato, Bull. Chem. Soc. Jpn. 63 (1990) 988.
[13] S. Inagaki, Y. Fukushima, K. Kuroda, J. Chem. Soc. Chem. Commun. (1993) 680.
[14] S. Inagaki, A. Koiwai, N. Suzuki, Y. Fukushima, K. Kuroda, Bull. Chem. Soc. Jpn. 69 (1996) 1449.
[15] A. Corma, Chem. Rev. 97 (1997) 2373.
[16] U. Ciesla, F. Schüth, Micropor. Mesopor. Mater. 27 (1999) 131.
[17] M. Lindén, S. Schacht, F. Schüth, A. Steel, K. Unger, J. Porous. Mater. 5 (1998) 177.
[18] A. Tuel, Micropor. Mesopor. Mater. 27 (1999) 151.
[19] P. Selvam, S.K. Bhatia, C.G. Sonwane, Ind. Eng. Chem. Res. 40 (2001) 3237.
[20] Y. Liu, T.J. Pinnavaia, J. Mater. Chem. 12 (2002) 3179.
[21] J.M. Thomas, Angew. Chem. Int. Ed. 38 (1999) 3588.
[22] R. Anwander, Chem. Mater. 13 (2001) 4419.
[23] J.Y. Ying, C.P. Mehnert, M.S. Wong, Angew. Chem. Int. Ed. 38 (1999) 56.
[24] X. He, D. Antonelli, Angew. Chem. Int. Ed. 41 (2002) 214.
[25] A.P. Wight, M.E. Davis, Chem. Rev. 102 (2002) 3589.
[26] D.E. De Vos, M. Dams, B.F. Sels, P.A. Jacobs, Chem. Rev. 102 (2002) 3615.
[27] G.J. de A.A. Soler-Illia, C. Sanchez, B. Leveau, J. Patarin, Chem. Rev. 102 (2002) 4093.
[28] D. Trong On, D. Desplantier-Giscard, C. Danumah, S. Kaliaguine, Appl. Catal. A: Gen. 253 (2003) 545.
[29] A. Wingen, F. Kleitz, F. Schüth, in: M. Baerns (Ed.), Basic Principles in Applied Catalysis, Springer, Berlin, 2003, p. 281.
[30] F. Schüth, Chem. Mater. 13 (2001) 3184.
[31] F. Di Renzo, A. Galarneau, P. Trens, F. Fajula, in: F. Schüth, K.S.W. Sing, J. Weitkamp (Eds.), Handbook of Porous Solids, Wiley-VCH, Weinheim, 2002, p. 1311.
[32] A. Monnier, F. Schüth, Q. Huo, D. Kumar, D. Margolese, R.S. Maxwell, G. Stucky, M. Krishnamurty, P. Petroff, A. Firouzi, M. Janicke, B. Chmelka, Science 261 (1993) 1299.
[33] Q. Huo, D. Margolese, U. Ciesla, P. Feng, T. Gier, P. Sieger, R. Leon, P.M. Petroff, U. Ciesla, F. Schüth, G. Stucky, Nature 368 (1994) 317.
[34] Q. Huo, D. Margolese, U. Ciesla, D. Demuth, P. Feng, T. Gier, P. Sieger, A. Firouzi, B. Chmelka, F. Schüth, G.D. Stucky, Chem. Mater. 6 (1994) 1176.
[35] G.S. Attard, J.C. Glyde, C.G. Göltner, Nature 378 (1995) 366.
[36] R. Ryoo, S.H. Joo, S. Jun, J. Phys. Chem. B 103 (1999) 7743.
[37] A.H. Lu, W. Schmidt, A. Taguchi, B. Spliethoff, B. Tesche, F. Schüth, Angew. Chem. Int. Ed. 41 (2002) 3489.

[38] J.N. Israelachivili, D.J. Mitchell, B.W. Ninham, J. Chem. Soc. Faraday Trans. 72 (2) (1976) 1525.
[39] J.N. Israelachivili, Intermolecular and Surface Forces, Academic Press, London, 1991.
[40] G.D. Stucky, A. Monnier, F. Schüth, Q. Huo, D. Margolese, D. Kumar, M. Krishnamurty, P. Petroff, A. Firouzi, M. Janicke, B.F. Chmelka, Mol. Cryst. Liq. Cryst. 240 (1994) 187.
[41] A. Firouzi, D. Kumar, L.M. Bull, T. Besier, P. Sieger, Q. Huo, S.A. Walker, J.A. Zasadzinski, C. Glinka, J. Nicol, D.I. Margolese, G.D. Stucky, B.F. Chmelka, Science 267 (1995) 1138.
[42] J.C. Vartuli, K.D. Schmitt, C.T. Kresge, W.J. Roth, M.E. Leonowicz, S.B. McCullen, S.D. Hellring, J.S. Beck, J.L. Schlenker, D.H. Olson, E.W. Sheppard, Chem. Mater. 6 (1994) 2317.
[43] Q. Huo, R. Leon, P.M. Petroff, G.D. Stucky, Science 268 (1995) 1324.
[44] Q. Huo, D.I. Margolese, G.D. Stucky, Chem. Mater. 8 (1996) 1147.
[45] S. Che, A.E. Garcia-Bennett, T. Yokoi, K. Sakamoto, H. Kunieda, O. Terasaki, T. Tatsumi, Nature Mater. 2 (2003) 801.
[46] A.E. Garcia-Bennett, O. Terasaki, S. Che, T. Tatsumi, Chem. Mater. 16 (2004) 813.
[47] M. Lindén, P. Ågren, S. Karlsson, P. Bussian, H. Amenitsch, Langmuir 16 (2000) 5831.
[48] N. Ulagappan, C.N.R. Rao, Chem. Commun. (1996) 2759.
[49] A. Lind, J. Andersson, S. Karlsson, P. Ågren, P. Bussian, H. Amenitsch, M. Lindén, Langmuir 18 (2002) 1380.
[50] S. Namba, A. Mochizuki, M. Kito, Chem. Lett. (1998) 569.
[51] U. Ciesla, D.G. Demuth, R. Leon, P.M. Petroff, G.D. Stucky, K.K. Unger, F. Schüth, J. Chem. Soc. Chem. Commun. (1994) 1387.
[52] D.M. Antonelli, J.Y. Ying, Angew. Chem. Int. Ed. 34 (1995) 2014.
[53] U. Ciesla, S. Schacht, G.D. Stucky, K. Unger, F. Schüth, Angew. Chem. Int. Ed. Engl. 35 (1996) 541.
[54] P.T. Tanev, T.J. Pinnavaia, Science 267 (1995) 865.
[55] P.T. Tanev, M. Chibwe, T.J. Pinnavaia, Nature 368 (1994) 321.
[56] S.A. Bagshaw, E. Prouzet, T.J. Pinnavaia, Science 269 (1995) 1242.
[57] T.R. Pauly, Y. Liu, T.J. Pinnavaia, S.J.L. Billige, T.P. Rieker, J. Am. Chem. Soc. 121 (1997) 8835.
[58] E. Prouzet, T.J. Pinnavaia, Angew. Chem. Int. Ed. 36 (1997) 516.
[59] K. Cassiers, P. Van Der Voort, E.F. Vansant, Chem. Commun. (2000) 2489.
[60] P.T. Tanav, T.J. Pinnavaia, Chem. Mater. 8 (1996) 2068.
[61] W. Zhang, T.R. Pauly, T.J. Pinnavaia, Chem. Mater. 9 (1997) 2491.
[62] D. Zhao, Q. Huo, J. Feng, B.F. Chmelka, G.D. Stucky, J. Am. Chem. Soc. 120 (1998) 6024.
[63] D. Zhao, J. Feng, Q. Huo, N. Melosh, G.H. Fredrickson, B.F. Chmelka, G.D. Stucky, Science 279 (1998) 548.
[64] P. Yang, D. Zhao, D.I. Margolese, B.F. Chmelka, G.D. Stucky, Nature 396 (1998) 152.
[65] P. Yang, D. Zhao, D.I. Margolese, B.F. Chmelka, G.D. Stucky, Chem. Mater. 11 (1999) 2813.
[66] A. Galarneau, H. Cambon, F.D. Renzo, R. Ryoo, M. Choi, F. Fajula, New J. Chem. 27 (2003) 73.
[67] M. Impéror-Clerc, P. Davidson, A. Davidson, J. Am. Chem. Soc. 122 (2000) 11925.
[68] R. Ryoo, C.H. Ko, M. Kruk, V. Antochshuk, M. Jaroniec, J. Phys. Chem. B 104 (2000) 11465.
[69] Z. Liu, O. Terasaki, T. Ohsuna, K. Hiraga, H.J. Shin, R. Ryoo, Chem. Phys. Chem. 2 (2001) 229.
[70] S.A. Bagshaw, T.J. Pinnavaia, Angew. Chem. Int. Ed. 35 (1996) 1102.
[71] B. Lee, D. Lu, J.N. Kondo, K. Domen, Chem. Commun. (2001) 2118.
[72] D.M. Antonelli, J.Y. Ying, Angew. Chem. Int. Ed. 35 (1996) 426.
[73] D.M. Antonelli, J.Y. Ying, Chem. Mater. 8 (1996) 874.
[74] D.M. Antonelli, A. Nakahira, J.Y. Ying, Inorg. Chem. 35 (1996) 3126.
[75] J.J.E. Moreau, L. Vellutini, M.W.C. Man, C. Bied, J.-L. Bantignies, P. Dieudonné, J.-L. Sauvojol, J. Am. Chem. Soc. 123 (2001) 7957.
[76] E. Ruiz-Hitzky, S. Letaïef, V. Prévot, Adv. Mater. 14 (2002) 439.
[77] A. Shimojima, K. Kuroda, Angew. Chem. Int. Ed. 42 (2003) 4057.
[78] G.S. Attard, C.G. Göltner, J.M. Corker, S. Henke, R.H. Templer, Angew. Chem. Int. Ed. 36 (1997) 1315.
[79] C.G. Göltner, M. Antonietti, Adv. Mater. 9 (1997) 431.
[80] G.S. Attard, P.N. Bartlett, N.R.B. Coleman, J.M. Elliott, J.R. Owen, J.H. Wang, Science 278 (1997) 838.
[81] A.H. Whitehead, J.M. Elliott, J.R. Owen, G.S. Attard, Chem. Commun. (1999) 331.
[82] P.V. Braun, P. Osenar, S.I. Stupp, Nature 380 (1996) 325.
[83] H. Kang, Y.-W. Jun, J.-I. Park, K.-B. Lee, J. Cheon, Chem. Mater. 12 (2000) 3530.
[84] S.A. Johnson, D. Khushalani, N. Coombs, T.E. Mallouk, G.A. Ozin, J. Mater. Chem. 8 (1998) 13.
[85] J.Y. Kim, S.B. Yoon, F. Kooli, J.-S. Yu, J. Mater. Chem. 11 (2001) 2912.
[86] S.C. Laha, R. Ryoo, Chem. Commun. (2003) 2138.
[87] K. Zhu, B. Yue, W. Zhou, H. He, Chem. Commun. (2003) 98.
[88] B. Tian, X. Liu, H. Yang, S. Xie, C. Yu, B. Tu, D. Zhao, Adv. Mater. 15 (2003) 1370.
[89] K. Lee, Y.-H. Kim, S.B. Han, H. Kang, S. Park, W.S. Seo, J.T. Park, B. Kim, S. Chang, J. Am. Chem. Soc. 125 (2003) 6844.
[90] H. Yang, Q. Shi, B. Tian, Q. Lu, F. Gao, S. Xie, J. Fan, C. Yu, B. Tu, D. Zhao, J. Am. Chem. Soc. 125 (2003) 4724.
[91] B. Tian, X. Liu, L.A. Solovyov, Z. Liu, H. Yang, Z. Zhang, S. Xie, F. Zhang, B. Tu, C. Yu, O. Terasaki, D. Zhao, J. Am. Chem. Soc. 126 (2004) 865.
[92] Y. Wang, C.M. Yang, W. Schmidt, B. Spliethoff, F. Schüth, Adv. Mater. (in press).
[93] M. Kang, S.H. Yi, H.I. Lee, J.E. Yie, J.M. Kim, Chem. Commun. (2002) 1944.
[94] A. Lu, W. Schmidt, F. Schüth, Chem. Eur. J. (in press).
[95] A. Galarneau, A. Barodawalla, T.J. Pinnavaia, Nature 374 (1995) 529.
[96] A. Galarneau, D. Desplantier-Giscard, F. di Renzo, F. Fajula, Catal. Today 68 (2001) 191.
[97] K. Cassiers, T. Linssen, M. Mathieu, M. Benjelloun, K. Schrijnemakers, P. Van Der Voort, P. Cool, E.F. Vansant, Chem. Mater. 14 (2002) 2317.
[98] N. Igarashi, K.A. Koyano, Y. Tanaka, S. Nakata, K. Hashimoto, T. Tatsumi, Micropor. Mesopor. Mater. 59 (2003) 43.
[99] R. Ryoo, S. Jun, J. Phys. Chem. B 101 (1997) 317.
[100] J.M. Kisler, M.L. Gee, G.W. Stevens, A.J. O'Connor, Chem. Mater. 15 (2003) 619.
[101] A.S. O'Neil, R. Mokaya, M. Poliakoff, J. Am. Chem. Soc. 124 (2002) 10636.
[102] S.L. Burkett, S.D. Sim, S. Mann, Chem. Commun. (1996) 1367.
[103] D.J. Macquarrie, Chem. Commun. (1996) 1961.
[104] S. Inagaki, S. Guan, Y. Fukushima, T. Ohsuna, O. Terasaki, J. Am. Chem. Soc. 121 (1999) 9611.
[105] D. Brunel, Micropor. Mesopor. Mater. 27 (1999) 329.
[106] A. Stein, B.J. Melde, R.C. Schroden, Adv. Mater. 12 (2000) 1403.

[107] M.J. MacLachlan, T. Asefa, G.A. Ozin, Chem. Eur. J. 6 (2000) 2507.
[108] A. Sayari, S. Hamoudi, Chem. Mater. 13 (2001) 3151.
[109] F. Schüth, Y. Wang, C.-M. Yang, B. Zibrowius, in: N. Auner (Ed.), Organosilicon Chemistry VI, Wiley-VCH, in press.
[110] R. Mokaya, Angew. Chem. Int. Ed. 38 (1999) 2930.
[111] R. Mokaya, W. Jones, J. Mater. Chem. 9 (1999) 555.
[112] R.D. Oldroyd, G. Sankar, J.M. Thomas, D. Özkaya, J. Phys. Chem. B. 102 (1998) 1849.
[113] M. Jia, A. Seifert, W.R. Thiel, Chem. Mater. 15 (2003) 2174.
[114] M.J. Climent, A. Corma, S. Iborra, S. Miquel, J. Primo, F. Rey, J. Catal. 183 (1999) 76.
[115] A. Bhaumik, T. Tatsumi, J. Catal. 189 (2000) 31.
[116] M.L. Peña, V. Dellarocca, F. Rey, A. Corma, S. Coluccia, L. Marchese, Micropor. Mesopor. Mater. 44–45 (2001) 345.
[117] P. Wu, T. Tatsumi, T. Komatsu, T. Yashima, Chem. Mater. 14 (2002) 1657.
[118] D.-W. Park, S.-D. Choi, S.-J. Choi, C.-Y. Lee, G.-J. Kim, Catal. Lett. 78 (2002) 145.
[119] L. Vradman, M.V. Landau, M. Herskowitz, V. Ezersky, M. Talianker, S. Nikitenko, Y. Koltypin, A. Gedanken, J. Catal. 213 (2003) 163.
[120] S.-T. Wong, H.-P. Lin, C.-Y. Mou, Appl. Catal. A: Gen. 198 (2000) 103.
[121] H.P. Lin, C.Y. Mou, Science 273 (1996) 765.
[122] H.-P. Lin, S. Cheng, C.-Y. Mou, Micropor. Mater. 10 (1997) 111.
[123] W.-H. Chen, Q. Zhao, H.-P. Lin, Y.-S. Yang, C.-Y. Mou, S.-B. Liu, Micropor. Mesopor. Mater. 66 (2003) 209.
[124] H. Yang, A. Kuperman, N. Coombs, S. Mamiche-Afara, G.A. Ozin, Nature 379 (1996) 703.
[125] S. Schacht, Q. Huo, G.D. Stucky, F. Schüth, Science 273 (1996) 768.
[126] D. Zhao, P. Yang, N. Melosh, J. Feng, B.F. Chmelka, G.D. Stucky, Adv. Mater. 10 (1998) 1380.
[127] Q. Huo, D. Zhao, J. Feng, K. Weston, S.K. Buratto, G.D. Stucky, S. Schacht, F. Schüth, Adv. Mater. 9 (1997) 974.
[128] F. Marlow, F. Kleitz, Micropor. Mesopor. Mater. 44–45 (2001) 671.
[129] F. Kleitz, F. Schüth, G.D. Stucky, F. Marlow, Chem. Mater. 13 (2001) 3587.
[130] J. Wang, J. Zhang, B.Y. Asoo, G.D. Stucky, J. Am. Chem. Soc. 125 (2003) 13966.
[131] F. Kleitz, U. Wilczok, F. Schüth, F. Marlow, Phys. Chem. Chem. Phys. 3 (2001) 3486.
[132] P.J. Bruinsma, A.Y. Kim, J. Liu, S. Baskaran, Chem. Mater. 9 (1997) 2507.
[133] Y.F. Lu, H.Y. Fan, A. Stump, T.L. Ward, T. Rieker, C.J. Brinker, Nature 398 (1999) 223.
[134] Q. Huo, J. Feng, F. Schüth, G.D. Stucky, Chem. Mater. 9 (1997) 14.
[135] S.H. Tolbert, A. Firouzi, G.D. Stucky, B.F. Chmelka, Science 278 (1997) 264.
[136] M. Ogawa, Chem. Commun. (1996) 1149.
[137] B.T. Holland, L. Abrams, A. Stein, J. Am. Chem. Soc. 121 (1999) 4308.
[138] J.-H. Smått, S. Schunk, M. Lindén, Chem. Mater. 15 (2003) 2354.
[139] L.T. Zhuravlev, Langmuir 3 (1987) 316.
[140] M. Widenmeyer, R. Anwander, Chem. Mater. 14 (2002) 1827.
[141] X.S. Zhao, G.Q. Lu, A.K. Whittaker, G.J. Millar, H.Y. Zhu, J. Phys. Chem. B 101 (1997) 6525.
[142] H. Landmesser, H. Kosslick, W. Storek, R. Fricke, Solid State Ion. 101–103 (1997) 271.
[143] J. Jarupatrakorn, T.D. Tilley, J. Am. Chem. Soc. 124 (2002) 8380.
[144] C. Nozaki, C.G. Lugmair, A.T. Bell, T.D. Tilley, J. Am. Chem. Soc. 124 (2002) 13194.
[145] M.F. Ottaviani, A. Galarneau, D. Desplantiers-Giscard, F. Di Renzo, F. Fajula, Micropor. Mesopor. Mater. 44–45 (2001) 1.
[146] A. Corma, M.T. Navarro, M. Renz, J. Catal. 219 (2003) 242.
[147] C.Y. Chen, H.X. Li, M.E. Davis, Micropor. Mater. 2 (1993) 17.
[148] A. Corma, V. Fornés, M.T. Navarro, J. Pérez-Pariente, J. Catal. 148 (1994) 569.
[149] M. Hunger, U. Schenk, M. Breuninger, R. Gläser, J. Weitkamp, Micropor. Mesopor. Mater. 27 (1999) 261.
[150] A. Jentys, K. Kleestorfer, H. Vinek, Micropor. Mesopor. Mater. 27 (1999) 321.
[151] B. Chakraborty, B. Viswanathan, Catal. Today 49 (1999) 253.
[152] H. Landmesser, H. Kosslick, U. Kürschner, R. Fricke, J. Chem. Soc. Faraday Trans. 94 (1998) 971.
[153] L.Y. Chen, Z. Ping, G.K. Chuah, S. Jaenicke, G. Simon, Micropor. Mesopor. Mater. 27 (1999) 231.
[154] A. Auroux, Top. Catal. 19 (2002) 205.
[155] R. Schmidt, D. Akporiaye, M. Stöcker, O.H. Ellestad, Chem. Commun. (1994) 1493.
[156] Z. Luan, C.-F. Cheng, H. He, J. Klinowski, J. Phys. Chem. 99 (1995) 10590.
[157] R.B. Borade, A. Clearfield, Catal. Lett. 31 (1995) 267.
[158] M.L. Occelli, S. Biz, A. Auroux, G.J. Ray, Micropor. Mesopor. Mater. 26 (1998) 193.
[159] Y. Yue, A. Gédéon, J.-L. Bonardet, N. Melosh, J.-B. D'Espinose, J. Fraissard, Chem. Commun. (1999) 1967.
[160] T. Takeguchi, J.-B. Kim, M. Kang, T. Inui, W.-T. Cheuh, G.L. Haller, J. Catal. 175 (1998) 1.
[161] M.V. Landau, E. Dafa, M.L. Kaliya, T. Sen, M. Herskowitz, Micropor. Mesopor. Mater. 49 (2001) 65.
[162] R. Ryoo, S. Jun, J.M. Kim, M.J. Kim, Chem. Commun. (1997) 2225.
[163] Y. Zhu, S. Jaenicke, G.K. Chuah, J. Catal. 218 (2003) 396.
[164] K.R. Kloetstra, H. van Bekkum, J.C. Jansen, Chem. Commun. (1997) 2281.
[165] Z. Zhang, Y. Han, L. Zhu, R. Wang, Y. Yu, S. Qiu, D. Zhao, F.-S. Xiao, Angew. Chem. Int. Ed. 40 (2001) 1258.
[166] Y. Liu, W. Zhang, T.J. Pinnavaia, Angew. Chem. Int. Ed. 40 (2001) 1255.
[167] W. Guo, L. Huang, P. Deng, Z. Xue, Q. Li, Micropor. Mesopor. Mater. 44–45 (2001) 427.
[168] X. Meng, D. Li, X. Yang, Y. Yu, S. Wu, Y. Han, Q. Yang, D. Jiang, F.-S. Xiao, J. Phys. Chem. B 107 (2003) 8972.
[169] S.P.B. Kremer, C.E.A. Kirschhock, A. Aerts, K. Villani, J.A. Martens, O.I. Lebedev, G. Van Tendeloo, Adv. Mater. 15 (2003) 1705.
[170] D. Trong On, S. Kaliaguine, Angew. Chem. Int. Ed. 41 (2002) 1036.
[171] D. Trong-On, A. Ungureanu, S. Kaliaguine, Phys. Chem. Chem. Phys. 5 (2003) 3534.
[172] D. Trong On, S. Kaliaguine, in: S.-E. Park, R. Ryoo, W.-S. Ahn, C.W. Lee, J.-S. Chang (Eds.), Nanotechnology in Mesostructured Materials, Studies in Surface Science Catalysis, vol. 146, Elsevier, Amsterdam, 2003, p. 561.
[173] M. Onaka, R. Yamazaki, Chem. Lett. (1998) 259.
[174] R.T. Yang, T.J. Pinnavaia, W. Li, W. Zhang, J. Catal. 172 (1997) 488.
[175] C. Liu, X. Ye, Y. Wu, Catal. Lett. 36 (1996) 263.
[176] C. Liu, Y. Shan, X. Yang, X. Ye, Y. Wu, J. Catal. 168 (1997) 35.
[177] S.S. Kim, W.Z. Zhang, T.J. Pinnavaia, Catal. Lett. 43 (1997) 149.
[178] J. Połtowicz, E.M. Serwicka, E. Bastardo-Gonzalez, W. Jones, R. Mokaya, Appl. Catal. A: Gen. 218 (2001) 211.
[179] L. Frunza, H. Kosslick, H. Landmesser, E. Höft, R. Fricke, J. Mol. Catal. A: Chem. 123 (1997) 179.

[180] G.J. Kim, S.H. Kim, Catal. Lett. 57 (1999) 139.
[181] D. Trong On, P.N. Joshi, S. Kaliaguine, J. Phys. Chem. 100 (1996) 6743.
[182] K. Okumura, K. Nishigaki, M. Niwa, Micropor. Mesopor. Mater. 44–45 (2001) 509.
[183] M.D. Alba, Z. Luan, J. Klinowski, J. Phys. Chem. 100 (1996) 2178.
[184] A. Corma, M.T. Navarro, J. Pérez Pariente, J. Chem. Soc. Chem. Commun. (1994) 147.
[185] J. El Haskouri, S. Cabrera, M. Gutierrez, A. Beltrán-Porter, D. Beltrán-Porter, M.D. Marcos, P. Amorós, Chem. Commun. (2001) 309.
[186] M.A. Markowitz, S. Jayasundera, J.B. Miller, J. Klaehn, M.C. Burleigh, M.S. Spector, S.L. Golledge, D.G. Castner, B.P. Gaber, Dalton Trans. (2003) 3398.
[187] T. Maschmeyer, F. Rey, G. Sankar, J.M. Thomas, Nature 378 (1995) 159.
[188] B.J. Aronson, C.F. Blanford, A. Stein, Chem. Mater. 9 (1997) 2842.
[189] P. Wu, M. Iwamoto, J. Chem. Soc. Faraday Trans. 94 (1998) 2871.
[190] A. Hagen, D. Wei, G.L. Haller, in: L. Bonneviot, F. Béland, C. Danuhma, S. Giasson, S. Kaliaguine (Eds.), Mesoporous Molecular Sieves 1998, Studies in Surface Science Catalysis, vol. 117, Elsevier, Amsterdam, 1998, p. 191.
[191] M. Widenmeyer, S. Grasser, K. Köhler, R. Anwander, Micropor. Mesopor. Mater. 44–45 (2001) 327.
[192] Z. Luan, E.M. Maes, P.A.W. van der Heide, D. Zhao, R.S. Czernuszewicz, L. Kevan, Chem. Mater. 11 (1999) 3680.
[193] M. Yonemitsu, Y. Tanaka, M. Iwamoto, Chem. Mater. 9 (1997) 2679.
[194] M. Yonemitsu, Y. Tanaka, M. Iwamoto, J. Catal. 178 (1998) 207.
[195] Q. Zhang, Y. Wang, Y. Ohishi, T. Shishido, K. Takehira, J. Catal. 202 (2001) 308.
[196] N. Lang, P. Delichere, A. Tuel, Micropor. Mesopor. Mater. 56 (2002) 203.
[197] Y. Wang, Q. Zhang, T. Shishido, K. Takehira, J. Catal. 209 (2002) 186.
[198] P. Van Der Voort, M. Morey, G.D. Stucky, M. Mathieu, E.F. Vansant, J. Phys. Chem. B 102 (1998) 585.
[199] M. Morey, A. Davidson, H. Eckert, G. Stucky, Chem. Mater. 8 (1996) 486.
[200] V. Caps, S.C. Tshang, Catal. Today 61 (2000) 19.
[201] P. Van Der Voort, E.F. Vansant, J. Phys. Chem. B 103 (1999) 10102.
[202] P. Van Der Voort, E.F. Vansant, Micropor. Mesopor. Mater. 38 (2000) 385.
[203] P. Van Der Voort, E.F. Vansant, in: A. Sayari, M. Jaroniec, T.J. Pinnavaia (Eds.), Nanoporous Materials II, Studies in Surface Science Catalysis, vol. 129, Elsevier, Amsterdam, 2000, p. 317.
[204] A. Roucoux, J. Schulz, H. Patin, Chem. Rev. 102 (2002) 3757.
[205] U. Junges, W. Jacobs, I. Voigt-Martin, B. Krutzsch, F. Schüth, J. Chem. Soc. Chem. Commun. (1995) 2283.
[206] M.Á. Aramendia, V. Borau, C. Jiménez, J.M. Marinas, F.J. Romero, Chem. Commun. (1999) 873.
[207] N. Yao, C. Pinckney, S. Lim, C. Pak, G.L. Haller, Micropor. Mesopor. Mater. 44–45 (2001) 377.
[208] J.A. Darr, M. Poliakoff, Chem. Rev. 99 (1999) 495.
[209] H. Wakayama, N. Setoyama, Y. Fukushima, Adv. Mater. 15 (2003) 742.
[210] P.L. Dhepe, A. Fukushima, M. Ichikawa, Chem. Commun. (2003) 590.
[211] C.M. Yang, P.H. Liu, Y.F. Ho, C.Y. Chiu, K.J. Chao, Chem. Mater. 15 (2002) 275.
[212] A.H. Janssen, C.-M. Yang, Y. Wang, F. Schüth, A.J. Koster, K.P. de Jong, J. Phys. Chem. B 107 (2003) 10552.
[213] C.M. Yang, M. Kalwei, F. Schüth, K.J. Chao, Appl. Catal. A: Gen. 254 (2003) 289.
[214] S. Suvanto, T.A. Pakkanen, L. Backman, Appl. Catal. A: Gen. 177 (1999) 25.
[215] S. Suvanto, J. Hukkamäki, T.T. Pakkanen, T.A. Pakkanen, Langmuir 16 (2000) 4109.
[216] T. Yamamoto, T. Shido, S. Inagaki, Y. Fukushima, M. Ichikawa, J. Am. Chem. Soc. 118 (1996) 5810.
[217] T. Yamamoto, T. Shido, S. Inagaki, Y. Fukushima, M. Ichikawa, J. Phys. Chem. B 102 (1998) 3866.
[218] W. Zhou, J.M. Thomas, D.S. Shephard, B.F.G. Johnson, D. Ozkaya, T. Maschmeyer, R.G. Bell, Q. Ge, Science 280 (1998) 705.
[219] D.S. Shephard, T. Maschmeyer, G. Sankar, J.M. Thomas, D. Ozkaya, B.F.G. Johnson, R. Raja, R.D. Oldroyd, R.G. Bell, Chem. Eur. J. 4 (1998) 1214.
[220] S. Hermans, R. Raja, J.M. Thomas, B.F.G. Johnson, G. Sankar, D. Gleeson, Angew. Chem. Int. Ed. 40 (2001) 1211.
[221] R. Raja, T. Khimyak, J.M. Thomas, S. Hermans, B.F.G. Johnson, Angew. Chem. Int. Ed. 40 (2001) 4638.
[222] E. Brivio, A. Ceriotti, R.D. Pergola, L. Garlaschelli, F. Domartin, M. Manassero, M. Sansoni, P. Zanello, F. Laschi, B.T. Heaton, J. Chem. Soc. Dalton Trans. (1994) 3237.
[223] R. Raja, G. Sankar, S. Hermans, D.S. Shephard, S. Bromley, J.M. Thomas, B.F.G. Johnson, Chem. Commun. (1999) 1571.
[224] F. Schüth, A. Wingen, J. Sauer, Micropor. Mesopor. Mater. 44–45 (2001) 465.
[225] W. Stichert, F. Schüth, Chem. Mater. 10 (1998) 2020.
[226] M.V. Landau, L. Titelman, L. Vradman, P. Wilson, Chem. Commun. (2003) 594.
[227] T. Abe, Y. Tachibana, T. Uematsu, M. Iwamoto, J. Chem. Soc. Chem. Commun. (1995) 1617.
[228] M. Iwamoto, T. Abe, Y. Tachibana, J. Mol. Catal. A: Chem. 155 (2000) 143.
[229] M. Fröba, R. Köhn, G. Bouffaud, Chem. Mater. 11 (1999) 2858.
[230] L. Zhang, G.C. Papaefthymiou, J.Y. Ying, J. Phys. Chem. B 105 (2001) 7414.
[231] M. Eswaramoorthy, Neeraj, C.N.R. Rao, Chem. Commun. (1998) 615.
[232] M. Clemente-León, E. Coronado, A. Forment-Aliaga, J.M. Martínez-Agudo, P. Amorós, Polyhedron 22 (2003) 2395.
[233] K.R. Kloetstra, H. van Bekkum, in: H. Chon, S.-K. Ihm, Y.S. Uh (Eds.), Progress in Zeolite and Mesoporous Materials, Studies in Surface Science Catalysis, vol. 105, Elsevier, Amsterdam, 1997, p. 431.
[234] V.R. Choudhary, S.K. Jana, B.P. Kiran, J. Catal. 192 (2000) 257.
[235] V.R. Choudhary, S.K. Jana, J. Mol. Catal. A: Chem. 184 (2002) 247.
[236] J.-M. Clacens, Y. Pouilloux, J. Barrault, Appl. Catal. A: Gen. 227 (2002) 181.
[237] F. Yagi, N. Kanuka, H. Tsuji, H. Kita, H. Hattori, in: H. Hattori, M. Misono, Y. Ono (Eds.), Acid–Base Catalysis II, Studies in Surface Science and Catalysis, vol. 90, Elsevier, Amsterdam, 1994, p. 349.
[238] J. Sauer, F. Marlow, B. Spliethoff, F. Schüth, Chem. Mater. 14 (2002) 217.
[239] S.V. Nguyen, V. Szabo, D. Trong On, S. Kaliaguine, Micropor. Mesopor. Mater. 54 (2002) 51.
[240] I.V. Kozhevnikov, K.R. Kloetstra, A. Sinnema, H.W. Zandbergen, H. van Bekkum, J. Mol. Catal. A: Chem. 114 (1996) 287.
[241] T. Blasco, A. Corma, A. Martínez, P. Martínez-Escolano, J. Catal. 177 (1998) 306.

[242] M.J. Verhoef, P.J. Kooyman, J.A. Peters, H. van Bekkum, Micropor. Mesopor. Mater. 27 (1999) 365.
[243] A. Ghanbari-Siahkali, A. Philippou, J. Dwyer, M.W. Anderson, Appl. Catal. A: Gen. 192 (2000) 57.
[244] Q.-H. Xia, K. Kidajat, S. Kawi, J. Catal. 209 (2002) 433.
[245] T. Okuhara, N. Mizuno, M. Misono, Adv. Catal. 41 (1996) 113.
[246] I.V. Kozhevnikov, Chem. Rev. 98 (1998) 171.
[247] N. Mizuno, M. Misono, Chem. Rev. 98 (1998) 199.
[248] A. Maldotti, A. Molinari, G. Varani, M. Lenarda, L. Storaro, F. Bigi, R. Maggi, A. Mazzacani, G. Sartori, J. Catal. 209 (2002) 210.
[249] T. Ookoshi, M. Onaka, Chem. Commun. (1998) 2399.
[250] K.M. Reddy, B. Wei, C. Song, Catal. Today 43 (1998) 261.
[251] C. Song, K.M. Reddy, Appl. Catal. A: Gen. 176 (1999) 1.
[252] S. Krijnen, H.C.L. Abbenhuis, R.W.J.M. Hanssen, J.H.C. van Hooff, R.A. van Santen, Angew. Chem. Int. Ed. 37 (1998) 356.
[253] E. Rivera-Muñoz, D. Lardizabal, G. Alonso, A. Aguilar, M.H. Siadati, R.R. Chianelli, Catal. Lett. 85 (2003) 147.
[254] P.-P. Knops-Gerrits, D. De Vos, F. Thibault-Starzyk, P.A. Jacobs, Nature 369 (1994) 543.
[255] B. Pugin, J. Mol. Catal. A: Chem. 107 (1996) 273.
[256] H.H. Wagner, H. Hausmann, W.F. Hölderich, J. Catal. 203 (2001) 150.
[257] F.M. de Rego, D.K. Morita, K.C. Ott, W. Tumas, R.D. Broene, Chem. Commun. (2000) 1797.
[258] J. Jamis, J.R. Anderson, R.S. Dickson, E.M. Campi, W.R. Jackson, J. Organomet. Chem. 603 (2000) 80.
[259] C. Bianchini, D.G. Burnaby, J. Evans, P. Frediani, A. Meli, W. Oberhauser, R. Pasaro, L. Sordelli, F. Vizza, J. Am. Chem. Soc. 121 (1999) 5961.
[260] C. Bianchini, V. Dal Santo, A. Meli, W. Oberhauser, R. Pasaro, F. Vizza, Organometallics 19 (2000) 2433.
[261] J.F. Díaz, K.J. Balkus Jr., J. Mol. Catal. B: Enzym. 2 (1996) 115.
[262] H.H.P. Yiu, P.A. Wright, N.P. Botting, Micropor. Mesopor. Mater. 44–45 (2001) 763.
[263] C. Lei, Y. Shin, J. Liu, E.J. Ackerman, J. Am. Chem. Soc. 124 (2002) 11242.
[264] Y.-J. Han, J.T. Watson, G.D. Stucky, A. Butler, J. Mol. Catal. B: Enzym. 17 (2002) 1.
[265] H. Takahashi, B. Li, T. Sasaki, C. Miyazaki, T. Kajino, S. Inagaki, Micropor. Mesopor. Mater. 44–45 (2001) 755.
[266] H.H.P. Yiu, P.A. Wright, N.P. Botting, J. Mol. Catal. B: Enzym. 15 (2001) 81.
[267] A. Kinting, H. Krause, M. Čapka, J. Mol. Catal. 33 (1985) 215.
[268] A. Bleloch, B.F.G. Johnson, S.V. Ley, A.J. Price, D.S. Shephard, A.W. Thomas, Chem. Commun. (1999) 1907.
[269] H.M. Hultman, M. de Lang, M. Nowotny, I.W.C.E. Arends, U. Hanefeld, R.A. Sheldon, T. Maschmeyer, in: E. Gaigneaux, D.E. De Vos, P. Grange, P.A. Jacobs, J.A. Martens, P. Ruiz, G. Poncelet (Eds.), Scientific Bases for the Preparation of Heterogeneous Catalysts, Studies in Surface Science and Catalysis, vol. 143, Elsevier, Amsterdam, 2002, p. 277.
[270] B.F.G. Johnson, S.A. Raynor, D.S. Shephard, T. Maschmeyer, J.M. Thomas, G. Sankar, S. Bromley, R. Oldroyd, L. Gladden, M.D. Mantle, Chem. Commun. (1999) 1167.
[271] S.A. Raynor, J.M. Thomas, R. Raja, B.F.G. Johnson, R.G. Bell, M.G. Mantle, Chem. Commun. (2000) 1925.
[272] R. Anwander, C. Palm, G. Gerstberger, O. Groeger, G. Engelhardt, Chem. Commun. (1998) 1811.
[273] G. Gerstberger, C. Palm, R. Anwander, Chem. Eur. J. 5 (1999) 997.
[274] I. Nagl, M. Widenmeyer, S. Grasser, K. Köhler, R. Anwander, J. Am. Chem. Soc. 122 (2000) 1544.
[275] G. Gerstberger, R. Anwander, Micropor. Mesopor. Mater. 44–45 (2001) 303.
[276] J.M. Thomas, T. Maschmeyer, B.F.G. Johnson, D.S. Shephard, J. Mol. Catal. A: Chem. 141 (1999) 139.
[277] A. Corma, M. Iglesias, C. del Piño, F. Sánchez, J. Organomet. Chem. 431 (1992) 233.
[278] M.V. Landau, in: F. Schüth, K.S.W. Sing, J. Weitkamp (Eds.), Handbook of Porous Solids, Wiley-VCH, Weinheim, 2002, p. 1677.
[279] A. Stein, M. Fendorf, T.P. Jarvie, K.T. Muller, A.J. Benesi, T.E. Mallouk, Chem. Mater. 7 (1995) 304.
[280] F. Kleitz, S.J. Thomson, Z. Liu, O. Terasaki, F. Schüth, Chem. Mater. 14 (2002) 4134.
[281] B. Tian, X. Liu, B. Tu, C. Yu, J. Fan, L. Wang, S. Xie, G.D. Stucky, D. Zhao, Nature Mater. 2 (2003) 159.
[282] H. Yoshitake, T. Tatsumi, Chem. Mater. 15 (2003) 1695.
[283] M.P. Kapoor, Y. Ichihashi, K. Kuraoka, Y. Matsumura, J. Mol. Catal. A: Chem. 198 (2003) 303.
[284] D.J. Macquarrie, D.B. Jackson, Chem. Commun. (1997) 1781.
[285] T. Asefa, M.J. MacLachlan, N. Coombs, G.A. Ozin, Nature 402 (1999) 867.
[286] S. Inagaki, S. Guan, T. Ohsuna, O. Terasaki, Nature 416 (2002) 304.
[287] A. Bhaumik, T. Tatsumi, Catal. Lett. 66 (2000) 181.
[288] A. Bhaumik, M.P. Kapoor, S. Inagaki, Chem. Commun. (2003) 470.
[289] R. Ryoo, S.H. Joo, M. Kruk, M. Jaroniec, Adv. Mater. 13 (2001) 677.
[290] S.H. Joo, S.J. Choi, I. Oh, J. Kwak, Z. Liu, O. Terasaki, R. Ryoo, Nature 412 (2001) 169.
[291] T.-W. Kim, I.-S. Park, R. Ryoo, Angew. Chem. Int. Ed. 42 (2003) 4375.
[292] F. Schüth, Angew. Chem. Int. Ed. 42 (2003) 3604.
[293] Z. Liu, Y. Sakamoto, T. Ohsuna, K. Hiraga, O. Terasaki, C.H. Ko, H.J. Shin, R. Ryoo, Angew. Chem. Int. Ed. 39 (2000) 3107.
[294] H.J. Shin, R. Ryoo, Z. Liu, J. Am. Chem. Soc. 123 (2001) 1246.
[295] H.J. Shin, C.H. Ko, R. Ryoo, J. Mater. Chem. 11 (2001) 260.
[296] J.Y. Kim, S.B. Yoon, J.-S. Yu, Chem. Mater. 15 (2003) 1932.
[297] C.J.H. Jacobsen, C. Madsen, J. Houzvicka, I. Schmidt, A. Carlsson, J. Am. Chem. Soc. 122 (2000) 7116.
[298] Y. Tao, H. Kanoh, K. Kaneko, J. Am. Chem. Soc. 125 (2003) 6044.
[299] O.D. Velev, T.A. Jede, R.F. Lobo, A.M. Lenhoff, Nature 389 (1997) 447.
[300] A. Imhof, D.J. Pine, Nature 389 (1997) 948.
[301] H. Yan, C.F. Blanford, B.T. Holland, W.H. Smyrl, A. Stein, Chem. Mater. 12 (2000) 1134.
[302] M.A. Al-Daous, A. Stein, Chem. Mater. 15 (2003) 2638.
[303] M.A. Carreon, V.V. Guliants, Chem. Commun. (2001) 1438.
[304] M.A. Carreon, V.V. Guliants, Chem. Mater. 14 (2002) 2670.
[305] C.H. Christensen, K. Johannsen, I. Schmidt, C.H. Christensen, J. Am. Chem. Soc. 125 (2003) 13370.
[306] F.A. Twaiq, A.R. Mohamed, S. Bhatia, Micropor. Mesopor. Mater. 64 (2003) 95.
[307] E. Byambajav, Y. Ohtuska, Fuel 82 (2003) 1571.
[308] M.A. Uddin, Y. Sakata, A. Muto, Y. Shiraga, K. Koizumi, Y. Kanada, K. Murata, Micropor. Mesopor. Mater. 21 (1998) 557.
[309] A. Corma, M.S. Grande, V. Gonzalez-Alfaro, A.V. Orchilles, J. Catal. 159 (1996) 375.
[310] J.P.G. Pater, P.A. Jacobs, J.A. Martens, J. Catal. 184 (1999) 262.
[311] G. Seo, N.H. Kim, Y.H. Lee, J.H. Kim, Catal. Lett. 57 (1999) 209.
[312] A. Corma, V. González-Alfaro, A.V. Orchillés, J. Catal. 200 (2001) 34.
[313] D. Eliche-Quesada, J. Mérida-Robles, P. Maireles-Torres, E. Rodríguez-Castellón, A. Jiménez-López, Langmuir 19 (2003) 4985.
[314] Y. Sun, L. Zhu, H. Lu, R. Wang, S. Lin, D. Jiang, F.-S. Xiao, Appl. Catal. A: Gen. 237 (2002) 21.

[315] B. Chiche, E. Sauvage, F. Di Renzo, I.I. Ivanova, F. Fajula, J. Mol. Catal. A: Chem. 134 (1998) 145.
[316] X. Hu, M.L. Foo, G.K. Chuah, S. Jaenicke, J. Catal. 195 (2000) 412.
[317] E. Armengol, M.L. Cano, A. Corma, H. Garcia, M.T. Navarro, J. Chem. Soc. Chem. Commun. (1995) 519.
[318] N. He, S. Bao, Q. Xu, Appl. Catal. A: Gen. 169 (1998) 29.
[319] M.J. Climent, A. Corma, S. Iborra, M.C. Navarro, J. Primo, J. Catal. 161 (1996) 783.
[320] M.J. Climent, A. Corma, R. Guil-Lopez, S. Iborra, J. Primo, J. Catal. 175 (1998) 70.
[321] M. Iwamoto, Y. Tanaka, N. Sawamura, S. Namba, J. Am. Chem. Soc. 125 (2003) 13032.
[322] M. Onaka, N. Hashimoto, Y. Kitabata, R. Yamasaki, Appl. Catal. A: Gen. 241 (2003) 307.
[323] T. Kugita, S.K. Jana, T. Owada, N. Hashimoto, M. Onaka, S. Namba, Appl. Catal. A: Gen. 245 (2003) 353.
[324] L.-X. Dai, K. Koyama, T. Tatsumi, Catal. Lett. 53 (1998) 211.
[325] A.L. Villade, P.E. Alarcón, C.M. de Correa, Chem. Commun. (2002) 2654.
[326] H. Yoshida, K. Kimura, Y. Inaki, T. Hattori, Chem. Commun. (1997) 129.
[327] Y. Inaki, H. Yoshida, K. Kimura, S. Inagaki, Y. Fukushima, T. Hattori, Phys. Chem. Chem. Phys. 2 (2000) 5293.
[328] Y. Inaki, H. Yoshida, T. Yoshida, T. Hattori, J. Phys. Chem. B 106 (2002) 9098.
[329] A. Corma, S. Iborra, S. Miquel, J. Primo, J. Catal. 173 (1998) 315.
[330] S.C. Laha, P. Mukherjee, S.R. Sainkar, R. Kumar, J. Catal. 207 (2002) 213.
[331] D.R.C. Huybrechts, L. De Bruycher, P.A. Jacobs, Nature 345 (1990) 240.
[332] G. Bellusi, A. Carati, M.G. Clerici, G. Meddinelli, R. Millini, J. Catal. 133 (1992) 220.
[333] S. Gontier, A. Tuel, Appl. Catal A: Gen. 118 (1994) 173.
[334] O. Franke, J. Rathousky, G. Schulz-Ekloff, J. Starek, A. Zukal, in: J. Weitkamp, H.G. Karge, H. Pfeifer, W. Hölderich (Eds.), Zeolites and Related Microporous Materials: State of the Art 1994, Studies in Surface Science Catalysis, vol. 84, Elsevier, Amsterdam, 1994, p. 77.
[335] I.W.C.E. Arends, R.A. Sheldon, Appl. Catal. A: Gen. 212 (2001) 175.
[336] L.J. Davies, P. McMorn, D. Bethell, P.C.B. Page, F. King, F.E. Hancock, G.J. Hutchings, J. Mol. Catal. A: Chem. 165 (2001) 243.
[337] T. Blasco, A. Corma, M.T. Navarro, J. Pérez Pariente, J. Catal. 156 (1995) 65.
[338] V. Parvulescu, C. Constantin, B.L. Su, J. Mol. Catal. A: Chem. 202 (2003) 171.
[339] W.A. Carvalho, M. Wallau, U. Schuchardt, J. Mol. Catal. A: Chem. 144 (1999) 91.
[340] A. Sakthivel, P. Selvam, J. Catal. 211 (2002) 134.
[341] E. Armengol, A. Corma, V. Fornés, H. García, J. Primo, Appl. Catal. A: Gen. 181 (1999) 305.
[342] R.K. Rana, B. Viswanathan, Catal. Lett. 52 (1998) 25.
[343] L. Noreñga-Franco, I. Hernandez-Perez, J. Aguilar-Oliego, A. Maubert-Franco, Catal. Today 75 (2002) 189.
[344] V. Parvulescu, B.-L. Su, Catal. Today 69 (2001) 315.
[345] V. Parvulescu, C. Anastasescu, C. Constantin, B.L. Su, in: R. Aiello, G. Giordano, F. Testa (Eds.), Impact of Zeolites and Other Porous Materials on the New Technologies at the Beginning of the New Millennium, Studies in Surface Science and Catalysis, vol. 142, Elsevier, Amsterdam, 2002, p. 1213.
[346] K. Lemke, H. Ehrick, U. Lohse, H. Berndt, K. Jähnisch, Appl. Catal. A: Gen. 243 (2003) 41.
[347] J. Okamura, S. Nishiyama, S. Tsuruya, M. Masai, J. Mol. Catal. A: Chem. 135 (1998) 133.
[348] A. Corma, M.T. Navarro, L. Nemeth, M. Renz, Chem. Commun. (2001) 2190.
[349] T. Miyaji, P. Wu, T. Tatsumi, Catal. Today 71 (2001) 169.
[350] Y.A. Kalvachev, T. Hayashi, S. Tsubota, M. Haruta, in: R.K. Grasselli, S.T. Oyama, A.M. Gaffney, J.E. Lyons (Eds.), Third World Congress on Oxidation Catalysis, Studies in Surface Science and Catalysis, vol. 110, Elsevier, Amsterdam, 1997, p. 965.
[351] B.S. Uphade, Y. Yamada, T. Akita, T. Nakamura, M. Haruta, Appl. Catal. A: Gen. 215 (2001) 137.
[352] B.S. Uphade, T. Akita, T. Nakamura, M. Haruta, J. Catal. 209 (2002) 331.
[353] A.K. Sinha, S. Seelan, T. Akita, S. Tsubota, M. Haruta, Catal. Lett. 85 (2003) 223.
[354] P.P. Olivera, E.M. Patrito, H. Sellers, Surf. Sci. 313 (1994) 25.
[355] A.K. Sinha, S. Seelan, S. Tsubota, M. Haruta, Angew. Chem. Int. Ed. 43 (2004) 1546.
[356] B. Solsona, T. Blasco, J.M. López Nieto, M.L. Pena, F. Rey, A. Vidal-Moya, J. Catal. 203 (2001) 443.
[357] B. Sulikowski, Z. Olejniczak, E. Włoch, J. Rakoczy, R.X. Valenzuela, V.C. Corberán, Appl. Catal. A: Gen. 232 (2002) 189.
[358] H. Berndt, A. Martin, A. Brückner, E. Schreier, D. Müller, H. Kosslick, G.U. Wolf, B. Lücke, J. Catal. 191 (2000) 384.
[359] B. Lin, X. Wang, Q. Guo, W. Yang, Q. Zhang, Y. Wang, Chem. Lett. 32 (2003) 860.
[360] L.-X. Dai, Y.H. Teng, K. Tabata, E. Suzuki, T. Tatsumi, Micropor. Mesopor. Mater. 44–45 (2001) 573.
[361] X. Gao, I.E. Wachs, M.S. Wong, J.Y. Ying, J. Catal. 203 (2001) 18.
[362] A. Wingen, N. Anastasievič, A. Hollnagel, D. Werner, F. Schüth, J. Catal. 193 (2000) 248.
[363] A. Corma, A. Martinez, V. Marinez-Soria, J. Catal. 169 (1997) 480.
[364] K.M. Reddy, C. Song, Catal. Today 31 (1996) 137.
[365] M. Jacquin, D.J. Jones, J. Roziere, S. Albertazzi, A. Vaccari, M. Lenarda, L. Storaro, R. Ganzerla, Appl. Catal. A: Gen. 251 (2003) 131.
[366] S. Coman, V.I. Parvulescu, B. Tesche, H. Bönnemann, J.F. Roux, S. Kaliaguine, P.A. Jacobs, J. Mol. Catal. A: Chem. 146 (1999) 247.
[367] S.N. Coman, V.I. Parvulescu, M. De Bruyn, D.E. De Vos, P.A. Jacobs, J. Catal. 206 (2002) 218.
[368] C. Schüth, S. Disser, F. Schüth, M. Reinhard, Appl. Catal. B: Environ. 28 (2000) 147.
[369] C.P. Mehnert, J.Y. Ying, Chem. Commun. (1997) 2215.
[370] C.P. Mehnert, D.W. Weaver, J.Y. Ying, J. Am. Chem. Soc. 120 (1998) 12289.
[371] B.G. Johnson, C.H. Bartholomew, D.W. Goodman, J. Catal. 128 (1991) 231.
[372] E. Iglesia, S.L. Soled, R.A. Fiato, J. Catal. 137 (1992) 212.
[373] A.Y. Khodakov, A. Griboval-Constant, R. Bechara, V.L. Zholobenko, J. Catal. 206 (2002) 230.
[374] J. Panpranot, J.G. Goodwin Jr., A. Sayari, Catal. Today 77 (2002) 269.
[375] J. Panpranot, J.G. Goodwin Jr., A. Sayari, J. Catal. 211 (2002) 530.
[376] J. Panpranot, J.G. Goodwin Jr., A. Sayari, J. Catal. 213 (2003) 78.
[377] A. Lewandowska, S. Monteverdi, M. Bettahar, M. Ziolek, J. Mol. Catal. A: Chem. 188 (2002) 85.
[378] M. Okumura, S. Tsubota, M. Iwamoto, M. Haruta, Chem. Lett. (1998) 315.
[379] U. Junges, F. Schüth, G. Schmid, Y. Uchida, R. Schlögl, Ber. Bunsenges. Phys. Chem. 101 (1997) 1631.

[380] A. Fukuoka, N. Higashimoto, Y. Sakamoto, M. Sasaki, N. Sugimoto, S. Inagaki, Y. Fukushima, M. Ichikawa, Catal. Today 66 (2001) 23.
[381] M. Sasaki, M. Osada, N. Higashimoto, T. Yamamoto, A. Fukuoka, M. Ichikawa, J. Mol. Catal. A: Chem. 141 (1999) 223.
[382] W.S. Ahn, K.I. Min, Y.M. Chung, H.-K. Rhee, S.H. Joo, R. Ryoo, in: A. Galarneau, F. di Renzo, F. Fajula, J. Vedrine (Eds.), Zeolites and Mesoporous Materials at the Dawn of the 21st Century, Studies in Surface Science and Catalysis, vol. 135, Elsevier, Amsterdam, 2001, p. 313.
[383] I. Yuranov, P. Moeckli, E. Suvorova, P. Buffat, L. Kiwi-Minsker, A. Renken, J. Mol. Catal. A: Chem. 192 (2003) 239.
[384] R. Burch, N. Cruise, D. Gleeson, S.C. Tsang, Chem. Commun. (1996) 951.
[385] S. Kawi, S.Y. Liu, S.-C. Shen, Catal. Today 68 (2001) 237.
[386] Y. Liu, K. Murata, M. Inaba, N. Mimura, Catal. Commun. 4 (2003) 281.
[387] H.U. Wüstefeld, Ph.D. Thesis, Ruhr-Universität Bochum, 2004.
[388] P. Piaggio, P. McMorn, C. Langham, D. Bethell, P.C. Bulman-Page, F.E. Hancock, G.J. Hutchings, New J. Chem. (1998) 1167.
[389] S.-H. Lau, V. Caps, K.-W. Yeung, K.-Y. Yeung, K.-Y. Wong, S.C. Tsang, Micropor. Mesopor. Mater. 32 (1999) 279.
[390] S. Ernst, M. Selle, Micropor. Mesopor. Mater. 27 (1999) 355.
[391] M.L. Kantam, T. Bandyopadhyay, A. Rahman, N.M. Reddy, B.M. Choudary, J. Mol. Catal. A: Chem. 133 (1998) 293.
[392] M.L. Kantam, A. Rahman, T. Bandyopadhyzy, Y. Haritha, Synth. Commun. 29 (1999) 691.
[393] T. Joseph, S.S. Deshpande, S.B. Halligudi, A. Vinu, S. Ernst, M. Harmann, J. Mol. Catal. A: Chem. 206 (2003) 13.
[394] S.-G. Shyu, S.-W. Cheng, D.-L. Tzou, Chem. Commun. (1999) 2337.
[395] C.M. Crudden, D. Allen, M.D. Mikoluk, J. Sun, Chem. Commun. (2001) 1154.
[396] A. Marteel, J.A. Davies, M.R. Mason, T. Tack, S. Bektesevic, M.A. Abraham, Catal. Commun. 4 (2003) 309.
[397] C.E. Song, S.G. Lee, Chem. Rev. 102 (2002) 3495.
[398] J. Jamis, J.R. Anderson, R.S. Dickson, E.M. Campi, W.R. Jackson, J. Organomet. Chem. 627 (2001) 37.
[399] C. Pérez, S. Pérez, G.A. Fuentes, A. Corma, J. Mol. Catal. A: Chem. 197 (2003) 275.
[400] M.D. Jones, R. Raja, J.M. Thomas, B.F.G. Johnson, D.W. Lewis, J. Rouzaud, K.D.M. Harris, Angew. Chem. Int. Ed. 42 (2003) 4326.
[401] J.K. Park, S.-W. Kim, T. Hyeon, B.M. Kim, Tetrahedron: Asymmetry 12 (2001) 2931.
[402] A. Corma, H. García, A. Moussaif, M.J. Sabater, R. Zniber, A. Redouane, Chem. Commun. (2002) 1058.
[403] R.J. Clarke, I.J. Shannon, Chem. Commun. (2001) 1936.
[404] H. Kosslick, I. Mönnich, E. Paetzold, H. Fuhrmann, R. Fricke, D. Müller, G. Oehme, Micropor. Mesopor. Mater. 44–45 (2001) 537.
[405] E. Paetzold, G. Oehme, H. Fuhrmann, M. Richter, R. Eckelt, M.-M. Pohl, H. Kosslick, Micropor. Mesopor. Mater. 44–45 (2001) 517.
[406] K. Melis, D. De Vox, P. Jacobs, F. Verpoort, J. Mol. Catal. A: Chem. 169 (2001) 47.
[407] M. Pillinger, I.S. Gonçalves, A.D. Lopes, P. Ferreira, J. Rocha, G. Zhang, M. Schäfer, O. Nuyken, F.E. Kühn, Phys. Chem. Chem. Phys. 4 (2002) 696.
[408] R.R. Rao, B.M. Weckhuysen, R.A. Schoonheydt, Chem. Commun. (1999) 445.
[409] B.M. Weckhuysen, R.R. Rao, J. Pelgrims, R.A. Schoonheydt, P. Bodart, G. Debras, O. Collart, P. Van Der Voort, E.F. Vansant, Chem. Eur. J. 6 (2000) 2960.
[410] J. Tudor, D. O'Hare, Chem. Commun. (1997) 603.
[411] S. O'Brien, J. Tudor, T. Maschmeyer, D. O'Hare, Chem. Commun. (1997) 1905.
[412] H. Rahiala, I. Beurroies, T. Eklund, K. Hakara, R. Gougeon, P. Trens, J.B. Rosenholm, J. Catal. 188 (1999) 14.
[413] T. Sano, K. Doi, H. Hagimoto, Z. Wang, T. Uozumi, K. Soga, Chem. Commun. (1999) 733.
[414] H. Schneider, G.T. Puchta, F.A.R. Kaul, G. Raudaschl-Sieber, F. Lefebvre, G. Saggio, D. Mihalios, W.A. Herrmann, M. Basset, J. Mol. Catal. A: Chem. 170 (2001) 127.
[415] K. Kageyama, J. Tamazawa, T. Aida, Science 285 (1999) 2113.
[416] K. Tajima, G. Ogawa, T. Aida, J. Polym. Sci. A: Poly. Chem. 38 (2000) 4821.
[417] Z. Yang, Z. Niu, X. Cao, Z. Yang, Y. Lu, Z. Hu, C.C. Han, Angew. Chem. Int. Ed. 42 (2003) 4201.
[418] R. Anwander, I. Nagl, C. Zapilko, M. Widenmeyer, Tetrahedron 59 (2003) 10567.
[419] A. Fischbach, M.G. Klimpel, M. Widenmeyer, E. Herdtweck, W. Scherer, R. Anwander, Angew. Chem. Int. Ed. 43 (2004) 2234.
[420] X. Feng, G.E. Fryxell, L.Q. Wang, A.Y. Kim, J. Liu, K.M. Kemmer, Science 276 (1997) 923.
[421] J. Brown, L. Mercier, T.J. Pinnavaia, Chem. Commun. (1999) 69.
[422] J. Weitkamp, M. Hunger, U. Rymsa, Micropor. Mesopor. Mater. 48 (2001) 255.
[423] I. Rodriguez, S. Iborra, A. Corma, F. Rey, J.L. Jorda, Chem. Commun. (1999) 593.
[424] I. Rodriguez, G. Sastre, A. Corma, S. Iborra, J. Catal. 183 (1999) 14.
[425] A. Corma, S. Iborra, I. Rodríguez, F. Sánchez, J. Catal. 211 (2002) 208.
[426] S.T. Tavener, J.H. Clark, G.W. Gray, P.A. Heath, D.J. Macquarrie, Chem. Commun. (1997) 1147.
[427] D.J. Macquarrie, S.J. Tavener, G.W. Gray, P.A. Heath, J.S. Rafelt, S.I. Saulzet, J.J.E. Hardy, J.H. Clark, P. Sutra, D. Brunel, F. di Renzo, F. Fajula, New. J. Chem. 23 (1999) 725.
[428] D. Brunel, F. Fajula, J.B. Nagy, B. Deroide, M.J. Verhoef, L. Veum, J.A. Peters, H. van Bekkum, Appl. Catal. A: Gen. 213 (2001) 73.
[429] M.P. Kapoor, A. Bhaumik, S. Inagaki, K. Kuraoka, T. Yazawa, J. Mater. Chem. 12 (2002) 3078.
[430] M.J. MacLachlan, N. Coombs, G.A. Ozin, Nature 397 (1999) 681.
[431] P.N. Trikalitis, K.K. Rangan, T. Bakas, M.G. Kanatzidis, Nature 410 (2001) 671.
[432] C. Serre, A. Auroux, A. Gervasini, M. Hervieu, G. Rérey, Angew. Chem. Int. Ed. 41 (2002) 1594.
[433] M. Onaka, T. Oikawa, Chem. Lett. (2002) 850.
[434] A. Bhaumik, S. Inagaki, J. Am. Chem. Soc. 123 (2001) 691.
[435] S. Velu, M.P. Kapoor, S. Inagaki, K. Suzuki, Appl. Catal. A: Gen. 245 (2003) 317.
[436] V.F. Stone Jr., R.J. Davis, Chem. Mater. 10 (1998) 1468.
[437] Y. Takahara, J.N. Kondo, T. Takata, D. Lu, K. Domen, Chem. Mater. 13 (2001) 1194.
[438] M. Uchida, J.N. Kondo, D. Lu, K. Domen, Chem. Lett. (2002) 498.
[439] M. Vettraino, X. He, M. Trudeau, J.E. Drake, D.M. Antonelli, Adv. Func. Mater. 12 (2002) 174.
[440] M. Vettraino, M. Trudeau, A.Y.H. Lo, R.W. Schurko, D. Antonelli, J. Am. Chem. Soc. 124 (2002) 9567.
[441] D. Farrusseng, K. Schlichte, B. Spliethoff, A. Wingen, S. Kaskel, J.S. Bradley, F. Schüth, Angew. Chem. Int. Ed. 40 (2001) 4204.
[442] S. Yoon, J. Lee, T. Hyeon, S.M. Oh, J. Electrochem. Soc. 147 (2000) 2507.

[443] H. Zhou, S. Zhu, M. Hibino, I. Honma, J. Power, Source 122 (2003) 219.
[444] H. Zhou, S. Zhu, M. Hibino, I. Honma, M. Ichihara, Adv. Mater. 15 (2003) 2107.
[445] M. Choi, R. Ryoo, Nature Mater. 2 (2003) 473.
[446] A. Lu, W. Schmidt, N. Matoussevitch, B. Spliethoff, B. Tesche, E. Bill, W. Kiefer, F. Schüth, Angew. Chem. Int. Ed. 43 (2004) 4303.
[447] M. Iwamoto, H. Kitagawa, Y. Watanabe, Chem. Lett. (2002) 814.